

**Microscale Structure and Activity of  
Complex Nitrifying Wastewater Biofilms**

---

**Feinstruktur und *in situ*-Aktivität komplexer  
nitrifizierender Abwasserbiofilme**

Dissertation  
zur Erlangung des Grades eines  
Doktors der Naturwissenschaften  
– Dr. rer. nat. –

dem Fachbereich Biologie/Chemie der  
Universität Bremen  
vorgelegt von

Armin Gieseke  
aus Rotenburg/Wümme

Bremen  
Februar 2001

Die vorliegende Arbeit wurde in der Zeit vom Februar 1998 bis Februar 2001 am Max-Planck-Institut für marine Mikrobiologie in Bremen angefertigt.

1. Gutachter: PD Dr. Rudolf Amann
2. Gutachterin: Prof. Dr. Barbara Reinhold-Hurek

Tag des Promotionskolloquiums: 07. März 2001

Meinen Eltern Helga und Robert

## Preface

This thesis is concerned with the investigation of nitrifying communities in biofilms grown in complex environments of various wastewater treatment systems. Whereas lab-scale experimental reactors are run under very defined conditions, the applied scale often lacks this high degree of control leading to structural and functional heterogeneity also on the micro-scale. The aim of this thesis was to identify mechanisms that govern the structure and function of nitrifying communities and their interaction with other processes in such complex environments. By use of techniques adapted to the microscale, i.e., microsensors and fluorescence *in situ* hybridization, the microenvironment, activity, and microbial structure of nitrifying biofilms were studied *in situ*. The insights gained by this approach contribute to the understanding of the ecology of nitrifiers and might help, on the long run, in the handling and control of the treatment techniques.

The following introduction (chapter 1) presents a short overview on the methods used in this work and previous *in situ* studies on nitrification and nitrifying bacteria. The subsequent chapters (chapter 2 to 6) are publications (already published or in preparation) that in detail present and discuss the results. In chapter 7, this thesis is summarized and some ulterior discussion points are reviewed.

It goes without saying that this work was dependent on the help of a lot of people. During the last three years, my supervisor Rudi Amann, was always available for advice and motivating discussions. I am grateful for all his help. Barbara Reinhold-Hurek is thanked for rendering her expert opinion on this thesis. I am deeply indebted to Andreas Schramm, who introduced me to the techniques and the exciting world of nitrifiers, and discussed many results with me in depth. I am also most thankful to Dirk de Beer for his unconventional ideas, his expert opinion, and his motivating optimism. Patrik Arnz, Eva Arnold and their colleagues (Garching) maintained the reactor systems in Garching and Ingolstadt, and were of great help during three measuring campaigns in these places. I thank Michi Wagner, Holger Daims, Andi Brühl and Uli Purkhold (Munich), who infected me with new ideas and inspiring discussions. Anja Eggers, Gaby Eickert, Vera Hübner, and Ines Schröder were the essential

components to avoid oxygen sensor limitations during the last three years. Also, nitrate measurements would have come to a soon end without the help of Thomas Etterer (Garching), who synthesized a new batch of the ionophor. Thanks to all the helpful nice colleagues in both, the microsensor group and the molecular ecology group! I felt home in both groups the last three years. Many of them provided practical help or discussed ideas with me. Thank you all! Henk, Quique, and Rebecca are acknowledged for their important help in the last minute.

Finally, I am much obliged to Christine Pranz for all her patience and help, and to my parents, who paved my way with their continuous support.

Bremen, February 2001

Armin Gieseke



# Contents

<b>Chapter 1</b>	<i>Introduction</i>	9
<b>Chapter 2</b>	<i>Microenvironments and Distribution of Nitrifying Bacteria in a Membrane-Bound Biofilm</i>	37
<b>Chapter 3</b>	<i>Simultaneous P and N Removal in a Sequencing Batch Biofilm Reactor: Insights from Reactor- and Microscale Investigations</i>	51
<b>Chapter 4</b>	<i>Community Structure and Activity Dynamics of Nitrifying Bacteria in a Phosphate-Removing Biofilm</i>	67
<b>Chapter 5</b>	<i>Structure and Activity of Multiple Nitrifying Bacterial Populations Coexisting in a Biofilm</i>	95
<b>Chapter 6</b>	<i>In situ Substrate Conversion and Assimilation in a Nitrifying Model Biofilm as Studied with a Combination of Methods</i>	121
<b>Chapter 7</b>	<i>Discussion and Summary</i>	145
<b>Appendix</b>	List of Publications	



# **Chapter 1**

## **Introduction**

Parts of this chapter are included in a manuscript for "Fossil and Recent Biofilms"  
by Krumbein, W. E., Paterson, D. M., Zavarzin, G. A. (eds.), Dordrecht, Kluwer  
Academic Publishers



# Introduction

## 1 Nitrification

### 1.1 Nitrifying bacteria in nature and biotechnology

Nitrifying bacteria are among the earliest described microorganisms in the history of microbiology (97). In the natural N cycle they act as essential catalysts for the key steps of oxidation of ammonia to the oxidized state of nitrate (Fig. 1). This oxidation is performed in two sequential steps by different groups of bacteria: the aerobic chemolithoautotrophic ammonia-oxidizing bacteria (AOB) convert ammonia to nitrite, and nitrite-oxidizing bacteria (NOB) perform further conversion to nitrate by (7):



In the conventional N cycle, no pathway exists for the direct reduction of ammonium nitrogen to gaseous nitrogen (for a discussion of newly described pathways and their relevance see below). Therefore, both steps of nitrification are an important precondition for the release of bound nitrogen to the atmosphere via denitrification. From a human perspective, nitrification bears both benefits and drawbacks. In agricultural soils it may cause extensive loss of fertilizers by conversion of the cationic and well-bound ammonium into the easily soluble nitrate, which is washed out, causing eutrophication in surface and ground waters (29). Accumulation of ammonia, e.g., through dumping of untreated sewage waters into the environment is critical due to its toxicity to aquatic life (3). Therefore, nitrification is used intensively in wastewater treatment, where it is the first step in the removal of nitrogen from the bound pool (58). The removal of the secondary pollutants, nitrogen and phosphorus, has become increasingly

important in sewage treatment. Consequently, the stable and reproducible growth and activity of AOB and NOB play an important role in such applied systems.

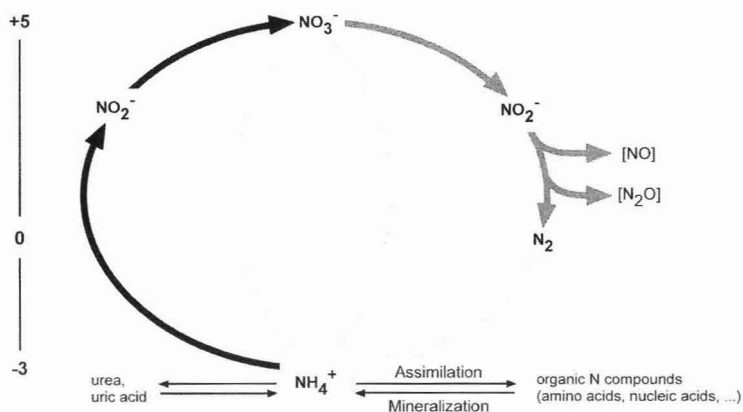


FIG. 1. Main components of the nitrogen cycle and their redox state (left). The outer circle represents nitrification performed by nitrifying bacteria (black arrows), denitrifying reactions catalyzed by facultatively anaerobic heterotrophic bacteria (dark grey), and nitrogen fixation as found, e.g., in the heterocysts of some *Cyanobacteria* or in *Rhizobium* (light grey). The central light grey arrows symbolize the assimilatory nitrate reduction performed by many aerobic bacteria in the absence of ammonium as a nitrogen source, and nitrate ammonification, that can be observed in several facultatively anaerobic fermenting bacteria [after (43), modified].

The process of nitrification and the organisms involved have been, and are still, of interest for microbiological research. Much efforts have been centered on isolating and cultivating pure strains of AOB and NOB. Use of common media for the cultivation of ammonia- and nitrite-oxidizing bacteria typically result in the isolation of members of the genera *Nitrosomonas* and *Nitrobacter*. This led to the general opinion that these microorganisms are the dominating AOB and NOB in many environments. Until the early eighties, however, no methods were available to detect and quantify the organisms and their activity directly in various habitats. Therefore, the reasons for failure in stable establishment of nitrification or breakdown of existing nitrification systems could not be directly analyzed. In a more general view, this also hampered deeper insights into the microbial ecology of nitrifying bacteria in general, i.e., the study of relationships with their environment.

## 1.2 Novel pathways in the N cycle

On the other hand, interesting new processes with respect to the N cycle have been described in recent years. This involves the discovery of an anaerobic oxidation of ammonium

(Anammox) (37, 52) with nitrite (88) by a "missing lithotroph" , which has been shown to be affiliated to the order of *Planctomycetales* (82). A likely stoichiometry for the reaction is (89):



A denitrifying activity with nitrite as an electron acceptor has also been demonstrated for the typical AOB *Nitrosomonas europaea* and *N. eutropha* (8, 69). When subjected to low oxygen concentrations, formation of dinitrogen oxide and molecular nitrogen were observed. Under anoxic conditions, molecular hydrogen or even ammonium could be used as alternative electron donors, with a stoichiometry analogous to reaction [3]. Causing a significant loss of bound nitrogen, both, the Anammox process and the "nitrifier denitrification" (36) might be of importance in applied sewage treatment systems working with activated sludge (37, 53) or with biofilms (31, 68, 75). The maximum oxidation rate for the Anammox organism was shown to be 25-fold higher than that for *N. europaea* (37). The presence of *N. europaea*, however, has been demonstrated for many wastewater treatment systems, and these newly described processes may play a certain role in practical applications.

The central focus of this thesis is set on the process of nitrification and nitrifying microbial communities, their structure and activity in modern wastewater treatment biofilm systems. The following sections will give an overview of the methods applied for this purpose.

## 2 Analysis of the structure of nitrifying microbial communities

### 2.1 The cultivation-based approach and its limitations

To study the ecology of microbial communities in biofilms out of environmental or applied systems it is necessary to have insights into their microbial structure, i.e., the abundance, distribution, and identity of their members. In microbiology, identification is usually addressed by isolation and subsequent description of morphological, physiological and biochemical traits of a pure culture of a microorganism. For several reasons, it is difficult to approach the ecology of microorganisms in biofilms with this method. Firstly, isolation removes the organism from the biofilm and out of its structured microenvironment (see below). Culture conditions might not precisely reproduce this *in situ* microenvironment, which often is not even

fully characterized. As a consequence, cultivation bears the risk of biases because of selective enrichment of certain strains due to different, non-natural conditions. This might result in failure to qualitatively determine the main microbial components of a system (90). Attempts of quantification frequently result in a discrepancy between direct total cell counts and cell abundance estimated by most-probable-number quantification or colony forming units. Only between 0.1% and 10% of directly counted cells are often found actively growing in culture (35, 78). The occurrence of cells in microcolonies, the presence of inactive cells, and inefficiency of the culture medium might explain this discrepancy (9, 35). Cultivation of slow-growing or fastidious organisms like the nitrifying bacteria is time-consuming. The free energy nitrifiers gain from reaction [1] or [2] is low: about  $-287 \text{ kJ mol}^{-1}$  from oxidation of ammonia under standard conditions and pH 7, and even less from oxidation of nitrite ( $-74.1 \text{ kJ mol}^{-1}$ ) (46). As a result, the maximum specific growth rates and growth yields are low compared to that of heterotrophic bacteria (61). Thus, cultivation might not be the most suitable tool if, e.g., rapid transient or successional events in biofilms are to be studied.

However, cultivation of microorganisms is essential to investigate their physiological and biochemical potentials. This data is often necessary to interpret *in situ* observations in an ecological context.

## 2.2 Cultivation-independent techniques

### *Molecular bacterial phylogeny*

The expansion of molecular methods in the late seventies led to new possibilities for the study of microbial diversity. An independent and phylogenetically meaningful classification system of bacteria was established based on molecular evidence. This classification was built on comparative sequence analysis of the gene fragments coding for the small subunit rRNA (SSU rRNA) (98). Among other elements such as the gene coding for the elongation factor Tu (EF-Tu), or for the  $\beta$ -subunit of the ATP synthase (45), the gene fragments coding for 16S rRNA proved suitable targets for phylogenetic analyses, because their products are indispensable parts of the structural components for protein biosynthesis and, thus, are ubiquitous among prokaryotes. Parts of these sequences are highly conserved whereas other domains are variable to different degrees. This allows a proper alignment on one hand, and, on the other hand, differentiation on various taxonomic scales from the level of kingdoms down to the

individual genera or species. After extraction of DNA from an environmental sample or a pure culture, the 16S rDNA is amplified in a polymerase chain reaction (PCR) by use of a universal primer pair that specifically binds near the ends of the 16S rRNA-coding sequence of all prokaryotes. For separation of the mixture of different sequences, the products are then ligated into vectors (usually plasmids) and transformed into competent cells. After plating, each individual colony of this clone library ideally should carry copies of a unique 16S rRNA sequence, which can be separately extracted and sequenced. This cloning and sequencing approach has been intensively used and has led to the accumulation of more than 18,000 16S rRNA sequences from either isolates or molecular clones out of diverse environments (47).

### *Diversity of nitrifying bacteria*

The diversity of nitrifying communities has been intensively studied by these methods in soils (40, 41, 80), freshwater (76, 79), sediments (95), activated sludge (83), and marine environments (49, 80). Continuous efforts have been made to establish a general phylogeny of nitrifying bacteria (30, 33, 60, 63, 86). In case of the AOB, the molecular analysis recently included as well sequences of the functional gene coding for the key enzyme of ammonia oxidation, the ammonia monooxygenase (*amoA*) (39, 63, 67). Sequence analysis based on *amoA* and 16S rRNA sequences leads to a similar, although not identical, phylogeny. However, *amoA* sequence comparison allows a higher resolution (below the species level). Fig. 2 gives an overview of the current 16S rRNA-based phylogeny of AOB. All currently described species and several isolates and molecular clones are grouped into two monophyletic lineages. The major part of species belongs to the  $\beta$ -subclass of *Proteobacteria* including the genera *Nitrosomonas* and *Nitrospira*, whereas some sequences are related to the  $\gamma$ -subclass of *Proteobacteria*. Based on nearly full length 16S rRNA sequences it is now fairly accepted that five stable lineages exist among the  $\beta$ -subclass AOB. They are represented by the following: (i) *Nitrospira* sp. (cluster 0 to 4); (ii) cluster 5, *N. oligotropha*/*N. ureae*, and *N. aestuarii*/*N. marina* (clusters 5, 6a, and 6b); (iii) *N. europaea*/*Nitrosococcus mobilis* (cluster 7); (iv) *N. communis* (cluster 8); (v) *Nitrosomonas cryotolerans*. The *Nitrospira*-lineage includes the genera *Nitrosolobus* and *Nitrosovibrio*. *N. cryotolerans* represents a separate lineage. Strains affiliated to the group mentioned under (ii) form three subgroups: the cluster 6a encompassing *N. oligotropha* and *N. ureae*; cluster 6b, which include *N. aestuarii* and *N. marina*; and cluster 5, which only consist of molecular clones (not shown in Fig. 2) (60, 63). The branching order between these five lineages can not unequivocally be determined.

Up to now, all members of this monophyletic branch of the  $\beta$ -subclass of *Proteobacteria* have been shown to be chemolithoautotrophic AOB.

Isolates related to the AOB *Nitrosococcus oceani* and *Nitrosococcus halophilus* have been shown to belong to the  $\gamma$ -subclass of *Proteobacteria*.

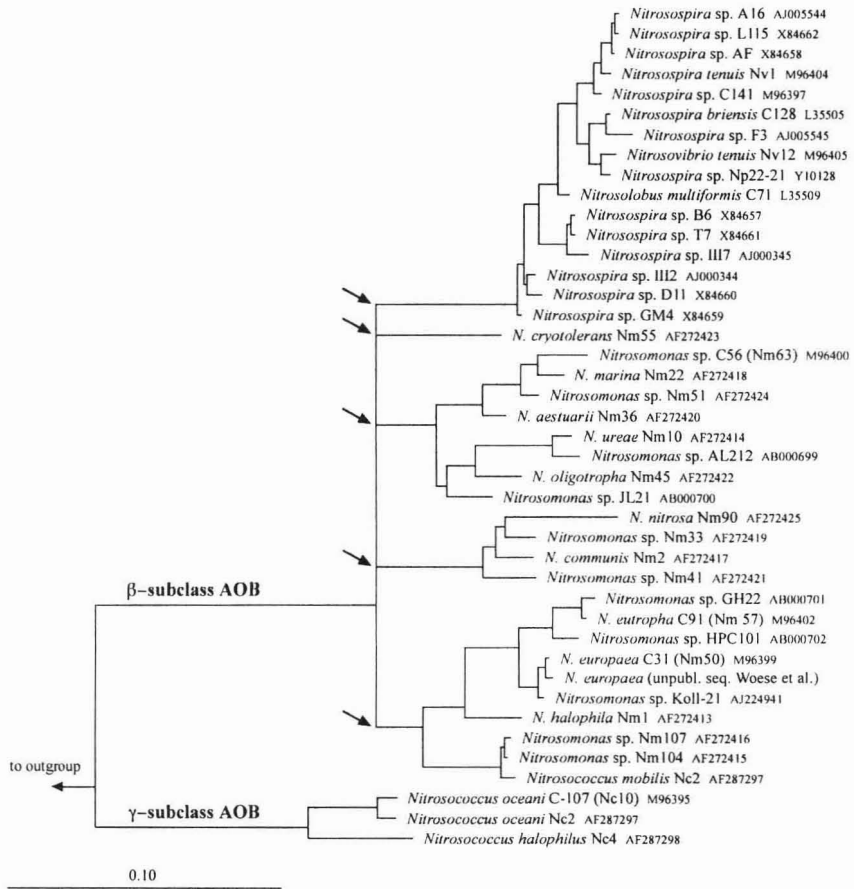


FIG. 2. Phylogenetic tree of ammonia-oxidizing bacteria (type strains, isolates, and environmental clones) inferred from comparative analysis of 16S rRNA sequences (>1300 informative positions; 50% conservation filter for *Bacteria*). The tree is based on a maximum likelihood calculation (FastDNAML), and topology was tested by distance matrix and maximum parsimony methods. Multifurcations were drawn as a consensus, where the relative branching order could not be determined. Arrows indicate the five lineages of  $\beta$ -subclass AOB as described in the text. *Nitrosomonas* cluster 5 is not included because of the lack of nearly full sequences for this cluster. The bar represents 10% estimated sequence divergence.

The nitrite-oxidizing bacteria (Fig. 3) are represented in several subclasses of the *Proteobacteria*: The well-studied strains of *Nitrobacter* sp. form a closely related cluster affiliated to the  $\alpha$ -subclass, whereas *Nitrospina* sp. strains are affiliated with the  $\delta$ -subclass (85). *Nitrosococcus mobilis* (not to be mistaken for the AOB *Nitrosococcus mobilis*) is a NOB related to

the  $\gamma$ -subclass. Recently, isolates and molecular clones of another group of NOB, *Nitrospira* sp. have been recovered from various habitats (14, 23, 34, 39, 72, 94). They very likely appeared already in earlier studies on nitrifying reactor systems but were judged as contamination (13). These newly described NOB (23, 94) are not related to any known bacterial group. Based on comparative 16S rRNA sequence analysis, a distinct phylum *Nitrospira* was proposed, which encompasses the genus *Nitrospira* (with the isolates of *Nitrospira moscoviensis* and *Nitrospira marina*) and non-nitrite-oxidizing isolates of *Thermodesulfovibrio yellowstonii* and *Leptospirillum ferrooxidans*, together with some environmental clones (23).

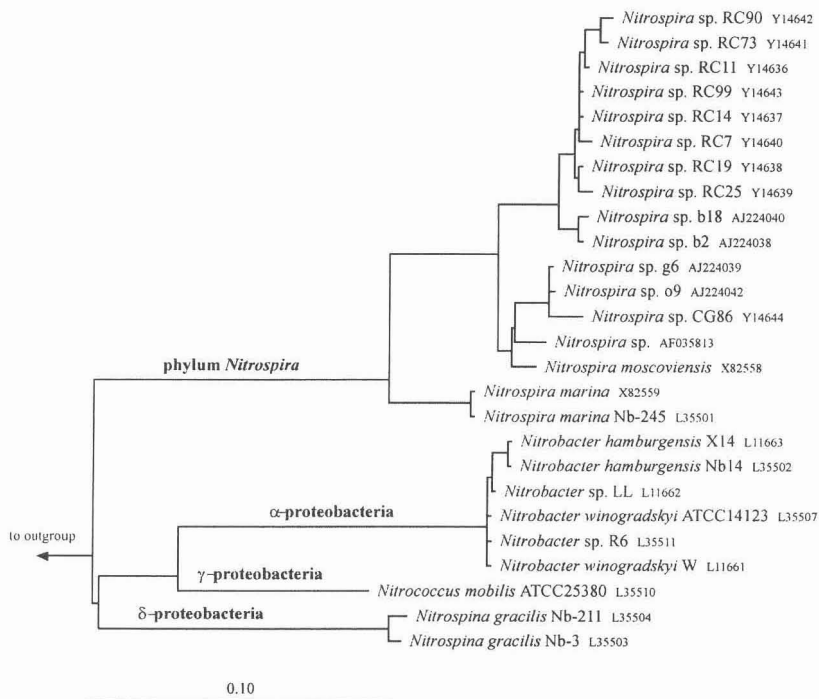


FIG. 3. Phylogenetic tree of nitrite-oxidizing bacteria (type strains, isolates, and environmental clones) inferred from comparative analysis of 16S rRNA sequences. Calculation and tree construction was performed as described in the legend of Fig. 2. The bar represents 10% estimated sequence divergence.

### *In situ analysis based on oligonucleotide probing*

The information content of 16S rRNA sequences is not only of use for investigating the phylogeny of various groups, but can be applied again for analytical purposes in the environment based on the principles of hybridization. In detail, sequence obtained from 16S clone libraries are compared to find small regions, usually of a length of 18 to 20 base pairs, with a

sequence specific for a certain taxon of interest. A small oligonucleotide labeled with a suitable marker (a fluorescent dye or a radiotracer) to be used as a probe is then synthesized with the complementary sequence. During hybridization, specific binding will take place only between the target nucleic acids and the probe, given that the conditions are stringent, i.e., close to the dissociation temperature of the hybrid (77). Hybridization can either be performed with extracted rRNA bound to a membrane (slot blot hybridization) or to rRNA directly in whole microbial cells *in situ*, that have been permeabilized before by appropriate fixation. Many oligonucleotide probes are available for hybridization of various groups of nitrifying bacteria (63, 87).

A whole cycle can thus be run of cloning, sequencing, and analysis of environmental 16S rRNA, the development of oligonucleotide probes against certain organisms represented in the clone library, and their detection in the original sample via hybridization. This investigation method has been described as the rRNA approach (57) and is illustrated in Fig. 4.

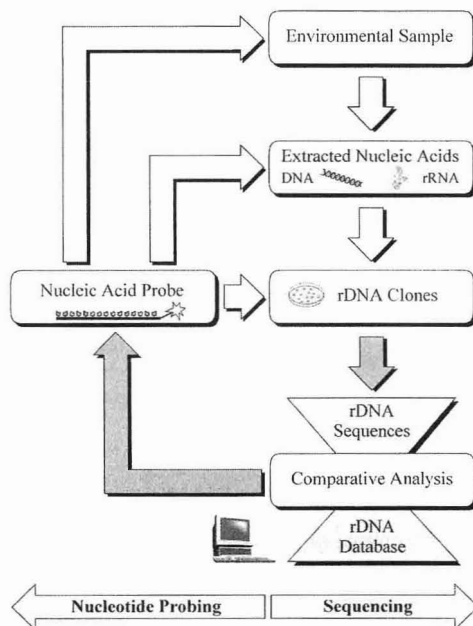


FIG. 4. Schematic overview of the rRNA approach [after (2), modified].

*In situ* hybridization is ideally performed with fluorescently labeled oligonucleotide probes. The sample can then be directly inspected by epifluorescence microscopy. An important precondition for this fluorescence *in situ* hybridization (FISH) is the fact, that usually the rRNA target exists in several hundreds to many thousands of copies in a single cell. Thus, the

hybridization between target and probe includes a natural amplification that enables the visualization. The FISH method allows direct identification and quantification of cells in a sample. Additionally, information is obtained on cell morphology and spatial organization of cells, giving hints on potential interactions (2). In contrast to other molecular tools for identification, this method *per se* does not include a polymerase chain reaction step and, thus, is not affected by biases like selectivity in the extraction (93) or amplification (24, 84). However, FISH bears its own drawbacks: (i) probe design can only be based on *existing* sequence information, leading to problems in case of "hidden" diversity in the sample; (ii) the ribosome content affects the signal intensity; as a consequence the detectability depends on recent activity and/or the strain-specific ability to preserve the ribosome content in case of inactivity; and (iii) care has to be taken that the probe target regions of the 16S rRNA molecule are accessible. Therefore, selection of suitable domains within the 16S rRNA during probe design (28) or additional application of helper probes (27) might be necessary.

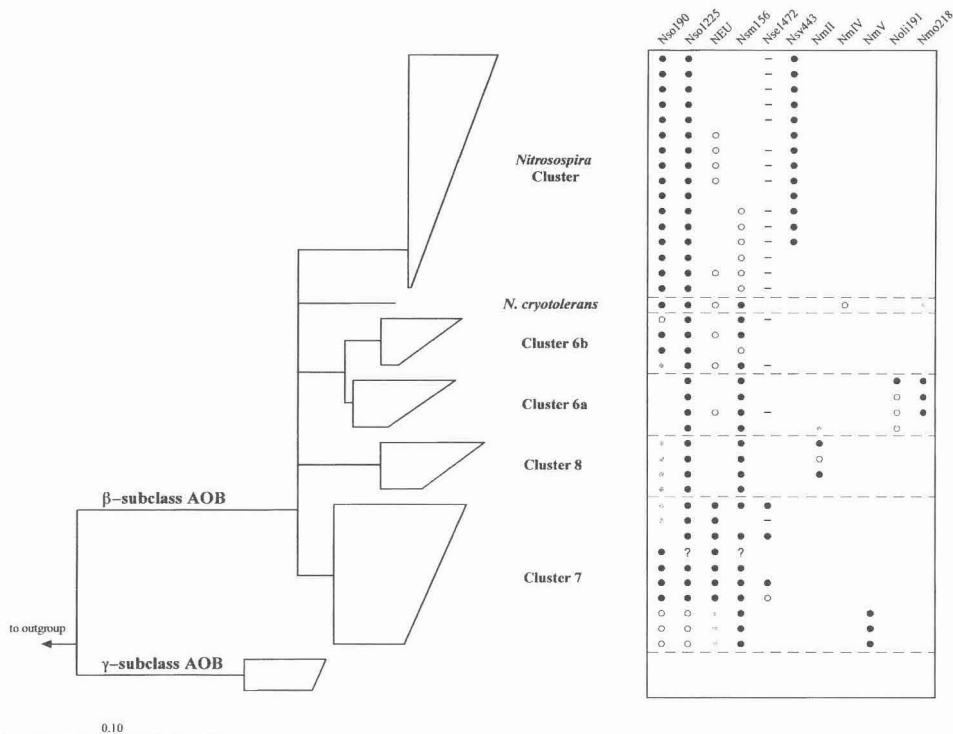


FIG. 5. Simplified phylogenetic tree of ammonia-oxidizing bacteria and matching situation of oligonucleotide probes for the detection of AOB with FISH. The symbols in the box are as follows: ● zero mismatches, ○ a weak mismatch ( $\leq 0.6$  weighted mismatches), and ○ one strong mismatch ( $\geq 1$  weighted mismatches) to the 16S target site of the respective strain in the tree; ? one or several ambiguities at the target site; - no sequence information at the target site. Lack of symbols indicates two or more mismatches. For details of phylogeny see Fig. 2.

The range of known target organisms covered by a probe may be affected by the increasing sequence information. New sequences with complementary target site appear originating from non-target organisms, causing false-positive results in FISH. Whereas the probe is still specific in terms of hybridization to the complementary target, its use in detecting a specific group of organisms may become restricted. This is illustrated in Fig. 5 showing the oligonucleotide probes currently used for the detection of the  $\beta$ -subclass AOB. Most of the probes do not fully and exclusively cover a certain subgroup. Thus, to ensure proper discrimination between target and non-target organisms, several probes can be applied sequentially in a nested approach (2). Combining probes of overlapping ranges and different fluorescent labels on one sample (1) helps to increase the reliability of the method and can reveal details on the spatial organization of different populations (Fig. 6).

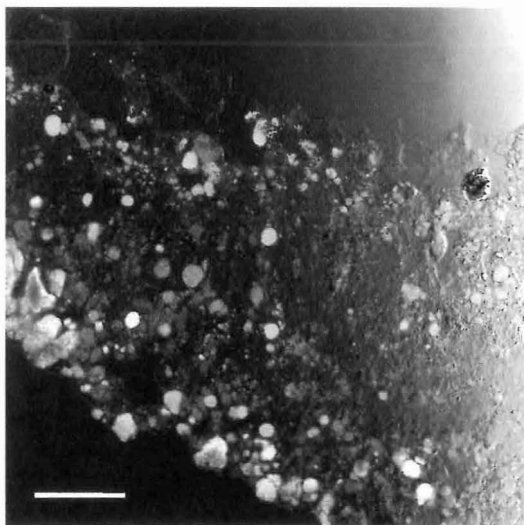


FIG. 6: Confocal micrograph of a vertical biofilm thin section illustrating the multiple probe concept. The section was hybridized with probes EUB338 (targeting *Bacteria*; blue), a mixture of Nso1225 and NmV (targeting most  $\beta$ -subclass AOB; red), and Ntspa 712 (targeting the phylum *Nitrospira*; green). Purple color results from an overlap of blue and red signal, turquoise from an overlap of blue and green signals. *Nitrospira* sp. is situated at the bottom part of the biofilm. Scale bar is 50  $\mu$ m.

Initial attempts of direct detection of nitrifying bacteria by FISH were made by Wagner et al. (91, 92). Based on 16S rDNA sequence information an oligonucleotide probe was designed specific for the halophilic and halotolerant *Nitrosomonas* spp. (NEU) and for all *Nitrobacter* sp. (NIT3) sequenced at that time. The successful detection demonstrated the approach to be useful even for complex microbial communities. Later, further probes

covering all  $\beta$ -subclass AOB (Nso190, Nso1225), different lineages among them (Nsv443, Nsm156, Nse1472), and the NOB *Nitrobacter* sp. were described (39, 50). Several studies in wastewater systems showed that *Nitrobacter* was either absent or occurred in low numbers. In contrast, these studies could demonstrate the presence of members of the phylum *Nitrospira* by cloning and/or oligonucleotide hybridization (14, 39, 56, 70-72). In a recent study on a nitrifying biofilm reactor, comprehensive probes were suggested covering the phylum (Ntspa712) and the genus *Nitrospira* (Ntspa662) on the basis of all currently known sequences affiliated to that group (14).

### 3 The biofilm function and its analysis

#### 3.1 Biofilm architecture and microenvironments

Biofilms as "...a collection of microorganisms and their extracellular products bound to a solid (living or inanimate) surface (termed as substratum)" (48) have been, for several reasons, the main study object during this work. First of all, biofilms are an ubiquitous way of life for many bacteria. The observation of attachment of bacteria as a common phenomenon in aquatic environments (32) and the study of its effects on bacterial activity (99) might be the earliest examples of biofilm research. Biofilm formation was suggested to be a multistep process of initial reversible attachment, followed by "cementation" and later growth and/or additional attachment (99). Thus, biofilms have been a well known phenomenon since decades, but their importance has been overlooked for a long time. Later discoveries of biofilms in many environments suggested that the attached growth is typical for many bacteria (11).

Many modern wastewater treatment systems make use of the advantages of biofilms. In contrast to sludges, biofilm systems ensure a longer retention of biomass, a higher biomass concentration in the reactor, the presence of mixed populations, and lower amounts of sludge waste (10). Especially the longer retention times allow the establishment of slow-growing organisms like nitrifying bacteria (58), which otherwise are easily outcompeted by heterotrophic bacteria (25, 61).

From the viewpoint of microbial ecology, biofilms are of interest because they provide a variety of distinct environments for the individual cells (16). Diffusion is the main transport process for substrates and metabolic products within biofilm structures. Due to the high local

metabolic activity steep concentration gradients are typically present across the liquid-biofilm interface and within the biofilm, causing a vertical stratification in terms of environments and function. While forming a flat layer in some cases (e.g., dental biofilms), heterogeneous physical structures, such as microcolonies and streamers, appear as a result of heterogeneous substrate supply and, thus, differential growth. This can lead to a more open architecture with channels and pores, which allow transport by advection (19, 81) and increased lateral heterogeneity (20). An overview of different models for biofilm architectures is given in (96).

The biofilm definition given above also includes suspended microbial aggregates, flocs, and granules. There is a quite arbitrary borderline between attached growth in the form of a biofilm of macroscopic dimensions and free-floating assemblages of only a few aggregated microbes. In ecological terms, this border is given by the quality of the environment: aggregation will cause a difference for the individual cell as soon as solute gradients and, thus, a different *local environment* develop. Transport of solutes by diffusion is very fast on the size scale of a microbial cell (38). An individual cell, or even a group of cells will not create a local gradient in the substrate or product concentration. When initial attachment to a surface is stimulated by certain environmental conditions (55), cells multiply and form microcolonies. After a critical size is exceeded, local solute concentrations will be affected. The problem of this critical size has been discussed, e.g., in conjunction with the occurrence of anoxic microenvironments in marine microbial aggregates (59) and activated sludge flocs (74). With the process of aggregation, the microorganisms have an effect on their local environment, thus actively creating "customized microniches" (12). Experiments in microbial ecology of biofilms therefore have to consider the scale of the environment of the target organisms, which is a *microscale*. Many studies in engineered and environmental ecosystems relate the detected aspects of microbial diversity and distribution in a biofilm to macroscopically measured parameters. The multitude of potential microenvironments within a biofilm are handled as a black box, or are included by theoretical considerations or modelling. However, experimental investigation of the microenvironment might reveal valuable information and can give insights into the ecology of the single microbial cell or population in a biofilm. Therefore, methods to address the environment of populations in a biofilm have to cope with the microscale.

### 3.2 Approaching functions on a microscale: Application of microsensors

#### *Microsensor types*

Methods for measurements on a microscale should have some important characteristics: high resolution, minimal disturbance of the microenvironment, and applicability *in situ*. New procedures which fulfill these needs strongly evolved during the last two decades. With respect to the microenvironment and the activity of microbial communities on a microscale, electrochemical and optical microsensors were adopted to the field of microbial ecology. Two types of microsensors have been mainly used in the present thesis: (i) an amperometric microelectrode for oxygen (65), and (ii) potentiometric ion-selective microelectrodes for ammonium, nitrite, nitrate, and pH (18, 21). These microelectrodes have tip diameters of 5 to 15  $\mu\text{m}$ , show a high sensitivity (usually less than  $1 \mu\text{mol l}^{-1}$ ), and have response times in the order of seconds (Fig. 7). Their dimensions allow measurements on a microscale, i.e., with a step size as small as 25  $\mu\text{m}$  and even less. However, as the transport efficiency of diffusion on short distances is very high (38), concentration differences along shorter distances caused by local activity will become small to nonexistent revealing no additional information.

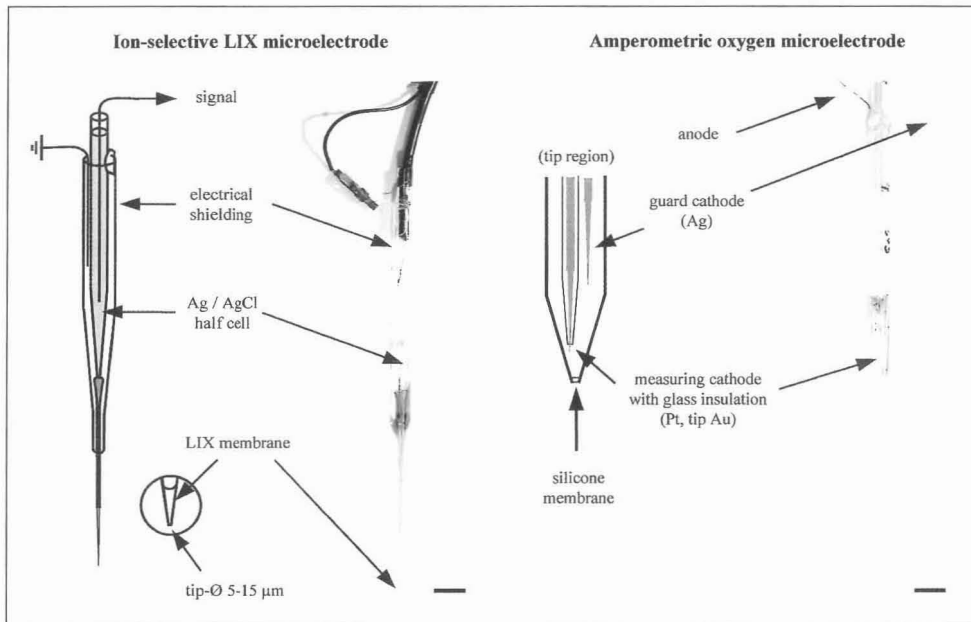


FIG. 7. Types of microelectrode applied in the biofilm studies: Ion-selective microelectrodes for ammonium, nitrite, nitrate, and pH (18), and amperometric oxygen microelectrodes (65). Scale bar is 1 cm.

*Microprofiles and functional informations*

The liquid above the biofilm is typically well mixed. With decreasing distance to the biofilm surface, the liquid layer becomes gradually stagnant. Transport of solutes out of and into the biofilm through this diffusive boundary layer (DBL) and within impermeable areas of the biofilm is driven by diffusion. Steady state microprofiles are interpreted with a one-dimensional diffusion-reaction model (66). Each depth-concentration point in a profile is assumed to reflect the result of two processes: transport and conversion of the respective solute. Solute transport towards or away from each point is driven by diffusion as described by Fick's first law:

$$J = D_o \frac{\partial c(x)}{\partial z} \quad [4]$$

with  $J$ : flux in [ $\mu\text{mol cm}^{-2} \text{ h}^{-1}$ ],  $D_o$ : molecular diffusion coefficient in water in [ $\text{cm}^2 \text{ h}^{-1}$ ],  $c$ : solute concentration in [ $\mu\text{mol cm}^{-3}$ ], and  $z$ : depth in [cm]. For the calculation of fluxes within the biofilm matrix, the molecular diffusion coefficient  $D_o$  has to be replaced by the apparent diffusion coefficient,  $D_{\text{eff}}$ , which accounts for tortuosity and porosity of the biofilm matrix (6). The flux through a certain area is then proportional to the local concentration gradient. Changes of solute concentration with time by diffusional transport are described by Fick's second law of diffusion. In steady state, the concentration change with time is zero, and the conversion rate in a given layer equals the diffusive transport:

$$r = -D_{\text{eff}} \frac{\partial^2 c(z, t)}{\partial z^2} \quad [5]$$

with  $r$ : volumetric conversion rate in [ $\mu\text{mol cm}^{-3} \text{ h}^{-1}$ ],  $D_{\text{eff}}$ : apparent diffusion coefficient in [ $\text{cm}^2 \text{ h}^{-1}$ ], and  $t$ : time in [h]. This model is simplified in that it assumes an equal diffusion coefficient throughout the biofilm, and zero or first order kinetics of the conversion reaction.

Typical informations that can be obtained from microprofiles are: (i) diffusive solute fluxes into or out of the biofilm calculated from the linear concentration gradient in the diffusive boundary layer; (ii) local production or consumption rates derived from the shape (curvature) of the profile within the biofilm; (iii) distribution and penetration depth of solutes, which visualizes the separation of different layers (e.g., oxic vs. anoxic horizons); and (iv) local irregularities as channels and voids with advective solute transport if these structures are large enough to cause a concentration gradient (see above). Results of (i) and (ii) are of prime interest since these rates represent the activity of the whole biofilm (fluxes or areal rates in

[ $\mu\text{mol cm}^{-2} \text{ h}^{-1}$ ]) or of local distinct horizons inside (volumetric rates in [ $\mu\text{mol cm}^{-3} \text{ h}^{-1}$ ]), respectively.

The term  $\partial^2 c(z,t)/\partial z^2$  in equation [5] represents the curvature of the concentration profile, i.e., the second derivative of the profile. Conversion rates in the biofilm can be calculated by differentiation of the profile in a simple stepwise calculation using adjacent values in the profile (17). The advantages of simplicity and direct use of measured data in this procedure are counterbalanced by a strong effect of noise on the resulting local rates. With increasing derivatives, minor irregularities in profiles typically cause stronger variations. By calculating stepwise rates for every profile and subsequently averaging all values of a certain depth, this noise can partly be reduced. Alternatively, parabolic functions (2<sup>nd</sup> order) can be fitted to different segments of the profile before differentiation. The second derivative of the parabolic function is represented by the coefficient of the quadratic term of the function, which multiplied by  $D_{\text{eff}}$  yields the conversion rate in the segment of the profile. Several more or less sophisticated methods have been described for this fitting procedure (5, 44, 54).

#### 4 The synthesis of structure and function: microbial ecology of biofilms

With the availability of FISH and microsensors both the microbial structure and function of biofilms could be addressed *in situ*.

Following the example of Ramsing et al. (64), who investigated sulfate reducing bacteria in a photosynthetic biofilm with these tools, Schramm et al. were the first who studied nitrification in biofilms (73). They examined a trickling filter biofilm treating wastewater from an aquaculture by use of microsensors for oxygen (65) and biosensors for nitrate (15). These microsensors had been formerly used successfully in other fields of microbial ecology (15, 42). The nitrifying populations were detected by FISH with described probes (91, 92). To maintain the spatial arrangement of the populations, a cryosectioning technique analogous to histological studies was applied. Typical microcolonies of *Nitrosomonas* and *Nitrobacter* (50, 91, 92) were found, most of them in the permanently aerobic upper 50 to 100  $\mu\text{m}$ . Correspondingly, nitrifying activity could be demonstrated near the very surface. The close vicinity of aggregates of both the AOB and the NOB were in agreement with analogous results from activated sludge (50). This arrangement was suggested to optimize the transfer of the intermediate nitrite. As reported earlier for nitrifying microbial granules (22), oxygen limitation

controlled nitrification. Some cell aggregates, however, were found in the anoxic layers of the biofilm, suggesting local presence of oxygen due to heterogeneity (20), anaerobic metabolism (8, 26), or a certain retention of ribosomes in overgrown, inactive cells (51, 71, 91). However, the nitrate biosensor used by Schramm et al. detected both nitrate and nitrite simultaneously. Thus, both metabolisms and especially efficient transfer of the intermediate nitrite could not be separately considered.

The development of a new nitrite microsensor for environmental applications (18) enabled the separate study of both processes. Among others, this sensor was applied in a study of nitrifying flocs from a lab-scale fluidized bed reactor system low in ammonium (72). All solutes involved in nitrification (oxygen, ammonium, nitrite, nitrate, pH) could be measured to characterize the microenvironment of the nitrifying bacteria. Despite a lack of oxygen depletion in the aggregates, again a thin actively nitrifying surface layer of 125  $\mu\text{m}$  was detected. Lack of nitrite accumulation indicated a very efficient internal coupling. In a nested FISH approach, a rather unusual composition of the nitrifying community was reported: members of the genera *Nitrosospira* and *Nitrospira* were found to be the dominating AOB and NOB, respectively. Surprisingly, the dominating AOB was *Nitrosospira* and not a member of the *Nitrosomonas* lineages, that are typically found in wastewater systems (50, 91). In contrast, *Nitrosospira*-like bacteria were detected by PCR-based methods in environments poor in ammonium (33, 40, 80). Schramm et al. assumed that the ammonia oxidation kinetics are different between both genera, suggesting the persistence of either as based on the concept of K and r strategy. The detection of a NOB population related to *Nitrospira* in the aggregates by FISH with newly developed probes was another *in situ* evidence for the importance of *Nitrospira*-like organisms as NOB in sewage treatment systems. In contrast, *Nitrobacter* sp. often could not be detected (39, 56, 71, 72). Microsensor-based rate measurements of both, the ammonia- and nitrite oxidation reactions and direct quantification of cell numbers of AOB and NOB by FISH allowed the determination of  $K_m$  values and cell-specific conversion rates *in situ* (71) for *Nitrosospira* sp. and *Nitrospira* sp. These cell-specific rates of ammonia and nitrite oxidation were found to be around 0.25 and 0.02  $\text{nmol cell}^{-1} \text{h}^{-1}$ , respectively, and correspond to what was found by FISH and theoretical activity considerations for AOB in activated sludge (39, 91). However, values were one to three orders of magnitude below those obtained from pure cultures of AOB and *Nitrobacter* (4, 61). *In situ*  $K_m$  values for the substrates were found around 40  $\mu\text{M}$  ammonium for *Nitrosospira*, and 10  $\mu\text{M}$  nitrite for *Nitrospira* (71), which are markedly low compared to data from pure cultures of *Nitrosomonas* sp. and *Nitrobacter* sp. (61). Based on this *in situ* affinity constants, both populations were suggested to be typical K

strategists. In the absence of pure cultures, this *in situ* data is of high value and demonstrates the potential of combined *in situ* methods.

In contrast to the mixed occurrence of AOB and NOB in the flocs, a spatial separation was reported from an autotrophic nitrifying biofilm investigated by FISH and microsensor measurements (56), and lower growth rates of *Nitrospira* compared to AOB were suggested to explain this finding. While the nitrification rates in this biofilm were lower than those determined in other systems (71, 73), ammonium uptake did not account for the oxidized products released, and, thus, the rates are probably underestimated for this autotrophic biofilm. The nitrifying community was dominated by a *N. europaea*/*N. europaea*-related population, obviously due to enrichment caused by increased concentration of ammonium.

In conclusion, several studies successfully made use of a combination of FISH and microsensor measurements. The results were promising steps towards an *in situ* ecology of nitrifying bacteria. So far, most of these studies, however, focussed on experimental systems on the lab-scale, e.g., a rotating disk reactor (56), a nitrifying fluidized bed reactor (72), a nitrifying/denitrifying membrane reactor (70), or biofilm samples were removed from the original system and studied under artificial experimental conditions (18, 73). Hence, the systems were strongly selective towards a nitrifying functionality, or were exclusively investigated under nitrifying conditions. Both, the AOB and NOB were present mostly with one (56, 71-73) or a few populations (70).

Biotechnological systems of the applied scale, however, often lack the high functional specificity of bench-scale reactors. In sewage treatment, various processes usually coexist, as the removal of carbon, phosphorus, and, via nitrification and subsequent denitrification, nitrogen. Furthermore, the substrate situation is much more complex and less controlled. Efforts to integrate different functions result from a practical interest in saving space for reactors and/or aeration and thereby money in the large-scale application. Under these conditions, nitrifiers are exposed to competition with heterotrophs and other organisms, for oxygen and nutrients, and have to cope with varying environmental conditions. It was the goal of this thesis to get insights into the key factors controlling the distribution and activity of various nitrifying populations in such complex multispecies biofilms by use of the combined approach depicted above. Findings could contribute to our understanding of the microbial ecology of nitrifying bacteria, and, on the long run, also might help in further optimizing sewage treatment techniques.

## Outline of this thesis

The aim of this thesis was to reveal important aspects of the ecology of nitrifying populations in complex biofilms on the applied scale. The composition and activity of nitrifying communities, and the role of competition and interaction should be addressed by combining *in situ* methods adapted to the microscale, like, e.g., microsensor measurements and fluorescence *in situ* hybridization. This combination has been successively used in experimental systems (56, 71-73). At the beginning of this thesis microelectrodes for all important compounds involved in nitrification had been available (18, 65), and a detailed set of several oligonucleotide probes for FISH targeting most described nitrifying bacteria had been described (39, 60, 72).

In the first study (Chapter 2) a nitrifying community in a membrane-grown biofilm with opposed substrate and oxygen gradients was investigated. The biofilm harbored two ammonia-oxidizing and two nitrite-oxidizing populations, related to *N. europaea* and *Nitrosospira sp.*, and to *Nitrobacter sp.* and *Nitrospira sp.*, respectively. The goal of this study was to reveal whether earlier hypotheses on their adaptation to high (*N. europaea*, *Nitrobacter sp.*) or low (*Nitrosospira sp.*, *Nitrospira sp.*) substrate levels based on *in situ* data could be supported by spatial organization and activity of this multispecies nitrifying community.

From a technical point of view, the combination of several nutrient removal processes is of interest. The potential of coexistence of nitrification with a heterotrophic process was addressed in a multifunctional sequencing batch biofilm reactor (SBBR) combining removal of phosphate with nitrification and denitrification (Chapter 3). The study focussed on long-term changes on the reactor- and the microscale associated with increased concentrations of ammonium. The aims were to find out to what extent nitrification could be combined with biological phosphate-removal, and how this affected the presence and microscale activity of the nitrifying populations. The results of this study suggested that competition for oxygen generated a sequential activity of the phosphate-removing and other heterotrophic bacteria, and nitrifiers during the aerated period. Oxygen budgets revealed the significant contribution of nitrification to total oxygen consumption.

In a second study, the nitrifying community and its *in situ* activity in this system were studied in detail. Microsensor analysis was combined with FISH, and cloning, sequencing, and analysis of the 16S rDNA and the *amoA* gene of AOB (Chapter 4). The questions were, which populations of AOB and NOB persisted under these only temporally favorable condi-

tions, which population was active during which part of the process, and how nitrifying activity managed to coexist with heterotrophic activity, especially biological phosphate removal. Whereas cell-specific nitrification rates reached values reported from other nitrifying systems in the final aerated period, the composition of the nitrifying community appeared to be unusually complex in this system.

Was this complexity caused by the combination of the two processes or was it due to the specific transient conditions in a sequencing batch system? Chapter 5 of this thesis presents a study of the role of varying conditions on nitrification during a sequencing batch cycle. A nitrifying biofilm of a pilot-scale SBBR treating ammonium-rich reject water was investigated under different experimental conditions in terms of oxygen and ammonium concentrations. The study revealed a clear N loss under conditions which typically occur in the pilot reactor for long time intervals during operation. The heterogeneous spatial distribution of the various populations of AOB and NOB, however, did not allow to assign distinct roles to the individual populations. This study demonstrated the limitations of this combination of methods in non- or poorly layered microbial communities.

To overcome this limitation and approach nitrification on both, the community as well as the single population/single cell level, a new approach integrating multiple *in situ* methods was used to study the function of a nitrifying model biofilm under various conditions (Chapter 6). Microsensor measurements and FISH were combined with quantitative beta-microimaging and microautoradiography (MAR) to quantify local uptake of carbonate and to assign it to certain populations.

## References

1. **Amann, R., J. Snaird, M. Wagner, W. Ludwig, and K.-H. Schleifer.** 1996. *In situ* visualization of high genetic diversity in a natural microbial community. *J. Bacteriol.* **178**:3496-3500.
2. **Amann, R. I., W. Ludwig, and K.-H. Schleifer.** 1995. Phylogenetic identification and *in situ* detection of individual microbial cells without cultivation. *Microbiol. Rev.* **59**:143-169.
3. **Arthur, J. W., C. W. West, K. N. Allen, and S. F. Hedke.** 1987. Seasonal toxicity of ammonia to five fish and nine invertebrate species. *Bull. Environ. Contam. Toxicol.* **38**:324-331.
4. **Belser, L. W.** 1979. Population ecology of nitrifying bacteria. *Annu. Rev. Microbiol.* **33**:309-333.
5. **Berg, P., N. Risgaard-Petersen, and S. Risgaard.** 1998. Interpretation of measured concentration profiles in sediment pore water. *Limnol. Oceanogr.* **43**:1500-1510.
6. **Beuling, E.** 1998. Mass Transfer Properties of Biofilms. PhD thesis. University of Amsterdam, Amsterdam (NL).
7. **Bock, E., H. P. Koops, B. Ahlers, and H. Harms.** 1992. Oxidation of inorganic nitrogen compounds as energy source, p. 414-430. *In* A. Balows, Trüper, HG, Dworkin, M, Harder, W, Schleifer, K-H (ed.), *The Prokaryotes (A Handbook of the Biology of Bacteria: Ecophysiology, Isolation, Identification, Applications)*, 2nd ed., vol. 1. Springer, New York Berlin Heidelberg.
8. **Bock, E., I. Schmidt, R. Stüven, and D. Zart.** 1995. Nitrogen loss caused by denitrifying *Nitrosomonas* cells using ammonium or hydrogen as electron donors and nitrite as electron acceptor. *Arch. Microbiol.* **163**:16-20.
9. **Brock, T. D.** 1987. The study of microorganisms *in situ*: progress and problems. *Symp. Soc. Gen. Microbiol.* **41**:1-17.
10. **Bryers, J. D., and W. G. Characklis.** 1990. Biofilms in water and wastewater treatment, p. 671-696. *In* W. G. Characklis and K. C. Marshall (eds.), *Biofilms*. John Wiley & Sons, Inc., New York Chichester Brisbane Toronto Singapore.
11. **Costerton, J. W., Z. Lewandowski, D. L. Caldwell, D. R. Korber, and H. M. Lappin-Scott.** 1995. Microbial biofilms. *Annu. Rev. Microbiol.* **49**:711-745.
12. **Costerton, J. W., Z. Lewandowski, D. de Beer, D. Caldwell, D. Korber, and G. James.** 1994. Biofilms, the customized microniche. *J. Bacteriol.* **176**:2137-2142.
13. **Cox, D. J., and M. J. Bazin.** 1980. Distribution of bacteria in a continuous-flow nitrification column. *Soil Biol. Biochem.* **12**:241-246.
14. **Daims, H., P. Nielsen, J. L. Nielsen, S. Juretschko, and M. Wagner.** 2000. Novel *Nitrospira*-like bacteria as dominant nitrite-oxidizers in biofilms from wastewater treatment plants: diversity and *in situ* physiology. *Water Sci. Technol.* **41**:85-90.
15. **Damsgaard, L. R., L. H. Larsen, and N. P. Revsbech.** 1995. Microscale biosensors for environmental monitoring. *Trends Anal. Chem.* **14**:300-303.
16. **de Beer, D.** 1990. Microelectrode studies in biofilms and sediments. PhD thesis. University of Amsterdam, Amsterdam (NL).
17. **de Beer, D.** 2000. Micro-electrodes. *In* R. H. Wijffels (ed.), *Immobilized Cells*. Springer, Heidelberg.

18. **de Beer, D., A. Schramm, C. M. Santegoeds, and M. Kühl.** 1997. A nitrite microsensor for profiling environmental biofilms. *Appl. Environ. Microbiol.* **63**:973-977.
19. **de Beer, D., P. Stoodley, and Z. Lewandowski.** 1994. Liquid flow in heterogeneous biofilms. *Biotechnol. Bioeng.* **44**:636-641.
20. **de Beer, D., P. Stoodley, F. Roe, and Z. Lewandowski.** 1994. Effects of biofilm structures on oxygen distribution and mass transport. *Biotechnol. Bioeng.* **43**:1131-1138.
21. **de Beer, D., and J. C. van den Heuvel.** 1988. Response of ammonium-selective microelectrodes based on the neutral carrier nonactin. *Talanta.* **35**:728-730.
22. **de Beer, D., J. C. van den Heuvel, and S. P. P. Ottengraf.** 1993. Microelectrode measurements of the activity distribution in nitrifying bacterial aggregates. *Appl. Environ. Microbiol.* **59**:573-579.
23. **Ehrich, S., D. Behrens, E. Lebedeva, W. Ludwig, and E. Bock.** 1995. A new obligately chemolithoautotrophic, nitrite-oxidizing bacterium, *Nitrospira moscoviensis* sp. nov. and its phylogenetic relationship. *Arch. Microbiol.* **164**:16-23.
24. **Farrelly, V., F. A. Rainey, and E. Stackebrandt.** 1995. Effect of genome size and *rrn* gene copy number on PCR amplification of 16S rRNA genes from a mixture of bacterial species. *Appl. Environ. Microbiol.* **61**:2798-2801.
25. **Focht, D. D., and W. Verstraete.** 1977. Biochemical ecology of nitrification and denitrification. *Adv. Microb. Ecol.* **1**:135-214.
26. **Freitag, A., M. Rudert, and E. Bock.** 1987. Growth of *Nitrobacter* by dissimilatoric nitrate reduction. *FEMS Microbiol. Lett.* **48**:105-109.
27. **Fuchs, B. M., F. O. Glöckner, J. Wulf, and R. Amann.** 2000. Unlabeled helper oligonucleotides increase the *in situ* accessibility to 16S rRNA fluorescently labeled oligonucleotide probes. *Appl. Environ. Microbiol.* **66**:3603-3607.
28. **Fuchs, B. M., G. Wallner, W. Beisker, I. Schwiippel, W. Ludwig, and R. Amann.** 1998. Flow cytometric analysis of the *in situ* accessibility of *Escherichia coli* 16S rRNA for fluorescently labeled oligonucleotide probes. *Appl. Environ. Microbiol.* **64**:4973-4982.
29. **Hall, G. H.** 1986. Nitrification in lakes, p. 127-156. *In* J. I. Prosser (ed.), *Nitrification*, vol. 20. Society for General Microbiology, Oxford (UK).
30. **Head, I. M., W. D. Hiorns, T. M. Embley, A. J. McCarthy, and J. R. Saunders.** 1993. The phylogeny of autotrophic ammonia-oxidizing bacteria as determined by analysis of 16S ribosomal RNA gene sequences. *J. Gen. Microbiol.* **139**:1147-1153.
31. **Helmer, C., S. Kunst, S. Juretschko, M. C. Schmid, K.-H. Schleifer, and M. Wagner.** 1999. Nitrogen loss in a nitrifying biofilm system. *Water Sci. Technol.* **39**:13-21.
32. **Henrici, A. T.** 1933. Studies of freshwater bacteria. I. A direct microscopic technique. *J. Bacteriol.* **25**:277-287.
33. **Hiorns, W. D., R. C. Hastings, I. M. Head, A. J. McCarthy, and J. R. Saunders.** 1995. Amplification of 16S ribosomal RNA genes of autotrophic ammonia-oxidizing bacteria demonstrates the ubiquity of nitrospiras in the environment. *Microbiology.* **141**:2793-2800.
34. **Hovanec, T. A., L. T. Taylor, A. Blakis, and E. F. Delong.** 1998. *Nitrospira*-like bacteria associated with nitrite oxidation in freshwater aquaria. *Appl. Environ. Microbiol.* **64**:258-264.

35. **Jannasch, H. W., and G. E. Jones.** 1959. Bacterial populations in seawater as determined by different methods of enumeration. *Limnol. Oceanogr.* **4**:128-139.
36. **Jetten, M. S. M., S. Logemann, G. Muyzer, L. A. Robertson, S. de Vries, M. C. M. van Loosdrecht, and J. G. Kuenen.** 1997. Novel principles in the microbial conversion of nitrogen compounds. *Ant. Leeuw.* **71**:75-93.
37. **Jetten, M. S. M., M. Strous, K. T. van de Pas-Schoonen, J. Schalk, U. G. J. M. van Dongen, A. A. van de Graaf, S. Logemann, G. Muyzer, M. C. M. van Loosdrecht, and J. G. Kuenen.** 1999. The anaerobic oxidation of ammonium. *FEMS Microbiol. Rev.* **22**:421-437.
38. **Jørgensen, B. B.** 2000. Life in the diffusive boundary layer, p. 348-373. *In* B. P. Boudreau (ed.), *The Benthic Boundary Layer: Transport Processes and Biogeochemistry*. Oxford University Press, Oxford (UK).
39. **Juretschko, S., G. Timmermann, M. Schmid, K.-H. Schleifer, A. Pommerening-Röser, H. P. Koops, and M. Wagner.** 1998. Combined molecular and conventional analysis of nitrifying bacterium diversity in activated sludge: *Nitrosococcus mobilis* and *Nitrospira*-like bacteria as dominant populations. *Appl. Environ. Microbiol.* **64**:3042-3051.
40. **Kowalchuk, G. A., J. R. Stephen, W. de Boer, J. I. Prosser, T. M. Embley, and J. W. Woldendorp.** 1997. Analysis of ammonia-oxidizing bacteria of the  $\beta$  subdivision of the class proteobacteria in coastal sand dunes by denaturing gradient gel electrophoresis and sequencing of PCR-amplified 16S ribosomal DNA fragments. *Appl. Environ. Microbiol.* **63**:1489-1497.
41. **Kowalchuk, G. A., A. W. Stienstra, H. J. Heilig, J. R. Stephen, and J. W. Woldendorp.** 2000. Molecular analysis of ammonia-oxidising bacteria in soil of successional grasslands of the Drentsche A (The Netherlands). *FEMS Microbiol. Ecol.* **31**:207-215.
42. **Larsen, L. H., N. P. Revsbech, and S. J. Binnerup.** 1996. A microsensor for nitrate based on immobilized denitrifying bacteria. *Appl. Environ. Microbiol.* **62**:1248-1251.
43. **Lengeler, J. W., G. Drews, and H. G. Schlegel.** 1999. *Biology of the Prokaryotes*. Thieme, Stuttgart New York.
44. **Lorenzen, J., L. H. Larsen, T. Kjær, and N. P. Revsbech.** 1998. Biosensor determination of the microscale distribution of nitrate, nitrate assimilation, nitrification, and denitrification in a diatom-inhabited freshwater sediment. *Appl. Environ. Microbiol.* **64**:3264-3269.
45. **Ludwig, W., J. Neumaier, N. Klugbauer, E. Brockmann, C. Roller, S. Jilg, K. Reetz, I. Schachtner, A. Ludvigsen, M. Bachleitner, U. Fischer, and K.-H. Schleifer.** 1993. Phylogenetic relationships of *Bacteria* based on comparative sequence analysis of elongation factor Tu and ATP-synthase  $\beta$ -subunit genes. *Ant. Leeuw.* **64**:285-305.
46. **Madigan, M. T., J. M. Martinko, and J. Parker.** 2000. *Biology of Microorganisms*, 9th ed. Prentice-Hall, Upper Saddle River (NJ, USA).
47. **Maidak, B. L., J. R. Cole, C. T. Parker, G. M. Garrity, N. Larsen, B. Li, T. G. Lilburn, M. J. McCaughey, G. J. Olsen, R. Overbeek, S. Pramanik, T. M. Schmidt, T. J. M., and C. R. Woese.** 1999. A new version of the RDP (Ribosomal Database Project). *Nucleic Acids Res.* **27**:171-173.
48. **Marshall, K. C.** 1984. *Microbial Adhesion and Aggregation*. Springer, Berlin.
49. **McCaig, A. E., T. M. Embley, and J. I. Prosser.** 1994. Molecular analysis of enrichment cultures of marine ammonia oxidizers. *FEMS Microbiol. Lett.* **120**:363-368.

50. **Mobarry, B. K., M. Wagner, V. Urbain, B. E. Rittmann, and D. A. Stahl.** 1996. Phylogenetic probes for analyzing abundance and spatial organization of nitrifying bacteria. *Appl. Environ. Microbiol.* **62**:2156-2162.
51. **Morgenroth, E., A. Obermayer, E. Arnold, A. Brühl, M. Wagner, and P. A. Wilderer.** 2000. Effect of long-term idle periods on the performance of sequencing batch reactors. *Water Sci. Technol.* **41**:105-113.
52. **Mulder, A., A. A. van de Graaf, L. A. Robertson, and J. G. Kuenen.** 1995. Anaerobic ammonium oxidation discovered in a denitrifying fluidized bed reactor. *FEMS Microbiol. Ecol.* **16**:177-184.
53. **Muller, E. B., A. H. Stouthamer, and H. W. van Verseveld.** 1995. Simultaneous NH<sub>3</sub> oxidation and N<sub>2</sub> production at reduced O<sub>2</sub> tensions by sewage sludge subcultured with chemolithotrophic medium. *Biodegradation.* **6**:339-349.
54. **Nielsen, L. P., P. B. Christensen, N. P. Revsbech, and J. Sørensen.** 1990. Denitrification and oxygen respiration in biofilms studied with a microsensor for nitrous oxide and oxygen. *Microb. Ecol.* **19**:63-72.
55. **O'Toole, G., H. B. Kaplan, and R. B. Kolter.** 2000. Biofilm formation as microbial development. *Annu. Rev. Microbiol.* **54**:49-79.
56. **Okabe, S., H. Satoh, and Y. Watanabe.** 1999. *In situ* analysis of nitrifying biofilms as determined by *in situ* hybridization and the use of microelectrodes. *Appl. Environ. Microbiol.* **65**:3182-3191.
57. **Olsen, G. J., D. J. Lane, S. J. Giovannoni, N. R. Pace, and D. A. Stahl.** 1986. Microbial ecology and evolution: a ribosomal RNA approach. *Annu. Rev. Microbiol.* **40**:337-365.
58. **Painter, H. A.** 1986. Nitrification in the treatment of sewage and wastewaters. *Spec. Publ. Soc. Gen. Microbiol.* **20**:185-213.
59. **Ploug, H., M. Kühl, B. Buchholz-Cleven, and B. B. Jørgensen.** 1997. Anoxic aggregates - an ephemeral phenomenon in the pelagic environment? *Aquat. Microb. Ecol.* **13**:285-294.
60. **Pommerening-Röser, A., G. Rath, and H.-P. Koops.** 1996. Phylogenetic diversity within the genus *Nitrosomonas*. *Syst. Appl. Microbiol.* **19**:344-351.
61. **Prosser, J. I.** 1989. Autotrophic nitrification in bacteria. *Adv. Microb. Physiol.* **30**:125-181.
62. **Prosser, J. I.** 1986. Nitrification, vol. 20. Society for General Microbiology, Oxford (UK).
63. **Purkhold, U., A. Pommerening-Röser, S. Juretschko, M. C. Schmid, H.-P. Koops, and M. Wagner.** 2000. Phylogeny of all recognized species of ammonia-oxidizers based on comparative 16S rRNA and *amoA* sequence analysis: Implications for molecular diversity surveys. *Appl. Environ. Microbiol.* **66**:5368-5382.
64. **Ramsing, N. B., M. Kühl, and B. B. Jørgensen.** 1993. Distribution of sulfate-reducing bacteria, O<sub>2</sub>, and H<sub>2</sub>S in photosynthetic biofilms determined by oligonucleotide probes and microelectrodes. *Appl. Environ. Microbiol.* **59**:3840-3849.
65. **Revsbech, N. P.** 1989. An oxygen microelectrode with a guard cathode. *Limnol. Oceanogr.* **34**:474-478.
66. **Revsbech, N. P., and B. B. Jørgensen.** 1986. Microelectrodes: their use in microbial ecology. *Adv. Microb. Ecol.* **9**:293-352.

67. **Rotthauwe, J.-H., K.-P. Witzel, and W. Liesack.** 1997. The ammonia monoxygenase structural gene *amoA* as a functional marker: molecular fine-scale analysis of natural ammonia-oxidizing populations. *Appl. Environ. Microbiol.* **63**:4704-4712.
68. **Schmid, M., U. Twachtmann, M. Klein, M. Strous, S. Juretschko, M. S. M. Jetten, J. W. Metzger, K.-H. Schleifer, and M. Wagner.** 2000. Molecular evidence for genus level diversity of bacteria capable of catalyzing anaerobic ammonium oxidation. *Syst. Appl. Microbiol.* **23**:93-106.
69. **Schmidt, I., and E. Bock.** 1997. Anaerobic ammonia oxidation with nitrogen dioxide by *Nitrosomonas eutropha*. *Arch. Microbiol.* **167**:106-111.
70. **Schramm, A., D. de Beer, A. Gieseke, and R. Amann.** 2000. Microenvironments and distribution of nitrifying bacteria in a membrane-bound biofilm. *Environ. Microbiol.* **2**:680-686.
71. **Schramm, A., D. de Beer, J. C. van den Heuvel, S. Ottengraf, and R. Amann.** 1999. Microscale distribution of populations and activities of *Nitrosospira* and *Nitospira* spp. along a macroscale gradient in a nitrifying bioreactor: Quantification by *in situ* hybridization and the use of microsensors. *Appl. Environ. Microbiol.* **65**:3690-3696.
72. **Schramm, A., D. de Beer, M. Wagner, and R. Amann.** 1998. Identification and activities *in situ* of *Nitrosospira* and *Nitospira* spp. as dominant populations in a nitrifying fluidized bed reactor. *Appl. Environ. Microbiol.* **64**:3480-3485.
73. **Schramm, A., L. H. Larsen, N. P. Revsbech, N. B. Ramsing, R. Amann, and K.-H. Schleifer.** 1996. Structure and function of a nitrifying biofilm as determined by *in situ* hybridization and the use of microelectrodes. *Appl. Environ. Microbiol.* **62**:4641-4647.
74. **Schramm, A., C. M. Santegoeds, H. K. Nielsen, H. Ploug, M. Wagner, M. Pribyl, J. Wanner, R. Amann, and D. de Beer.** 1999. On the occurrence of anoxic microniches, denitrification, and sulfate reduction in aerated activated sludge. *Appl. Environ. Microbiol.* **65**:4189-4196.
75. **Siegrist, H., S. Reithaar, G. Koch, and P. Lais.** 1998. Nitrogen loss in a nitrifying rotating contactor treating ammonium-rich wastewater without organic carbon. *Water Sci. Technol.* **38**:241-248.
76. **Speksnijder, A., G. Kowalchuk, K. Roest, and H. Laanbroek.** 1998. Recovery of a *Nitrosomonas*-like 16S rDNA sequence group from freshwater habitats. *Syst. Appl. Microbiol.* **21**:321-330.
77. **Stahl, D. A., and R. Amann.** 1991. Development and application of nucleic acid probes, p. 205-248. *In* E. Stackebrandt and M. Goodfellow (eds.), *Nucleic Acid Techniques in Bacterial Systematics*. John Wiley & Sons Ltd., Chichester (UK).
78. **Staley, J. T., and A. Konopka.** 1985. Measurement of *in situ* activities of nonphotosynthetic microorganisms in aquatic and terrestrial habitats. *Annu. Rev. Microbiol.* **39**:321-346.
79. **Stehr, G., B. Böttcher, P. Dittberner, G. Rath, and H. P. Koops.** 1995. The ammonia-oxidizing nitrifying population of the river Elbe estuary. *FEMS Microbiol. Ecol.* **17**:177-186.
80. **Stephen, J. R., A. E. McCaig, Z. Smith, J. I. Prosser, and T. M. Embley.** 1996. Molecular diversity of soil and marine 16S rRNA gene sequences related to  $\beta$ -subgroup ammonia-oxidizing bacteria. *Appl. Environ. Microbiol.* **62**:4147-4154.
81. **Stoodley, P., D. de Beer, and Z. Lewandowski.** 1994. Liquid flow in biofilm systems. *Appl. Environ. Microbiol.* **60**:2711-2716.

82. **Strous, M., J. A. Fuerst, E. H. M. Kramer, S. Logemann, G. Muyzer, K. T. van de Pas-Schoonen, R. Webb, J. G. Kuenen, and M. S. M. Jetten.** 1999. Missing lithotroph identified as new planctomycete. *Nature*. **400**:446-449.
83. **Suwa, Y., T. Sumino, and K. Noto.** 1997. Phylogenetic relationships of activated sludge isolates of ammonia oxidizers with different sensitivities to ammonium sulfate. *J. Gen. Appl. Microbiol.* **43**:373-379.
84. **Suzuki, M. T., and S. J. Giovannoni.** 1996. Bias caused by template annealing in the amplification of mixtures of 16S rRNA genes by PCR. *Appl. Environ. Microbiol.* **62**:625-630.
85. **Teske, A., E. Alm, J. M. Regan, S. Toze, B. E. Rittmann, and D. A. Stahl.** 1994. Evolutionary relationships among ammonia- and nitrite-oxidizing bacteria. *J. Bacteriol.* **176**:6623-6630.
86. **Utåker, J. B., L. Bakken, Q. Q. Jiang, and I. F. Nes.** 1995. Phylogenetic analysis of seven new isolates of ammonia-oxidizing bacteria based on 16S rRNA gene sequences. *Syst. Appl. Microbiol.* **18**:549-559.
87. **Utåker, J. B., and I. F. Nes.** 1998. A qualitative evaluation of the published oligonucleotides specific for the 16S rRNA gene sequences of the ammonia-oxidizing bacteria. *Syst. Appl. Microbiol.* **21**:72-88.
88. **van de Graaf, A. A., P. de Bruijn, L. A. Robertson, M. S. M. Jetten, and J. G. Kuenen.** 1997. Metabolic pathway of anaerobic ammonium oxidation on the basis of <sup>15</sup>N studies in a fluidized bed reactor. *Microbiology*. **143**:2415-2421.
89. **van de Graaf, A. A., A. Mulder, P. de Bruijn, M. S. M. Jetten, L. A. Robertson, and J. G. Kuenen.** 1995. Anaerobic oxidation of ammonium is a biologically mediated process. *Appl. Environ. Microbiol.* **61**:1246-1251.
90. **Wagner, M., R. Amann, H. Lemmer, and K.-H. Schleifer.** 1993. Probing activated sludge with *Proteobacteria*-specific oligonucleotides: inadequacy of culture-dependent methods for describing microbial community structure. *Appl. Environ. Microbiol.* **59**:1520-1525.
91. **Wagner, M., G. Rath, R. Amann, H. P. Koops, and K.-H. Schleifer.** 1995. *In situ* identification of ammonia-oxidizing bacteria. *Syst. Appl. Microbiol.* **18**:251-264.
92. **Wagner, M., G. Rath, H. P. Koops, J. Flood, and R. Amann.** 1996. *In situ* analysis of nitrifying bacteria in sewage treatment plants. *Water Sci. Technol.* **34**:237-244.
93. **Ward, D. M.** 1989. Molecular probes for analysis of microbial communities, p. 145-163. *In* W. G. Characklis and P. A. Wilderer (eds.), *Structure and Function of Biofilms*. John Wiley & Sons, Chichester.
94. **Watson, S. W., E. Bock, F. W. Valois, J. B. Waterbury, and U. Schlosser.** 1986. *Nitrospira marina* gen. nov. sp. nov.: a chemolithotrophic nitrite-oxidizing bacterium. *Arch. Microbiol.* **144**:1-7.
95. **Whitby, C. B., J. R. Saunders, J. Rodriguez, R. W. Pickup, and A. McCarthy.** 1999. Phylogenetic differentiation of two closely related *Nitrosomonas* spp. that inhabit different sediment environments in an oligotrophic freshwater lake. *Appl. Environ. Microbiol.* **65**:4855-4862.
96. **Wimpenny, J. W. T., and R. Colasanti.** 1997. A unifying hypothesis for the structure of microbial biofilms based on cellular automaton models. *FEMS Microbiol. Ecol.* **22**:1-16.
97. **Winogradsky, S.** 1890. Recherches sur les organismes de la nitrification. *Ann. Inst. Pasteur.* **4**:257-275.
98. **Woese, C. R.** 1987. Bacterial evolution. *Microbiol. Rev.* **51**:221-271.
99. **ZoBell, C.** 1943. The effect of solid surfaces upon bacterial activity. *J. Bacteriol.* **46**:39-56.



## **Chapter 2**

### **Microenvironments and Distribution of Nitrifying Bacteria in a Membrane-Bound Biofilm**

A. Schramm, D. de Beer, A. Gieseke, and R. Amann



## Microenvironments and Distribution of Nitrifying Bacteria in a Membrane-Bound Biofilm

Andreas Schramm<sup>1,2\*</sup>, Dirk de Beer<sup>1</sup>, Armin Gieseke<sup>1</sup>,  
and Rudolf Amann<sup>1</sup>

Max Planck Institute for Marine Microbiology, D-28359 Bremen, Germany<sup>1</sup>  
Department of Ecological Microbiology, BITOEK, University of Bayreuth,  
D-95440 Bayreuth, Germany<sup>2</sup>

The distribution of nitrifying bacteria of the genera *Nitrosomonas*, *Nitrosospira*, *Nitrobacter*, and *Nitrospira* was investigated in a membrane-bound biofilm system with opposed supply of oxygen and ammonium. Gradients of oxygen, pH, nitrite and nitrate were determined by means of microsensors while the nitrifying populations along these gradients were identified and quantified using fluorescence *in situ* hybridization in combination with confocal laser scanning microscopy. The oxic part of the biofilm which was subjected to high ammonium and nitrite concentrations was dominated by *Nitrosomonas europaea*-like ammonia oxidizers and by members of the genus *Nitrobacter*. Cell numbers of *Nitrosospira* sp. were 1-2 orders of magnitude lower than those of *Nitrosomonas europaea*. *Nitrospira* sp. were virtually absent in this part of the biofilm whereas they were most abundant at the oxic-anoxic interface. In the totally anoxic part of the biofilm cell numbers of all nitrifiers were relatively low. These observations support the hypothesis that *Nitrosomonas europaea* and *Nitrobacter* sp. can out-compete *Nitrosospira* and *Nitrospira* sp. at high substrate and oxygen concentrations. Additionally, they suggest microaerophilic behaviour of yet uncultured *Nitrospira* sp. as a factor of its environmental competitiveness.

### INTRODUCTION

Nitrifying bacteria which participate in the nitrogen cycle by the successive oxidation of ammonium via nitrite to nitrate have been intensively studied for years using *Nitrosomonas europaea* (Koops and Möller, 1992) and *Nitrobacter* sp. (Bock and Koops, 1992) as model organisms (Prosser, 1989; Laanbroek and Woldendorp, 1995). However, recent data obtained by molecular techniques show that yet uncultured ammonia- and nitrite-oxidizers of the

genera *Nitrosospira* (Hiorns *et al.*, 1995; Stephen *et al.*, 1996; Kowalchuk *et al.*, 1997) and *Nitrospira* (Burrell *et al.*, 1998; Hovanec *et al.*, 1998; Juretschko *et al.*, 1998; Schramm *et al.*, 1998; Okabe *et al.*, 1999) also frequently occur in the environment. What are the environmental factors that select for certain nitrifying populations in nature? This is a challenging question considering that many strains so far rejected cultivation. In the absence of pure cultures to study their ecophysiology, one might detect nitrifying bacteria in a cultivation-independent way in various habitats based on their 16S rDNA sequences and relate this to data of some important environmental factors like pH, nitrogen or oxygen concentrations (Kowalchuk *et al.*, 1997; Hastings *et al.*, 1998; Princic *et al.*, 1998). However, due to the occurrence of chemical microgradients and microniches in soil, sediment or biofilms, the information derived from such correlations is rather indirect and therefore limited. More direct information about microenvironments and distribution of nitrifying bacteria can be obtained by the combined use of microsensors and fluorescence *in situ* hybridization (FISH), as already previously demonstrated for biofilms (Schramm *et al.*, 1996; Schramm *et al.*, 1998; Okabe *et al.*, 1999). Recently, even the *in situ* kinetics of uncultured nitrifying bacteria have been estimated by this approach (Schramm *et al.*, 1999). Based upon these results, it was hypothesized that members of the *Nitrosomonas europaea*-lineage (Pommerening-Röser *et al.*, 1996) and *Nitrobacter* sp. could out-compete *Nitrosospira* sp. and *Nitrospira* sp. in habitats with high substrate concentrations due to their higher maximum growth rates whereas *Nitrosospira* sp. and *Nitrospira* sp. were better competitors in low-substrate environments as a result of their lower  $K_M$  values (Schramm *et al.*, 1999). The goal of this study was to test this hypothesis in a gradient system (Thomas and Wimpenny, 1992) containing these four genera of nitrifying bacteria. The distribution of the different nitrifiers (as shown by FISH) along chemical gradients (measured by microsensors) should yield information about their ecological adaptations if monitored over a longer time period, e.g. during the initial succession of the biofilm. A nitrifying pilot reactor (Özoguz, 1997) has recently been shown to exhibit microgradients of oxygen, nitrite, and nitrate within the biofilm (de Beer *et al.*, 1997) and to contain a diverse nitrifying community, i.e. *Nitrosomonas* sp., *Nitrosospira* sp., *Nitrobacter* sp. and *Nitrospira* sp. (de Beer and Schramm, 1999). In this reactor, the biofilm was supplied with oxygen via a gas-permeable membrane (the biofilm substratum) while ammonium was provided from the bulk water. The concept of separating oxygen supply from substrate supply in order to enhance nitrification and to enable simultaneous nitrification-denitrification in biofilms, has been reported previously

(Timberlake *et al.*, 1988). To facilitate microsensor measurements directly in the reactor and to enable multiple samplings for FISH analysis, a similar lab-scale system was set up for this study.

## EXPERIMENTAL PROCEDURES

**Biofilm reactor operation.** Design and performance of the pilot membrane reactor have been described previously (Özoguz, 1997). To facilitate biofilm sampling and true *in situ* microsensor measurements a slightly modified lab-scale reactor was established and inoculated with material from the pilot plant. Pieces of silicon tubing were mounted as substratum perpendicular to the flow in the lumen of a Plexiglas pipe. Above each tubing an opening in the pipe that was sealed with a rubber stopper during normal reactor operation enabled the insertion of microsensors. The model system had a volume of 20.8 l, a recirculation rate of 900 l h<sup>-1</sup>, and artificial wastewater lacking organic carbon (K<sub>2</sub>HPO<sub>4</sub> 0.14 g l<sup>-1</sup>, MgSO<sub>4</sub> 0.17 g l<sup>-1</sup>, (NH<sub>4</sub>)<sub>2</sub>SO<sub>4</sub> 1.32 g l<sup>-1</sup>, H<sub>3</sub>BO<sub>3</sub> 2 mg l<sup>-1</sup>, MnCl 1.25 mg l<sup>-1</sup>, Na<sub>2</sub>MoO<sub>4</sub> 0.27 mg l<sup>-1</sup>, ZnSO<sub>4</sub> 0.15 mg l<sup>-1</sup>, CuSO<sub>4</sub> 0.06 mg l<sup>-1</sup>, Co(NO<sub>3</sub>)<sub>2</sub> 0.035 mg l<sup>-1</sup>) was added at a rate of 5 l h<sup>-1</sup> to a conditioning vessel connected to the recirculation system. Oxygen was supplied by pumping pressurized air (3 bar) through the silicone tubing, temperature was kept at 28°C, pH was adjusted to 7.8, and the conditioning vessel was flushed with dinitrogen gas during start-up to prevent biofilm growth apart from the O<sub>2</sub>-supplying membrane. Occasionally, NH<sub>4</sub><sup>+</sup>, NO<sub>2</sub><sup>-</sup>, and NO<sub>3</sub><sup>-</sup> in the bulk water were determined by routine chemical analysis (LCK 303, 341, and 339, Dr. Lange, Düsseldorf, Germany). Oxygen and pH were monitored continuously in the conditioning vessel by macroelectrodes (WTW, Weilheim, Germany).

**Microsensor measurements.** Clark-type microsensors for O<sub>2</sub> (Revsbech, 1989), and liquid ion-exchanging membrane (LIX) microsensors for pH, NH<sub>4</sub><sup>+</sup>, NO<sub>2</sub><sup>-</sup>, and NO<sub>3</sub><sup>-</sup> (de Beer *et al.*, 1997) were prepared and calibrated as described previously. Tip diameters were <10 µm for O<sub>2</sub>, 5 µm for pH, NH<sub>4</sub><sup>+</sup> and NO<sub>3</sub><sup>-</sup>, and 15 µm for NO<sub>2</sub><sup>-</sup> microsensors. LIX microsensors were connected to a millivoltmeter, and the potential was recorded relative to a calomel reference electrode (Radiometer, Denmark), while O<sub>2</sub> sensors were connected to a picoamperemeter with internal polarisation unit. Microprofiles in the biofilm were recorded 5, 10, and 14 weeks after start-up of the lab-scale reactor. Measurements were done directly in the running reactor by inserting the microsensors through openings in the reactor pipe (de Beer *et al.*,

1997). The spatial resolution of the measurements was 50  $\mu\text{m}$  as controlled by a micromanipulator, and the profiles were read on a strip chart recorder. For each parameter at least ten profiles were measured at different sites in the biofilm for each measuring day. As the detection of the biofilm surface in the reactor proved difficult, the different profiles were aligned with respect to the biofilm base: the silicone membrane was easily recognized either by disappearance of signal (for LIX sensors as they lost electric contact to the reference electrode) or by a perfectly linear profile within the silicone membrane (for oxygen sensors).

**Biofilm preparation.** After the microsensors measurements, part of the tubing with the attached biofilm was sampled and immediately fixed in paraformaldehyde solution (4% w/v) for 60 min at 4°C (Amann *et al.*, 1990). The sample was washed in phosphate buffered saline, embedded over night in OCT compound (Tissue-Tek II, Miles, Elkhart, Ind.) and frozen in a cryomicrotome at -35°C as described previously (Schramm *et al.*, 1998). When frozen, it was possible to cut the tubing with the biofilm into two longitudinal sections by use of a scalpel and to remove the embedded biofilm material from the tubing without losses (Yu *et al.*, 1994; Schramm *et al.*, 1996). The biofilm was then mounted with OCT compound to the object holder of the cryomicrotome. Sections of 14  $\mu\text{m}$  thickness were made at a temperature of -17°C perpendicular to the biofilm surface (Schramm *et al.*, 1998), and immobilized on gelatine-coated microscopic slides (Amann *et al.*, 1990).

**Fluorescence *in situ* hybridization.** The sequences of all oligonucleotide probes used in this study, their target organisms, hybridization conditions, and references are given in Table 1. Probes were synthesized and fluorescently labelled with the hydrophilic sulfoindocyanine dyes CY3 or CY5 at the 5' end by Interactiva Biotechnologie GmbH (Ulm, Germany). *In situ* hybridization of dehydrated biofilm sections was carried out at 46°C in an isotonicity equilibrated humidity chamber according to the protocol of Amann *et al.* (Amann *et al.*, 1990). Stringent hybridization conditions for the different oligonucleotide probes were adjusted using the formamide and sodium chloride concentrations listed in Table 1 in the hybridization and washing buffers, respectively (Manz *et al.*, 1992). Double-hybridizations with two probes that require different stringencies (e.g. NSR826+NSR1156) were done as subsequent hybridizations starting with the probe of higher dissociation temperature.

The nitrifying populations were quantified using confocal laser scanning microscopy (LSM 510, Carl Zeiss, Jena, Germany) and image analysis as described in detail by Schramm *et al.* (1999). Shortly, threshold values were defined to exclude background fluorescence and the probe-positive cell area was quantified. This procedure was calibrated by comparative cell

counts, and the results were expressed as cells per volume. Each 50  $\mu\text{m}$ -layer of the biofilm, starting at the membrane, was quantified separately.

TABLE 1. Oligonucleotide probes.

Probe	Specificity	Sequence (5'-3') of probe	Target site <sup>a</sup> (rRNA positions)	%FA <sup>b</sup>	mM NaCl <sup>c</sup>	Reference
EUB338	<i>Bacteria</i>	GCTGCCTCCCGTAGGAGT	16S, 338-355	20	225	Amann <i>et al.</i> , 1990
NON	non-binding control	ACTCCTACGGGAGGCAGC	-	20	225	Manz <i>et al.</i> , 1992
NSO1225	ammonia-oxidizing $\beta$ -proteobacteria	CGCCATTGTATTACGTGTGA	16S, 1225-1244	35	80	Mobarry <i>et al.</i> , 1996
NSO190	ammonia-oxidizing $\beta$ -proteobacteria	CGATCCCCTGCTTTCTCC	16S, 190-208	55	20	Mobarry <i>et al.</i> , 1996
NSV443	<i>Nitrosospora</i> spp.	CCGTGACCGTTTCGTTCCG	16S, 444-462	30	112	Mobarry <i>et al.</i> , 1996
NSM156	<i>Nitrosomonas</i> spp.	TATTAGCACATCTTCGAT	16S, 156-174	5	636	Mobarry <i>et al.</i> , 1996
NEU23a	<i>Nitrosomonas europaea</i> -lineage	CCCCTCTGCTGCACTCTA	16S, 653-670	40	56	Wagner <i>et al.</i> , 1995
CTE	unlabelled competitor for NEU23a	TTCATCCCCCTCTGCCG	16S, 659-676	40	56	Wagner <i>et al.</i> , 1995
Nse1472 <sup>d</sup>	<i>N. europaea</i> , <i>N. eutropha</i> , <i>N. halophila</i>	ACCCAGTCATGACCCCC	16S, 1472-1489	50	28	Juretschko <i>et al.</i> , 1998
NmV	<i>Nitrosococcus mobilis</i>	TCCTCAGAGACTACGCGG	16S, 174-191	35	80	Juretschko <i>et al.</i> , 1998
NIT3	<i>Nitrobacter</i> spp.	CCTGTGCTCCATGCTCCG	16S, 1035-1048	40	56	Wagner <i>et al.</i> , 1996
cNIT3	unlabelled competitor for NIT3	CCTGTGCTCCAGGCTCCG	16S, 1035-1048	40	56	Wagner <i>et al.</i> , 1996
NSR826	freshwater <i>Nitrosospora</i> spp.	GTAACCCGCGACACTTA	16S, 826-843	20	225	Schramm <i>et al.</i> , 1998
NSR1156	freshwater <i>Nitrosospora</i> spp.	CCCCTCTCTCTGGGCAGT	16S, 1156-1173	30	112	Schramm <i>et al.</i> , 1998

<sup>a</sup> *E. coli* numbering (Brosius *et al.*, 1981)

<sup>b</sup> conc. formamide in the hybridization buffer

<sup>c</sup> conc. sodium chloride in the washing buffer

<sup>d</sup> published as S-<sup>\*</sup>-Nse-1472-a-A-18

## RESULTS AND DISCUSSION

**Biofilm development.** With the start-up of the lab-scale biofilm reactor,  $\text{NH}_4^+$  concentrations in the bulk water decreased while  $\text{NO}_2^-$  and  $\text{NO}_3^-$  concentrations fluctuated but constantly increased, with the concentration of  $\text{NO}_2^-$  always exceeding that of  $\text{NO}_3^-$ . After 5 weeks, the biofilm had grown to a thickness of about 300  $\mu\text{m}$ . Microsensor measurements revealed  $\text{O}_2$  concentrations of about 220  $\mu\text{M}$  directly at the membrane (the biofilm base) and around the detection limit at the biofilm surface.  $\text{NO}_2^-$  and  $\text{NO}_3^-$  concentrations were 220 and 210  $\mu\text{M}$  at the membrane and decreased to 105 and 75  $\mu\text{M}$  at the biofilm surface, respectively. Ammonium was shown to penetrate the whole biofilm during the succession experiment (week 5 to 14) at concentrations of 15-20 mM and was slightly decreasing from the biofilm surface towards the membrane. However, the resolution of the LIX microsensor in this concentration range was not high enough to record more accurate profiles. The combined microsensor results indicate an oxic, nitrifying zone of about 200  $\mu\text{m}$  thickness directly at the membrane, with ammonia-oxidation rates exceeding nitrite-oxidation rates. FISH analysis showed the occurrence of all four investigated genera of nitrifiers but a clear dominance of

*Nitrosomonas europaea*-like ammonia oxidizers ( $3.7 \times 10^{10}$  to  $1.8 \times 10^{11}$  cells  $\text{cm}^{-3}$ ) over *Nitrospira* sp. ( $1.7 \times 10^9$  to  $7.6 \times 10^9$  cells  $\text{cm}^{-3}$ ) within the first 100  $\mu\text{m}$  at the membrane. Nitrite-oxidizers (*Nitrobacter* sp. and *Nitrospira* sp.) were found in lower numbers ( $8.6 \times 10^7$  to  $2.4 \times 10^{10}$  cells  $\text{cm}^{-3}$ ) with no preference for a certain zone in the biofilm or for one of the two populations. As ammonia-oxidizing bacteria catalyze the first reaction of a two-step process and are faster growing than nitrite-oxidizing bacteria (Bock *et al.*, 1986; Prosser, 1989), dominance of ammonia oxidizers and accumulation of  $\text{NO}_2^-$  is to be expected for the start-up phase of a nitrifying bioreactor. In week 10, the biofilm thickness had increased to about 600  $\mu\text{m}$ . Microprofiles followed a similar trend as in week 5, and a stratification of the nitrifying community became evident (see below). From week 10 to 14, neither bulk water measurements (data not shown), microprofiles, nor the community structure of nitrifying bacteria showed any significant change (see below). Although the continuous accumulation of nitrite indicated that the system had not yet reached a steady state situation the chemical gradients were very similar over at least 9 weeks. Stratification and community structure of nitrifying bacteria, that were stable from week 10 to 14, are therefore assumed to be a result of the conditions prevailing in the biofilm during the succession.

**Microprofiles in weeks 10 and 14.** The concentration profiles of week 10 and 14 were very similar for all compounds measured, and the heterogeneity at one week was usually in the same range as the differences between the two weeks. Oxygen penetrated the biofilm up to 150 - 250  $\mu\text{m}$  distance from the membrane, with mean values of  $188 \pm 35$   $\mu\text{M}$  (week 10) and  $168 \pm 48$   $\mu\text{M}$  (week 14) directly at the membrane. pH decreased in week 10 from 7.6 at the biofilm surface to 7.0 at the membrane while the respective values were 7.8 and 6.4 in week 14. Ammonium was always in the range of 15 - 20 mM. In week 10, the concentrations of nitrate increased from  $90 \pm 8$   $\mu\text{M}$  (week 10) to  $77 \pm 38$   $\mu\text{M}$  (week 14) at the biofilm surface to  $262 \pm 93$   $\mu\text{M}$  (week 10) to  $389 \pm 157$   $\mu\text{M}$  (week 14) at the membrane. For nitrite, the same trend was observed but with higher values of  $216 \pm 77$   $\mu\text{M}$  (week 10) or  $356 \pm 96$  (week 14) at the biofilm surface and  $845 \pm 520$   $\mu\text{M}$  (week 10) or  $842 \pm 465$   $\mu\text{M}$  (week 14) at the membrane. These microprofiles (Fig. 1, profiles of week 10 are displayed) together show a stratified biofilm with an oxic, nitrifying core around the silicone membrane that accumulates high concentrations of especially nitrite and is completely saturated with ammonium. The anoxic, outer part of the biofilm is characterized mainly by diffusion of nitrite and nitrate out of the biofilm. Additionally, as the profiles of nitrite and nitrate are not perfectly linear, denitrification relying on endogenous organic carbon might occur.

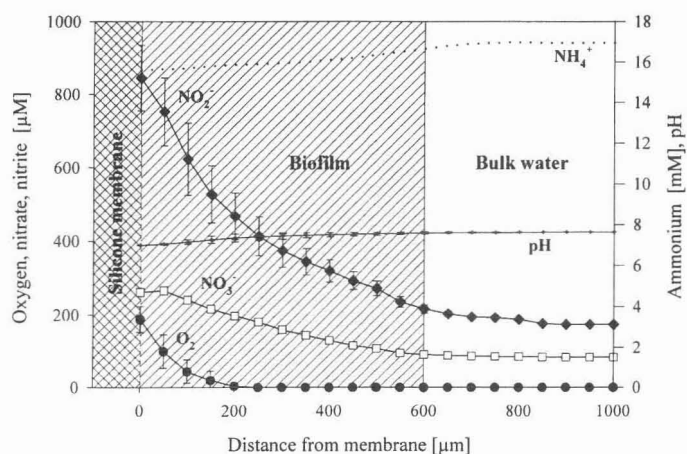


FIG. 1. Gradients of oxygen (●), pH (+), nitrite (◆), and nitrate (□) in the 10 week-old membrane-biofilm as measured with microsensors. For each data point, mean values and standard deviations out of 10 profiles are shown, except for the nitrate profile, where standard deviations were in the same range as mean values. Therefore they had to be omitted in order to keep the figure readable. The ammonium concentration (dotted line) was extrapolated from three measuring points, i.e., at the membrane, at the biofilm surface, and in the bulk water.

**Distribution of nitrifying bacteria in weeks 10 and 14.** Use of probe EUB338 as a positive control showed that probe penetration was sufficient to enable FISH in all parts of the biofilm. Unspecific binding of probe NON (as negative control) and autofluorescence were negligible, except for some easily distinguishable crystalline particles. A set of hierarchical oligonucleotide probes (Table 1) was applied to reliably identify ammonia-oxidizing bacteria of the  $\beta$ -subclass of *Proteobacteria* as outlined before (Amann *et al.*, 1995). Populations identified by the different probes were quantified and compared on the basis of their cell area, and in all samples a close match (within the standard deviations) was found for the areas detected by probes NSO190, NSO1225 and NSM156 + NSV443. However, only about 5% of all ammonia oxidizers hybridized with probe NSV443, specific for the genus *Nitrospira*. Furthermore, hybridizations with probes NSM156, NEU23a and Nse1472 yielded very similar area values. Thereby, the vast majority of the ammonia oxidizers is demonstrated to belong to the *Nitrosomonas europaea-eutropha-halophila* group while *Nitrospira* sp. accounted only for about 5% of all ammonia oxidizers. Additionally, few cells of *Nitrosococcus mobilis* have been detected by probe NmV in all samples. These, in no case constituted more than 0.1% of all ammonia oxidizers. This low number is not surprising as *N. mobilis* is a halophilic strain which is easily overgrown by *N. europaea* in low-salt environments (Juretschko *et al.*, 1998). A clear stratification of nitrifying bacteria (Fig. 2A and B) was established along the gradients (Fig. 1) within the biofilm. *N. europaea*-like ammonia oxidizers formed an extremely dense

layer of cells directly on the membrane surface ( $2.5 \times 10^{11}$  or  $2.1 \times 10^{11}$  cells  $\text{cm}^{-3}$  in weeks 10 or 14, respectively), and their numbers decreased gradually with decreasing oxygen concentrations. From 250  $\mu\text{m}$ , the distance from the membrane where oxygen disappeared, until almost to the biofilm surface cell numbers were in the range of  $3 \times 10^9$   $\text{cm}^{-3}$  in both weeks. In contrast, *Nitrosospira* sp. occurred throughout the biofilm in lower numbers of  $1 \times 10^9$  to  $6 \times 10^9$  cells  $\text{cm}^{-3}$  (week 10) or  $5 \times 10^7$  to  $5 \times 10^9$  cells  $\text{cm}^{-3}$  (week 14). Considering the high ammonium (15-20 mM) and nitrite (0.2-1.2 mM) concentrations in the reactor, this result confirms earlier reports on the adaptation of members of the *Nitrosomonas europaea*-group to high substrate and product concentrations (Pommerening-Röser *et al.*, 1996). Oxygen seems to be the main factor controlling the distribution of this population in the biofilm as their abundance correlates well with the oxygen concentration. A similar situation was reported previously for *Nitrosomonas* sp. in a trickling filter biofilm (Schramm *et al.*, 1996; Okabe *et al.*, 1999). *Nitrosospira* sp. was not competitive under the conditions prevailing in the oxic part of the biofilm. Whether this was due to a lower specific growth rate as suggested by pure culture (Belser, 1979) and *in situ* studies (Schramm *et al.*, 1998, Schramm *et al.*, 1999), or due to substrate and/or product inhibition (Prosser, 1989), can not be resolved on the basis of our data.

Nitrite-oxidizing bacteria were identified using probe NIT3, specific for all sequenced strains of *Nitrobacter* (Wagner *et al.*, 1996) and a combination of probes NSR826 + NSR1156 which together target all known *Nitrospira*-like sequences from freshwater habitats (Schramm *et al.*, 1998). *Nitrobacter* sp. showed a preference for the high oxygen and nitrite concentrations within the first 100  $\mu\text{m}$  at the membrane, with maximum cell numbers of  $5.9 \times 10^{10}$  (week 10) or  $4.4 \times 10^{10}$  cells  $\text{cm}^{-3}$  (week 14).

When oxygen became very low or zero cell numbers of *Nitrobacter* sp. decreased while *Nitrospira* sp., which was absent from the first 100  $\mu\text{m}$  at the membrane, reached maximum abundance with cell numbers of about  $9.7 \times 10^9$  (week 10) or  $6 \times 10^9$  cells  $\text{cm}^{-3}$  (week 14). This obvious spatial separation, with *Nitrobacter* sp. only occurring close to the membrane where oxygen and nitrite concentrations were highest, supports the idea that *Nitrobacter* sp. outgrows *Nitrospira* sp. at high substrate concentrations (Schramm *et al.*, 1999), at least if oxygen is not limiting. Low growth rates have been reported for pure cultures of *Nitrospira* sp. (Watson *et al.*, 1986; Ehrich *et al.*, 1995), and low nitrite-oxidation rates were proposed for uncultured *Nitrospira* spp. *in situ* (Schramm *et al.*, 1999). Why then did *Nitrospira* sp. establish in the micro-aerobic zone of the biofilm, i.e. between 150 and 300  $\mu\text{m}$  away from the membrane, even out-competing *Nitrobacter* sp.? Affinity for nitrite is unlikely to play a

selective role because the nitrite concentrations in this part of the biofilm are still about 400  $\mu\text{M}$  and thus above or about the  $K_M(\text{NO}_2^-)$  values reported for almost all *Nitrobacter* sp. (60 - 600  $\mu\text{M}$ , Prosser, 1989; Hunik *et al.*, 1993). Oxygen concentrations, however, are with 0 - 15  $\mu\text{M}$  well below the  $K_M(\text{O}_2)$  of *Nitrobacter* sp. (62 - 256  $\mu\text{M}$ , Prosser, 1989). A competitive advantage for *Nitrospira* sp. on the basis of oxygen affinity would therefore imply that its  $K_M(\text{O}_2)$  is significantly lower than that of *Nitrobacter* sp. The micro-aerophilic behaviour of *Nitrospira* sp. in our study is also in agreement with recent findings of Okabe *et al.* (1999) who showed maximum abundance of *Nitrospira* sp. in the micro-aerobic zone of two types of biofilms. Additionally, they speculated upon the inhibition of *Nitrospira* sp. by high levels of oxygen.

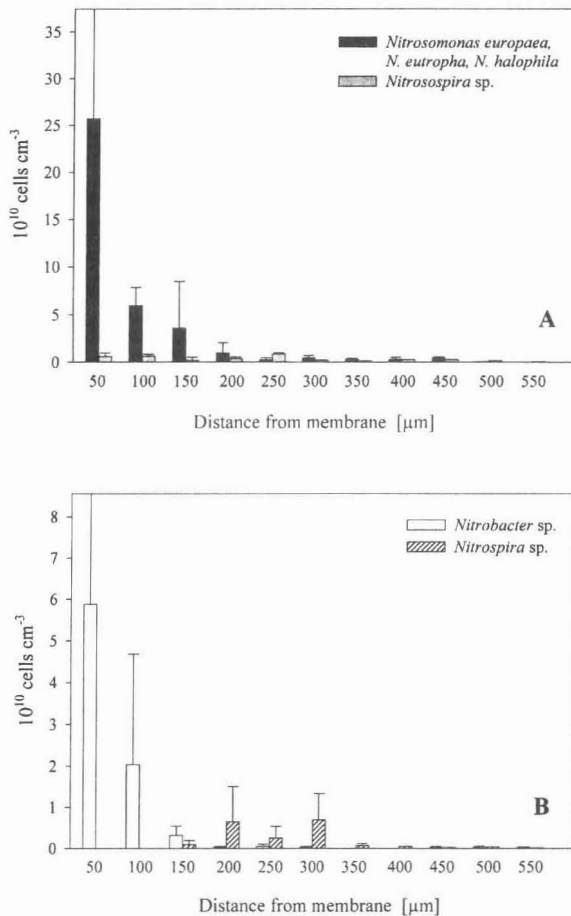


FIG. 2. Distribution of ammonia-oxidizing bacteria (A) and nitrite-oxidizing bacteria (B) in the 10 week-old membrane-biofilm as detected by FISH. Abundance of the different populations was quantified in steps of 50  $\mu\text{m}$  starting at the membrane (to the left). Mean values and standard deviations out of 9 replicates are shown. Note different scale.

In summary, our data support the idea that *Nitrospira* sp. might be a typical K-strategist compared to the r-strategist *Nitrobacter* sp. (Schramm et al., 1999), based on its putative higher affinities for nitrite and oxygen, and its lower growth rate. In many environments, where nitrite concentrations are negligible and nitrifiers have to compete for oxygen with heterotrophic bacteria, K-strategy might provide a selective advantage. However, physiological diversity is likely to occur in the phylogenetic diverse genus *Nitrospira*, and one should be cautious to generalize our findings as long as no information is available from in situ studies on the species level or from pure culture experiments.

In conclusion, the analysis of the distribution of nitrifying bacteria along gradients of oxygen and nitrite yielded insights into the factors that might govern the establishment of populations of different nitrite-oxidizing bacteria in the environment. Nevertheless, efforts should be made to isolate the respective strains to determine  $K_m$  values and growth rates for pure cultures and to evaluate their growth and competitiveness in defined co-cultures.

## ACKNOWLEDGEMENTS

We thank Bernd Walter and Norbert Rübiger, Institut für Umweltverfahrenstechnik, Universität Bremen, for design and maintenance of the biofilm reactor. Gaby Eickert, Anja Eggers, and Vera Hübner are acknowledged for constructing oxygen microsensors, and an anonymous reviewer for valuable comments on the manuscript.

This work was supported by the Körber Foundation, by the Max Planck Society, and by the Deutsche Forschungsgemeinschaft (SFB 411).

## REFERENCES

- Amann, R. I., Krumholz, L. and Stahl, D. A. (1990). Fluorescent-oligonucleotide probing of whole cells for determinative, phylogenetic, and environmental studies in microbiology. *J Bacteriol* 172, 762-770.
- Amann, R. I., Ludwig, W. and Schleifer, K. H. (1995). Phylogenetic identification and in situ detection of individual microbial cells without cultivation. *Microb Rev* 59, 143-169.
- Belser, L. W. (1979). Population ecology of nitrifying bacteria. *Annu Rev Microbiol* 33, 309-333.
- Bock, E. and Koops, H.-P. (1992). The genus *Nitrobacter* and related genera. In *The Prokaryotes*, pp. 2302-2309. Edited by A. Balows, H. G. Trüper, M. Dworkin, W. Harder and K.-H. Schleifer. New York: Springer Verlag.

- Bock, E., Koops, H.-P. and Harms, H. (1986). Cell biology of nitrifying bacteria. In *Nitrification*, pp. 17-38. Edited by J. I. Prosser. Oxford: IRL Press.
- Brosius, J., Dull, T. J., Sleeter, D. D. and Noller, H. F. (1981). Gene organization and primary structure of a ribosomal RNA operon from *Escherichia coli*. *J Mol Biol* 148, 107-127.
- Burrell, P. C., Keller, J. and Blackall, L. L. (1998). Microbiology of a nitrite-oxidizing bioreactor. *Appl Environ Microbiol* 64, 1878-1883.
- de Beer, D. and Schramm, A. (1999). Microenvironments and mass transfer phenomena in biofilms studied with microsensors. *Water Sci Technol* 39, 173-178.
- de Beer, D., Schramm, A., Santegoeds, C. M. and Kühl, M. (1997). A nitrite microsensor for profiling environmental biofilms. *Appl Environ Microbiol* 63, 973-977.
- Ehrich, S., Behrens, D., Lebedeva, E., Ludwig, W. and Bock, E. (1995). A new obligately chemolitho-autotrophic, nitrite-oxidizing bacterium, *Nitrospira moscoviensis* sp. nov. and its phylogenetic relationship. *Arch Microbiol* 164, 16-23.
- Hastings, R. C., Saunders, J. R., Hall, G. H., Pickup, R. W. and McCarthy, A. J. (1998). Application of molecular biological techniques to a seasonal study of ammonia oxidation in a eutrophic freshwater lake. *Appl Environ Microbiol* 64, 3674-3682.
- Hiorns, W. D., Hastings, R. C., Head, I. M., McCarthy, A. J., Saunders, J. R., Pickup, R. W. and Hall, G. H. (1995). Amplification of 16S ribosomal RNA genes of autotrophic ammonia-oxidizing bacteria demonstrates the ubiquity of nitrospiras in the environment. *Microbiology* 141, 2793-2800.
- Hovanec, T. A., Taylor, L. T., Blakis, A. and Delong, E. F. (1998). *Nitrospira*-like bacteria associated with nitrite oxidation in freshwater aquaria. *Appl Environ Microbiol* 64, 258-264.
- Hunik, J. H., Meijer, H. J. G. and Tramper, J. (1993). Kinetics of *Nitrobacter agilis* at extreme substrate, product and salt concentrations. *Appl Microbiol Biotech* 40, 442-448.
- Juretschko, S., Timmermann, G., Schmidt, M., Schleifer, K.-H., Pommerening-Röser, A., Koops, H.-P. and Wagner, M. (1998). Combined molecular and conventional analysis of nitrifying bacterial diversity in activated sludge: *Nitrosococcus mobilis* and *Nitrospira*-like bacteria as dominant populations. *Appl Environ Microbiol* 64, 3042-3051.
- Koops, H.-P. and Möller, U. C. (1992). The lithotrophic ammonia-oxidizing bacteria. In *The Prokaryotes*, pp. 2625-2637. Edited by A. Balows, H. G. Trüper, M. Dworkin, W. Harder and K.-H. Schleifer. New York: Springer Verlag.
- Kowalchuk, G. A., Stephen, J. R., de Boer, W., Prosser, J. I., Embley, T. M. and Woldendorp, J. W. (1997). Analysis of ammonia-oxidizing bacteria of the  $\beta$  subdivision of the class *Proteobacteria* in coastal sand dunes by denaturing gradient gel electrophoresis and sequencing of PCR-amplified 16S ribosomal DNA fragments. *Appl Environ Microbiol* 63, 1489-1497.
- Laanbroek, H. J. and Woldendorp, J. W. (1995). Activity of chemolithotrophic nitrifying bacteria under stress in natural soils. *Adv Microb Ecol* 14, 275-304.
- Manz, W., Amann, R., Ludwig, W., Wagner, M. and Schleifer, K.-H. (1992). Phylogenetic oligodeoxynucleotide probes for the major subclasses of proteobacteria: problems and solutions. *Syst Appl Microbiol* 15, 593-600.

- Mobarry, B. K., Wagner, M., Urbain, V., Rittmann, B. E. and Stahl, D. A.** (1996). Phylogenetic probes for analyzing abundance and spatial organization of nitrifying bacteria. *Appl Environ Microbiol* 62, 2156-2162.
- Okabe, S., Satoh, H., and Watanabe, Y.** (1999). In situ analysis of nitrifying biofilms as determined by in situ hybridization and the use of microelectrodes. *Appl Environ Microbiol* 65, 3182-3191.
- Özoguz, G.** (1997). *Stickstoffelimination durch immobilisierte Biomasse und entkoppelte Substratversorgung bei hochbelasteten Abwässern*. Düsseldorf, Germany, VDI-Verlag.
- Pommerening-Röser, A., Rath, G. and Koops, H.-P.** (1996). Phylogenetic diversity within the genus *Nitrosomonas*. *Syst Appl Microbiol* 19, 344-351.
- Princic, A., Mahne, I., Megusar, F., Paul, E. A. and Tiedje, J. M.** (1998). Effects of pH and oxygen and ammonium concentrations on the community structure of nitrifying bacteria from wastewater. *Appl Environ Microbiol* 64, 3584-3590.
- Prosser, J. I.** (1989). Autotrophic nitrification in bacteria. *Adv Microb Physiol* 30, 125-181.
- Revsbech, N. P.** (1989). An oxygen microelectrode with a guard cathode. *Limnol Oceanogr* 34, 474-478.
- Schramm, A., de Beer, D., van den Heuvel, H., Ottengraf, S., and Amann, R.** (1999). Microscale distribution of populations and activities of *Nitrosospira* and *Nitrospira* spp. along a macroscale gradient in a nitrifying bio-reactor: quantification by in situ hybridization and the use of microsensors. *Appl Environ Microbiol* 65, 3690-3696.
- Schramm, A., de Beer, D., Wagner, M. and Amann, R.** (1998). Identification and activity in situ of *Nitrosospira* and *Nitrospira* spp. as dominant populations in a nitrifying fluidized bed reactor. *Appl Environ Microbiol* 64, 3480-3485.
- Schramm, A., Larsen, L. H., Revsbech, N. P., Ramsing, N. B., Amann, R. and Schleifer, K.-H.** (1996). Structure and function of a nitrifying biofilm as determined by in situ hybridization and the use of microelectrodes. *Appl Environ Microbiol* 62, 4641-4647.
- Stephen, J. R., McCaig, A. E., Smith, Z., Prosser, J. I. and Embley, T. M.** (1996). Molecular diversity of soil and marine 16S rRNA gene sequences related to  $\beta$ -subgroup ammonia-oxidizing bacteria. *Appl Environ Microbiol* 62, 4147-4154.
- Thomas, L. V. and Wimpenny, J. W. T.** (1993). Method for investigation of competition between bacteria as a function of three environmental factors varied simultaneously. *Appl Environ Microbiol* 59, 1991-1997.
- Timberlake, D. L., Strand, S. E. and Williamson, K. J.** (1988). Combined aerobic heterotrophic oxidation, nitrification and denitrification in a permeable-support biofilm. *Water Res* 22, 1513-1517.
- Wagner, M., Rath, G., Amann, R., Koops, H.-P. and Schleifer, K.-H.** (1995). *In situ* identification of ammonia-oxidizing bacteria. *Syst Appl Microbiol* 18, 251-264.
- Wagner, M., Rath, G., Koops, H.-P., Flood, J. and Amann, R.** (1996). *In situ* analysis of nitrifying bacteria in sewage treatment plants. *Water Sci Technol* 34, 237-244.
- Watson, S. W., Bock, E., Valois, F. W., Waterbury, J. B. and Schlosser, U.** (1986). *Nitrospira marina* gen. nov. sp. nov.: a chemolithotrophic nitrite-oxidizing bacterium. *Arch Microbiol* 144, 1-7.
- Yu, F. P., Callis, G. M., Stewart, P. S., Griebbe, T. and McFeters, G. A.** (1994). Cryosectioning of biofilms for microscopic examination. *Biofouling* 8, 85-91.

## **Chapter 3**

# **Simultaneous P and N Removal in a Sequencing Batch Biofilm Reactor: Insights from Reactor- and Microscale Investigations**

A. Gieseke, P. Arnz, R. Amann, P. Wilderer, and A. Schramm



## Simultaneous P and N Removal in a Sequencing Batch Biofilm Reactor: Insights from Reactor- and Microscale Investigations

A. Gieseke<sup>1\*</sup>, P. Arnz<sup>2</sup>, R. Amann<sup>1</sup>, A. Schramm<sup>1,3</sup>

<sup>1</sup>Max-Planck-Institute for Marine Microbiology, Celsiusstr. 1, D-28359 Bremen, Germany

<sup>2</sup>Institute of Water Quality Control and Waste Management, TU Munich, Am Coulombwall,  
D-85748 Garching, Germany

<sup>3</sup>Present address: Department of Ecological Microbiology, BITOEK, University of Bayreuth,  
D-95440 Bayreuth, Germany

A sequencing batch biofilm reactor (SBBR) with well established enhanced biological phosphate removal (EBPR) was subjected to higher ammonium concentrations to stimulate and eventually implement simultaneous nitrification. Changes of activity and populations were investigated by a combination of online monitoring, microsensor measurements and fluorescence *in situ* hybridisation (FISH) of biofilm sections. Nitrification and nitrifying bacteria were always restricted to the periodically oxidic biofilm surface. Both, activity and population size increased significantly with higher ammonium concentrations. Nitrification always showed a delay after the onset of aeration, most likely due to competition for oxygen by coexisting P accumulating and other heterotrophic bacteria during the initial aeration phase. This view is also supported by comparing oxygen penetration and oxygen uptake rates under low and high ammonium conditions. Therefore, simultaneous nitrification and phosphorus removal in a P removing SBBR appears to be only possible with a sufficiently long oxidic period to ensure oxygen availability for nitrifiers.

### INTRODUCTION

Biofilms bear great potential for the simultaneous and efficient removal of organic carbon and nutrients like N and P in wastewater treatment (13, 22): They are spatially heterogeneous, providing space for both, aerobic and anaerobic processes; they are well suited for nitrification, since attached growth of the slow-growing nitrifying bacteria protects them from washout; and they can be exposed to alternating anaerobic and aerobic conditions as necessary for Enhanced Biological Phosphorus Removal (EBPR). First examples of multiple nutrient removal in biofilm systems have already been demonstrated (13). Recently, a Sequencing

Batch Biofilm Reactor (SBBR) was designed for very efficient EBPR (11) and successfully scaled up to the pilot scale (2). In each SBBR cycle, phosphorus is released during an initial anaerobic period. Subsequently, the reactor is aerated and phosphorus is taken up by Phosphorus-Accumulating Organisms (PAOs). This results in a net uptake of P over the cycle. The implementation of nitrification into this reactor type is a challenging but desired step in saving reactor volume and costs. As nitrification and P removal both consume oxygen, organisms in such a system are potentially subjected to competition for oxygen. Nitrifying bacteria in pure culture are known to have a lower affinity for oxygen compared to the heterotrophic bacteria as e.g., the PAOs (14), which may result in problems when integrating nitrifying activity. In contrast, recent *in situ* studies suggest certain nitrifiers to have relatively high affinities for oxygen (17). Understanding the underlying mechanisms of coexistence and competition of the organisms involved is therefore essential to reliably set up nitrification in the EBPR-SBBR system. Knowledge of microscale function and structure of the biological components in the biofilm can help to adjust both processes to a high efficiency.

In this study, a lab-scale SBBR operated for EBPR was subjected to higher ammonium concentrations to stimulate and eventually implement simultaneous nitrification. The resulting changes in system performance, microbial activity and populations were investigated on the reactor scale and on the microscale. For that purpose, online monitoring of the process was combined with microsensor measurements and fluorescence *in situ* hybridisations (FISH) of microorganisms in biofilm samples with oligonucleotide probes. Our goals were to examine to what extent nitrification can be combined with EBPR in a SBBR, and to get insights in how the processes might coexist spatially and temporally on the micro- and reactor scale.

## MATERIALS AND METHODS

**SBBR.** A biofilm reactor with a fixed-bed volume of 20 l and an exchangeable water volume of 19 L was operated in a sequencing batch mode for EBPR as described before (11). The 8 h operation cycle comprised a 20 min filling period, 160 min anaerobic recirculation, 260 min recirculation with aeration and 40 min draining (100 % water exchange). By completely draining the reactor at the end of each cycle carryover of nitrate to the following cycle was restricted to water remaining in pores and in the biofilm. Thus, competition for carbon by PAOs and denitrifying bacteria at the beginning of the cycle was minimised. Excess biomass was removed once a week by backwashing with pressurised air and water at the end of the aerated period. As support material for the biofilm, 8 x 8 mm (diameter x height) plastic

elements (Kaldnes, Purac, Merseburg, Germany) were used. These contained axial sheltered spaces that protected parts of the biomass from abrasion during backwashing (Fig. 1). Biofilm developed on the external and internal surfaces of the substratum elements, which in some cases filled the complete axial space of the substratum. Preceding observations on thin sections of the biomass hybridised with various fluorescently labelled oligonucleotide probes (see below) revealed no substantial difference in the microbial community structure of biofilm parts from the external surface and the surface part of biomass growing in the axial space.

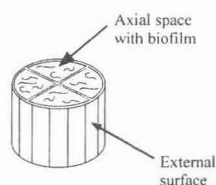


FIG. 1. Localisation of biofilm on the substratum elements.

During feeding of the reactor with a medium low in ammonium (LA operation mode), the reactor received a sterile solution containing acetate ( $224 \text{ mg L}^{-1}$ ),  $\text{PO}_4\text{-P}$  ( $10 \text{ mg L}^{-1}$ ),  $\text{NH}_4\text{-N}$  ( $13 \text{ mg L}^{-1}$ ),  $\text{K}^+$  ( $7 \text{ mg L}^{-1}$ ) and micronutrients. To enhance existing nitrifying activity, the feeding solution was enriched in ammonium, and acetate was replaced by a mixture of acetate ( $103 \text{ mg L}^{-1}$ ) and peptone ( $200 \text{ mg L}^{-1}$ ). Thereby, the COD was maintained at the same level (i.e.,  $230 \text{ mg COD L}^{-1}$ ), while ammonium (measured as Total Kjeldahl Nitrogen; TKN) was increased to  $38 \text{ mg L}^{-1}$  (HA operation mode). The system was allowed to adapt to the new conditions for 100 d before analyses were performed. Monitoring of phosphate and oxygen in the bulk medium was done routinely by online measurements with an oxygen electrode (Oxy 196, WTW), and with a P analyser (Phosphax Inter, Dr. Lange).  $\text{NO}_3\text{-N}$ , COD, and TKN were determined photometrically by use of standard test kits (Dr. Lange type LCK, digital photometer ISIS 6000).

**Microsensor measurements.** Vertical concentration profiles of oxygen, ammonium and nitrate in the biofilm were measured with microsensors (6, 15). For that purpose, substratum elements were placed in a flow chamber coupled directly to the recirculation of the SBBR, thus kept continuously under the conditions prevailing in the reactor. Measurements in biofilm grown on external surfaces or in the axial space of the substratum elements, respectively, showed no substantial differences in concentrations or shape of the profiles. All profiles presented were measured in the axial space biofilm. Measurements were performed at different times during the cycle to follow the concentration changes in the biofilm.

**Calculation of theoretical and measured oxygen uptake rate.** Theoretical oxygen requirements of the EBPR process were estimated based on the uptake of  $\text{PO}_4\text{-P}$  measured during the aerobic period, and the stoichiometry of the aerobic reactions of EBPR (19). These were compared to apparent oxygen uptake rates (OUR) for various times during the oxic period during both operation modes. Apparent OUR were calculated from microprofiles by use of the linear gradients of the oxygen profiles through the diffusive boundary layer above the biofilm as described earlier (16).

**FISH analysis of biofilms.** Biofilm material from the outer surface of the substratum and aggregated biomass from the axial space was sampled both during the LA and the HA operation. Samples were fixed with paraformaldehyde, cut in vertical sections on a cryomicrotome, and immobilised on microscopic slides for FISH (18). A hierarchical set of fluorescently labelled oligonucleotide probes was used: (i) probe EUB338 (1), specific for the domain Bacteria; (ii) probe HGC1351 (7), specific for Gram positive bacteria with a high GC content (HGCGPB); (iii) probes ALF968 (12), BET42a, GAM42a (8), and SRB385 (1) specific for most of the alpha, beta, gamma, and delta subclasses of *Proteobacteria*; (iv) probe NSO1225 (10) specific for ammonia oxidising bacteria (AOB) of the beta subclass of *Proteobacteria*; (v) NIT3 (21) specific for the nitrite oxidising bacteria (NOB) of the genus *Nitrobacter*; and (vi) Ntspa712 and Ntspa662 (5) specific for NOB of the phylum and genus *Nitrospira*, respectively. Hybridisation was performed according to the conditions described by Manz *et al.* (8). The distribution of hybridised cells was subsequently visualised by confocal laser scanning microscopy.

## RESULTS AND DISCUSSION

**SBBR performance.** During long-term LA operation, stable P removal was achieved in the SBBR system.  $\text{PO}_4\text{-P}$  concentrations were  $27 \text{ mg L}^{-1}$  and  $0.5 \text{ mg L}^{-1}$  at the end of the non-aerated and aerated period, respectively.  $\text{NH}_4\text{-N}$  concentration decreased from  $13 \text{ mg L}^{-1}$  to below  $0.8 \text{ mg L}^{-1}$  while the  $\text{NO}_3\text{-N}$  concentration increased to about  $1.5 \text{ mg L}^{-1}$  (Fig. 2A), indicating that nitrification (and a small amount of denitrification) already was present in the system. The oxygen concentration during LA operation instantly showed a constant level of  $5.4 \text{ mg L}^{-1}$  at the beginning of aeration, and after 80 min increased linearly up to  $6.8 \text{ mg L}^{-1}$  (Fig. 2C). After the system was switched to HA operation, a steady state was reached within a couple of days according to bulk data. For both, the  $\text{PO}_4\text{-P}$  and COD removal the same effi-

ciency as under LA operation was reached (data not shown). However,  $\text{NH}_4\text{-N}$  concentrations now decreased from  $40 \text{ mg L}^{-1}$  to  $11 \text{ mg L}^{-1}$ , while  $\text{NO}_3\text{-N}$  concentrations increased to  $14 \text{ mg L}^{-1}$  (Fig. 2B). In contrast to LA operation, the oxygen concentration remained constant at a level of  $6.3 \text{ mg L}^{-1}$  throughout the aerated period (Fig. 2D). No significant effect of back-washing on the bulk concentrations and, thus, on system performance could be detected in both the LA and HA operation mode.

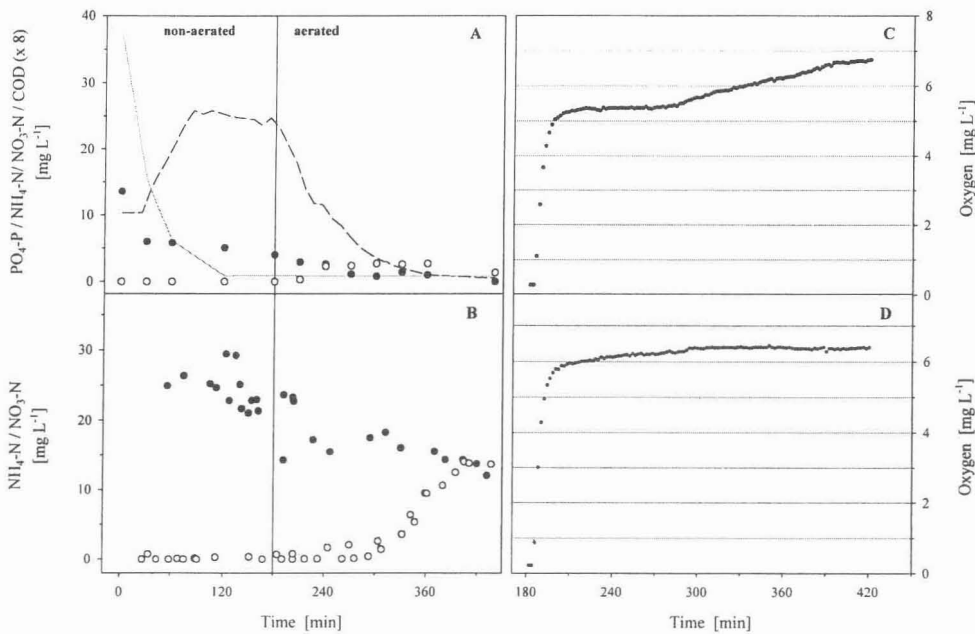


FIG. 2. Bulk concentration of  $\text{PO}_4\text{-P}$ , COD,  $\text{NH}_4\text{-N}$ , and  $\text{NO}_3\text{-N}$  during LA operation cycle (A), and  $\text{NH}_4\text{-N}$  and  $\text{NO}_3\text{-N}$  concentrations as measured with microsensors in the bulk during HA operation (B), and the appropriate bulk concentrations of oxygen during LA operation (C), and HA operation (D)

**Microprofiles.** Microprofiles and online monitoring data originated from various treatment cycles between 3 and 7 days after backwashing, and a certain variability occurred between cycles. The data shown represent typical observations.

In both operation modes, oxygen was initially limited to a penetration depth of 200 to  $250 \mu\text{m}$  during aeration. Between 80 and 140 min after start of aeration, a deeper penetration of oxygen up to a depth of 1.5 mm occurred during LA operation, coinciding with the increase of oxygen in the bulk liquid (Fig. 3). Although the absolute values differ between measurements with the online electrode and the microsensor due to different stirring sensitivity and micro-bial growth on the online electrode, the pattern of concentration changes was

the same. Both effects, the increase in bulk oxygen and penetration of oxygen during LA operation, are in accordance with results of a simulation of EBPR in a SBBR (11). A transition from partial to full penetration of oxygen was suggested for a 500  $\mu\text{m}$  thick biofilm during aeration. This effect was ascribed to a decrease in stored polyhydroxyalkanoates (PHA) and a subsequently reduced oxygen uptake by heterotrophic microorganisms. In contrast, the oxygen penetration depth and the bulk concentration of oxygen were constant throughout the oxic period of the reactor cycle during HA operation. An additional oxygen uptake by nitrification is likely to cause this difference in the oxygen uptake and will be discussed later.

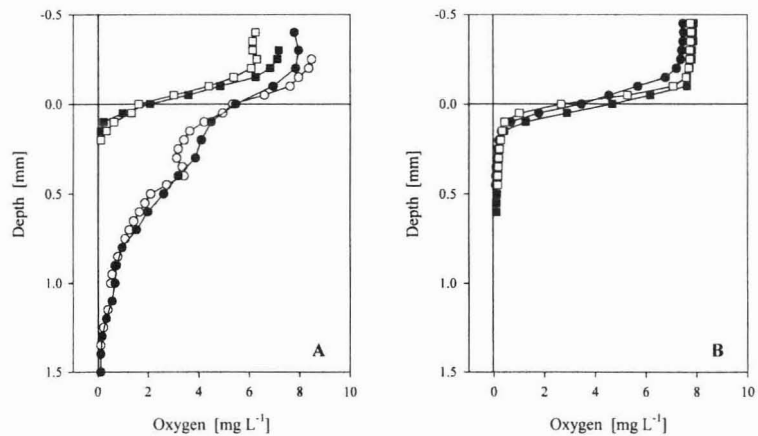


FIG. 3. Vertical concentration profiles of oxygen in the biofilm at different times of the reactor cycle during LA operation (A) and HA operation (B). Profiles were measured at 220 min (i.e., 40 min after start of aeration; □), 260 min (+80 min; ■), 320 min (+140 min; ○), and 360 to 370 min (+180 to +190 min; ●).

Steep ammonium profiles (data not shown) were measured during both operation modes at the beginning of the cycle that quickly levelled off thereafter. In a previous study it was shown that the biofilm strongly adsorbed ammonium (23), explaining the strong initial decrease of ammonium after filling without any production of nitrate. In contrast to LA operation, the higher amount of ammonium was not completely converted during HA operation, indicating that nitrification was not completed during the treatment cycle. In both operation modes, a low net uptake of ammonium into the biofilm was maintained throughout the cycle. However, no distinct zones of ammonium consumption could be determined from the micro-profiles. Assuming nitrification rates in the same order of magnitude as that found in other systems by use of microsensor techniques, the prevailing concentrations of ammonium were too high to support steep gradients and distinct zones of consumption.

The first occurrence of nitrate in the biofilm could be detected after approximately 60 min of aeration, and nitrate production was restricted to the oxic surface layer, i.e. to a depth of a few hundred  $\mu\text{m}$ . The delay in nitrification and its vertical distribution were the same in LA and HA operation mode. Nitrate production, however, was much higher in the latter (Figs. 2 and 4). Ammonium uptake without net nitrate production in the aerobic period has been demonstrated for a moving bed biofilm reactor combining nitrification and (13). It has been argued that nitrifier growth was favoured at the surface, whereas most PAOs grew in the inner parts of the biofilm and showed denitrifying activity, thereby consuming the nitrate. In our system, however, no nitrification took place in any biofilm layer at the beginning of the aeration according to the nitrate microprofiles. This can be explained by an initial competitive advantage of the heterotrophic bacteria in oxygen uptake. The putative heterotrophs might be PAOs and eventually also glycogen accumulating bacteria (GAOs; Mino *et al.*, 1998). Later in the cycle, the shortage of the endogenous C source and a resulting lower activity of the heterotrophs possibly enable nitrification. This hypothesis is strongly supported by the oxygen microprofiles of the second half of the aeration period. While during LA operation lower activity of the heterotrophs results in a higher oxygen penetration depth, during HA operation nitrifying activity replaces heterotroph activity at the surface in terms of oxygen consumption. As a result, the oxygen penetration depth remains constant. It can thus be inferred that nitrifying bacteria coexist spatially with the heterotrophic PAOs and GAOs, while their activity is separated in time.

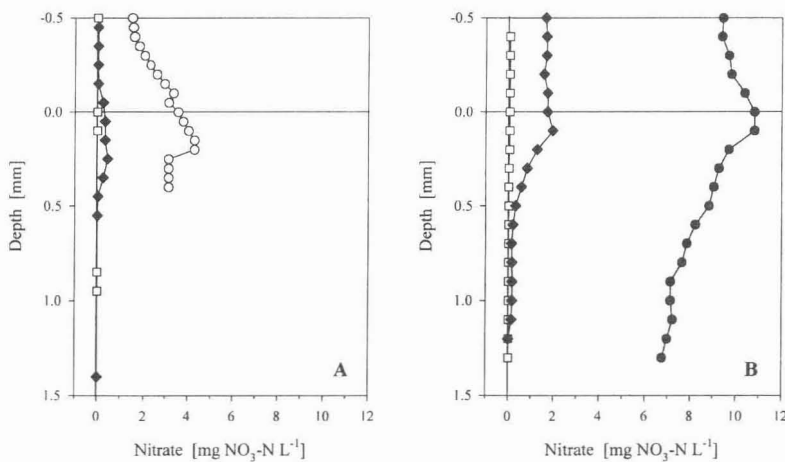


FIG. 4. Vertical nitrate microprofiles at various times of the oxic period during LA and HA operation. Concentration profiles were measured at 220 min (i.e., 40 min after start of aeration;  $\square$ ), 240 min (+60 min;  $\blacklozenge$ ), 320 min (+140 min;  $\circ$ ), and 360 min (+180 min;  $\bullet$ ).

The concentration of nitrate in the surface of the biofilm reached  $4.3 \text{ mg NO}_3\text{-N L}^{-1}$  during LA operation, and  $15.8 \text{ mg NO}_3\text{-N L}^{-1}$  during HA operation. Therefore, nitrification can be considered to provide nitrate for either conventional denitrification or denitrifying phosphorus uptake appearing in deeper anoxic layers. This would explain the N loss observed under LA as well as under HA operation. The potential carbon source for this heterotrophic process, however, remains unclear. Since the carbon source of the influent was completely sequestered in the anaerobic period, it may be assumed that storage products such as PHA were used for denitrification. It has been shown that at the beginning of the cycle acetate fully penetrated a  $500 \text{ }\mu\text{m}$  thick biofilm in a SBBR process (11). Thus, a carbon storage in deeper biofilm layers is possible.

**Theoretical and apparent OUR.** The required OUR for the phosphate uptake observed for both operation modes was calculated based on a stoichiometric model for EBPR in a sequencing batch process (19). The model assumes that four processes contribute to oxygen consumption: synthesis of polyphosphates, glycogen, and biomass, and maintenance of cell metabolism. For OUR calculation, we used a specific consumption of  $0.3 \text{ mol O}_2 \text{ mol}^{-1} \text{ P}$  (19), an oxygen demand for growth and glycogen formation of  $2.15 \text{ mmol L}^{-1} \text{ h}^{-1}$  (19), and a biomass composition comparable to that reported for a SBR biomass (19), i.e. a molecular weight of  $26 \text{ g mol}^{-1} \text{ C}$ . The biomass concentration in the SBBR was  $6.7 \text{ g L}^{-1}$ , and a maintenance demand of  $4.5 \times 10^{-3} \text{ mol O}_2 \text{ mol}^{-1} \text{ C h}^{-1}$  was assumed, leading to an oxygen demand of  $1.16 \text{ mmol O}_2 \text{ L}^{-1} \text{ h}^{-1}$ . In both operation modes, only the outer  $300 \text{ }\mu\text{m}$  of the biomass have been active and harboured potentially active cells, as shown by microsensor measurements and FISH analysis (see below). Thus, only one third of the total biomass was actively respiring. Consequently, the values for growth and glycogen formation and for maintenance have to be corrected to  $0.71$  and  $0.38 \text{ mmol O}_2 \text{ L}^{-1} \text{ h}^{-1}$ , respectively. This correction might underestimate the OUR of PAOs, as with LA operation oxygen penetrated to and partly was consumed in deeper layers during the final treatment. However, no putative PAOs were found in these layers, and oxygen consumption could not be assigned to a distinct population. The measured apparent areal uptake rates were converted to volumetric OUR by assuming an average biofilm surface of  $3250 \text{ cm}^2 \text{ L}^{-1}$ , obtained by geometric considerations of the substratum dimensions.

Apparent OUR calculated for the beginning of the aerated period did not show differences between LA and HA operation (Fig. 5), although the initial bulk concentration of oxygen during LA operation was found to be slightly lower than with HA (Fig. 2). For both operation modes, however, the apparent OUR were found to be twice as high as the estimated oxygen

requirements for the EBPR process after 80 min of aeration (Fig. 5). This suggests that either some of the parameters used in the calculation are underestimated, or that additional processes take up oxygen in the first part of the oxic period. Possibly, glycogen-accumulating organism, capable of anaerobic uptake and storage of organic carbon, were present in the system and caused this initially high oxygen uptake. However, during LA operation, OUR decreased in the second part of the aerobic period. Oxygen requirements of EBPR finally accounted for about 75% of the apparent OUR, thus indicating that at least the assumption for the maintenance demand of PAOs is realistic. Both, the decreased apparent OUR and the deeper oxygen penetration during LA operation is in accordance with predictions of an earlier model for EBPR in an SBBR (11). In contrast, oxygen consumption remained high during HA operation. It is obvious that nitrification contributed significantly to the apparent OUR. A constant activity of nitrifiers from 240 min to 450 min leading to  $14 \text{ mg L}^{-1} \text{ NO}_3\text{-N}$  during HA operation would explain an additional oxygen uptake of about  $18 \text{ mg L}^{-1} \text{ h}^{-1}$ . In contrast, during LA operation only  $2 \text{ mg L}^{-1} \text{ h}^{-1}$  of oxygen would have been used for nitrification. Furthermore, this calculation based on the accumulated  $\text{NO}_3\text{-N}$  clearly underestimates nitrifying activity by not accounting for simultaneous denitrification.

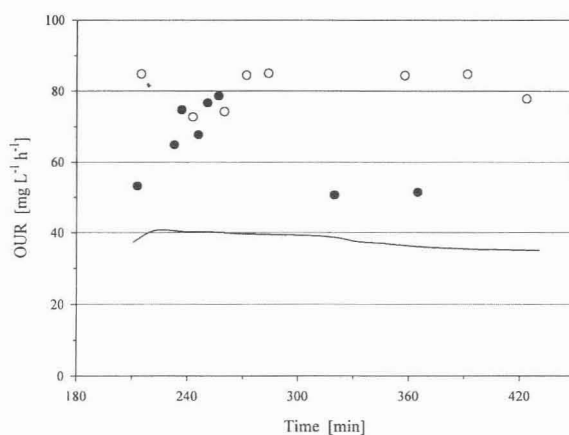


FIG. 5. Apparent OUR during LA (●) and HA operation (○), and predicted oxygen requirements for EBPR at different times of the aerobic period. For details see text.

**Biofilm structure.** Hybridisation with a general bacterial probe (EUB338) showed a clear stratification of the aggregated biomass during LA as well as HA operation (Fig. 6). In both cases, highest densities of bacteria could be detected in the uppermost 300  $\mu\text{m}$ . Cell densities visually decreased with depth. A high number of putatively active cells were thus located in

the periodically oxic biofilm layers (Fig. 6A, B), while a small amount was situated in the permanent anoxic layers of the biomass, thus possibly depending on anaerobic processes. The majority of EUB338 positive cells could be shown to belong to one of the groups described in the following.

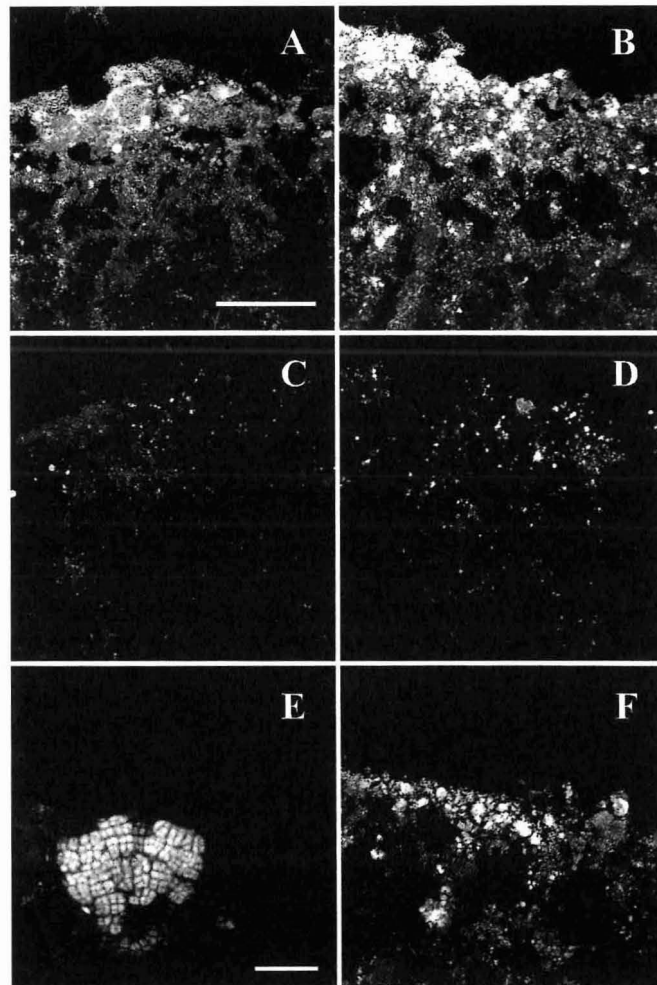


FIG. 6. Confocal fluorescent micrographs of vertical biofilm cross sections as hybridised with probes for *Bacteria* (EUB338; A and B), all nitrifying bacteria (mix of NSO1225 and Ntspa712; C and D), alpha subclass of *Proteobacteria* (ALF968; E), and Gram positive bacteria with a high GC content (HGC1351; F). A, C, and E refer to LA operation, whereas B, D and F refer to HA operation. White spots are hybridised cells or cell clusters, whereas grey areas reflect background. Scale bar is 50  $\mu\text{m}$  (A-D, F) and 10  $\mu\text{m}$  (E), respectively.

In LA operation, HGCGPB and members of the *Proteobacteria* appearing in tetrad-like clusters were most abundant, followed by members of the beta and delta subclasses of *Proteo-*

*bacteria*. As shown for other systems (4, 20) the HGCGPB population might be involved in the EBPR process. The majority of this population was found in the periodically oxic surface layer (Fig. 6F). Therefore, their contribution to a denitrifying P uptake is probably of minor importance in the system. This is in agreement with the fact that no nitrate was available during the first part of aerobic period, when the P uptake was found to be high. Furthermore, this result supports the assumption for OUR calculation that only one third of the biomass is involved in P uptake. The phylogenetic affiliation of the tetrad-like clustered cells (Fig. 6E) remained unclear, as they hybridised with both the probes specific for the alpha and gamma subclass of *Proteobacteria*. Similar structures were reported from reactors with poor EBPR properties and described as the so-called "G-Bacteria" (3). The phylogenetic affiliation of these GAOs (9) is yet unknown. The abundance of the tetrad-arranged cells visibly decreased when the system was switched to HA operation. This might indicate that these organisms have a reduced ability to utilise the substrate mixture. Despite the decline of this population, the P removal efficiency remained high, supporting the view that they play no major role in EBPR.

Beta-proteobacteria occurred in dense layers at the very surface as well as in typical spherical clusters of diameters from 4 to more than 20  $\mu\text{m}$ . The latter were restricted to the biofilm surface (300  $\mu\text{m}$ ). Their abundance appeared to be low during LA treatment, but visibly increased after the reactor was switched to HA operation. Subsequent hybridisations with sets of probes targeting different nitrifiers showed that these clusters belong to the ammonia oxidisers of the beta subclass of *Proteobacteria* (Fig. 6C, D). Nitrite oxidisers were found to belong to the genus *Nitrospira* while *Nitrobacter* spp. could not be detected in the system. In contrast to their visual frequency, neither the composition of the nitrifying community as detected by FISH nor the vertical distribution of various populations was affected by switching to HA mode. The vertical distribution of the nitrifying bacteria in the biomass correlated to the narrow zone of nitrifying activity as detected with microsensors. Thus, nitrification was higher both in terms of the amount of detectable cells and the activity as shown by the microsensor and bulk concentration data. Their spatial coexistence with putative PAOs (and GAOs) in the biofilm supports the hypothesis of oxygen competition and a separation of both processes in time. In contrast, a separation in space, as suggested for a moving bed biofilm (13), was not found in our system.

Small irregularly shaped clusters of delta-proteobacteria were present along the entire vertical biofilm section. Since this is the most abundant group in deeper zones of the biofilm, it could be hypothesised that it participates in a conventional anoxic denitrification. However,

there is not sufficient data from nitrate profiles to assign a certain zone to denitrification. Furthermore, the cell numbers appeared to be low compared to the numbers of other groups located at the surface, and the potential carbon source remains a matter of speculation.

## CONCLUSIONS

Efficient P removal and nitrification can be achieved simultaneously in a sequencing batch biofilm reactor. Based on macro- and microscale observations, we suggest that during the oxic period P uptake and nitrification occur sequentially in time within the oxic surface layer of the biofilm. The sequential action is a result of the oxygen limitation of nitrifiers caused by competition for oxygen with heterotrophic bacteria such as the PAOs (and eventually GAOs) at the biofilm surface. The observed delay in the nitrification supports this hypothesis. Thus, besides availability of substrate, successful nitrification as combined with EBPR relies on an aerobic period that is long enough for the nitrifiers to establish.

## ACKNOWLEDGEMENTS

The authors wish to thank A. Eggers, G. Eickert, and V. Hübner for providing oxygen microelectrodes, and D. de Beer for valuable comments on the manuscript. Thomas Etterer is acknowledged for providing the nitrate ionophor for the microelectrodes.

This work was carried out in the framework of the Research Center for Fundamental Studies of Aerobic Biological Wastewater Treatment (SFB 411), Munich, and financially supported by the German Research Foundation (DFG) and the Max-Planck-Society.

## REFERENCES

1. **Amann, R. I., B. J. Binder, R. J. Olson, S. W. Chisholm, R. Devereux, and D. A. Stahl.** 1990. Combination of 16S rRNA-targeted oligonucleotide probes with flow cytometry for analyzing mixed microbial populations. *Appl. Environ. Microbiol.* **56**:1919-1925.
2. **Arnz, P., E. Arnold, and P. A. Wilderer.** 2001. Enhanced biological phosphorus removal in a semi full-scale SBBR. *Water Sci. Technol.* **43**:167-174.
3. **Cech, J. S., and P. Hartman.** 1993. Competition between polyphosphate and polysaccharide accumulating bacteria in enhanced biological phosphate removal systems. *Water Res.* **7**:1219-1225.

4. **Christensson, M., L. L. Blackall, and T. Welander.** 1998. Metabolic transformations and characterisation of the sludge community in an enhanced biological phosphorus removal system. *Appl. Microbiol. Biotech.* **49**:226-234.
5. **Daims, H., P. Nielsen, J. L. Nielsen, S. Juretschko, and M. Wagner.** 2000. Novel *Nitrospira*-like bacteria as dominant nitrite-oxidizers in biofilms from wastewater treatment plants: diversity and *in situ* physiology. *Water Sci. Technol.* **41**:85-90.
6. **de Beer, D., A. Schramm, C. M. Santegoeds, and M. Kühl.** 1997. A nitrite microsensor for profiling environmental biofilms. *Appl. Environ. Microbiol.* **63**:973-977.
7. **Erhart, R.** 1997. *In situ* Analyse mikrobieller Biozönosen in Abwasserreinigungsanlagen. PhD thesis. Technical University Munich, Munich, Germany.
8. **Manz, W., R. Amann, W. Ludwig, M. Wagner, and K.-H. Schleifer.** 1992. Phylogenetic oligodeoxynucleotide probes for the major subclasses of proteobacteria: problems and solutions. *Syst. Appl. Microbiol.* **15**:593-600.
9. **Mino, T., M. C. M. van Loosdrecht, and J. J. Heijnen.** 1998. Microbiology and biochemistry of the enhanced biological phosphate removal process. *Water Res.* **32**:3193-3207.
10. **Mobarry, B. K., M. Wagner, V. Urbain, B. E. Rittmann, and D. A. Stahl.** 1996. Phylogenetic probes for analyzing abundance and spatial organization of nitrifying bacteria. *Appl. Environ. Microbiol.* **62**:2156-2162.
11. **Morgenroth, E., and P. A. Wilderer.** 1999. Controlled biomass removal - the key parameter to achieve enhanced biological phosphorus removal in biofilm systems. *Water Sci. Technol.* **39**:33-40.
12. **Neef, A.** 1997. Anwendung der *in situ*-Einzelzell-Identifizierung von Bakterien zur Populationsanalyse in komplexen mikrobiellen Biozönosen. PhD thesis. Technical University Munich, Munich, Germany.
13. **Pastorelli, G., R. Canziani, L. Pedrazzi, and A. Rozzi.** 1999. Phosphorus and nitrogen removal in moving-bed sequencing batch biofilm reactors. *Water Sci. Technol.* **40**:169-176.
14. **Prosser, J. I.** 1989. Autotrophic nitrification in bacteria. *Adv. Microb. Physiol.* **30**:125-181.
15. **Revsbech, N. P.** 1989. An oxygen microelectrode with a guard cathode. *Limnol. Oceanogr.* **34**:474-478.
16. **Revsbech, N. P., and B. B. Jørgensen.** 1986. Microelectrodes: their use in microbial ecology. *Adv. Microb. Ecol.* **9**:293-352.
17. **Schramm, A., D. de Beer, A. Gieseke, and R. Amann.** 2000. Microenvironments and distribution of nitrifying bacteria in a membrane-bound biofilm. *Environ. Microbiol.* **2**:680-686.
18. **Schramm, A., D. de Beer, M. Wagner, and R. Amann.** 1998. Identification and activities *in situ* of *Nitrosospira* and *Nitrospira* spp. as dominant populations in a nitrifying fluidized bed reactor. *Appl. Environ. Microbiol.* **64**:3480-3485.
19. **Smolders, G. J. F., J. van der Meij, M. C. M. van Loosdrecht, and J. J. Heijnen.** 1994. Stoichiometric model of the aerobic metabolism of the biological phosphorus removal process. *Biotechnol. Bioeng.* **44**:837-848.
20. **Wagner, M., R. Erhart, W. Manz, R. Amann, H. Lemmer, D. Wedi, and K.-H. Schleifer.** 1994. Development of an rRNA-targeted oligonucleotide probe specific for the genus *Acinetobacter* and its application for *in situ* monitoring in activated sludge. *Appl. Environ. Microbiol.* **60**:792-800.

21. **Wagner, M., G. Rath, H. P. Koops, J. Flood, and R. Amann.** 1996. *In situ* analysis of nitrifying bacteria in sewage treatment plants. *Water Sci. Technol.* **34**:237-244.
22. **Watanabe, Y., S. Okabe, K. Hirata, and S. Masuda.** 1995. Simultaneous removal of organic materials and nitrogen by micro-aerobic biofilms. *Water Sci. Technol.* **31**:195-203.
23. **Wilderer, P. A., P. Arnz, and E. Arnold.** 2000. Application of biofilms and biofilm support materials as a temporary sink and source. *Water Air Soil Poll.* **123**:147-158.

## **Chapter 4**

# **Community Structure and Activity Dynamics of Nitrifying Bacteria in a Phosphate-Removing Biofilm**

A. Gieseke, U. Purkhold, M. Wagner, R. Amann,  
and A. Schramm



## Community Structure and Activity Dynamics of Nitrifying Bacteria in a Phosphate-Removing Biofilm

Armin Gieseke<sup>1\*</sup>, Ulrike Purkhold<sup>2</sup>, Michael Wagner<sup>2</sup>, Rudolf Amann<sup>1</sup>,  
and Andreas Schramm<sup>1,3</sup>

<sup>1</sup>Molecular Ecology Group, Max Planck Institute for Marine Microbiology, D-28359 Bremen, Germany

<sup>2</sup>Department of Microbiology, Technical University Munich, D-85350 Freising, Germany

<sup>3</sup>Department of Ecological Microbiology, BITOEK, University of Bayreuth, D-95440 Bayreuth, Germany

The microbial community structure and activity dynamics of a phosphate removing biofilm from a sequencing batch biofilm reactor were investigated with special focus on the nitrifying community. O<sub>2</sub>, NO<sub>2</sub><sup>-</sup>, and NO<sub>3</sub><sup>-</sup> profiles in the biofilm were measured with microsensors at various times during the nonaerated-aerated reactor cycle. In the aerated period, nitrification was oxygen-limited and restricted to the first 200 μm at the biofilm surface. Additionally, a delayed onset of nitrification after the start of the aeration was observed. Nitrate accumulating in the biofilm in this period was denitrified during the nonaerated period of the next reactor cycle. Fluorescence in situ hybridization (FISH) revealed three distinct ammonia-oxidizing populations, related to the *Nitrosomonas europaea*, *N. oligotropha*, and *N. communis* lineages. This was confirmed by analysis of the genes coding for 16S rRNA and for ammonia monooxygenase (*amoA*). Based upon these results, a new 16S rRNA-targeted oligonucleotide probe specific for the *Nitrosomonas oligotropha* lineage was designed. FISH analysis revealed that the first 100 μm at the biofilm surface were dominated by members of the *N. europaea* and the *N. oligotropha* lineage, with a minor fraction related to *N. communis*. In deeper biofilm layers, exclusively members of the *N. oligotropha* lineage were found. This separation in space as well as a potential separation of activities in time are suggested as mechanisms to allow for the coexistence of the different ammonia-oxidizing populations. Nitrite-oxidizing bacteria belonged exclusively to the genus *Nitrospira* and could be assigned to a 16S rRNA sequence cluster found also in other sequencing batch systems.

## INTRODUCTION

Modern biological treatment of wastewater involves not only C removal but also elimination of the nutrients P and N (5, 20). This requires the combined or sequential action of

various groups of microorganisms like heterotrophic bacteria, phosphate-accumulating organisms (PAO), nitrifying and denitrifying bacteria. Consequently, purification plants and processes become increasingly complex to satisfy the needs of the different microorganisms, usually in several reactor stages (5, 27). The integration of different functions in a single reactor would save reaction space and time, and therefore is desirable from an economical point of view. However, difficulties often arise in establishing stable nitrification in such complex systems. Nitrifying bacteria [i.e., ammonia-oxidizing bacteria (AOB) and nitrite-oxidizing bacteria (NOB)], usually show low maximum growth rates, relatively low substrate affinities and high sensitivity to toxic shocks or sudden pH changes (17, 25, 41). In the presence of organic matter, they can be easily outcompeted by heterotrophs for oxygen (57) and ammonia (19). Other problems to be solved are the inhibition of denitrification by the presence of oxygen (5), and the need for cyclic changes of oxic and anoxic (i.e., free of oxygen and nitrate) conditions for biological phosphate removal (34). Biofilm systems are an obvious option for such multifunctional reactors. Slow growing organisms remain in the reactor by their attached growth; the biofilm matrix might protect bacteria from grazing, harmful substances or sudden pH shifts; and biofilms can be stratified and therefore provide oxic and anoxic reaction zones (11). During the last five years, several studies addressed nitrifying biofilms by a combination of microsensor measurements with 16S rRNA-based methods like fluorescence in situ hybridization (FISH; 39, 48, 50). This approach revealed, e.g., the identity and spatial arrangement of AOB and NOB in various nitrifying systems (39, 48-50), and a first estimate of their in situ reaction rates and substrate affinities (48). However, still very little is known of which and how nitrifying bacteria are adapted to the competition with heterotrophs in more complex systems, and how they interact with other processes.

Recently, a biofilm system was proposed, integrating enhanced biological phosphate removal (EBPR) and nitrification/denitrification in a single reactor (3, 18). The biofilm is subjected to a sequencing batch mode, where an anoxic treatment period is followed by an oxic period to allow for net accumulation of polyphosphate in the biomass, which is removed from the system by backwashing at regular intervals. Substrate balances revealed that the removal of organic carbon and EBPR were successfully combined with nitrogen removal via nitrification and denitrification (3).

In the present study, the microbial ecology of this combined nitrification-EBPR biofilm process was investigated by using microsensor analysis and various molecular techniques, i.e. FISH, and analysis of 16S rDNA and *amoA* gene sequences. The objectives were to reveal

which populations contribute to which part of the process, which AOB and NOB persist under these highly competitive and transient conditions, and how nitrifying activity overlaps, in time and space, with heterotrophic activity, especially EBPR.

## MATERIALS AND METHODS

**Process Description.** A 20 L sequencing batch biofilm reactor (SBBR) was established as described previously (18). The composition of the artificial wastewater used was as follows:  $\text{Na}(\text{CH}_3\text{COO}) \times 3 \text{H}_2\text{O}$  103 mg L<sup>-1</sup>, peptone 200 mg L<sup>-1</sup>,  $(\text{NH}_4)_2\text{SO}_4$  63 mg L<sup>-1</sup>,  $\text{KH}_2\text{PO}_4$  44 mg L<sup>-1</sup>, KCl 14 mg L<sup>-1</sup>, yeast extract 3 mg L<sup>-1</sup>, leading to influent concentrations of 12 mg L<sup>-1</sup> of P, 38 mg L<sup>-1</sup> of N, and a chemical oxygen demand (COD) of about 270 mg L<sup>-1</sup>. Oxygen and phosphate concentrations in the bulk water were regularly monitored by online measurements with an oxygen electrode (Oxy 196, WTW, Weilheim, Germany), and with a P analyzer (Phosphax Inter, Dr. Lange, Düsseldorf, Germany). Ammonium, nitrate, and COD were determined photometrically by use of standard test kits (LCK 303, 339, and 314, digital photometer ISIS 6000, Dr. Lange, Düsseldorf, Germany). The length of the operation periods were the following: 20 min of filling (min 0 to 20), 160 min of nonaerated recirculation (min 20 to 180), 260 min of recirculation with aeration (min 180 to 440), and 40 min draining (min 440 to 480). The process temperature was kept at 20°C. Biofilm was grown on substratum elements (Kaldnes, Purac, Merseburg, Germany), i.e. plastic rings (diameter 8 mm, height 8 mm), where biofilm could adhere to both, the outer surface and the central spaces within the ring. To remove biofilm material with incorporated polyphosphate, the system was back-washed once a week by use of pressurized air and water. Removal of biomass from the central spaces of the Kaldnes elements was not efficient, leading to complete clogging of these spaces. Preceding FISH analysis of the biofilm structure as described below revealed no visual difference in the composition and spatial organization of the main microbial populations in the upper part of biofilms originating from the external substratum surface and from the biofilm of clogged central spaces. Therefore, elements filled completely with biogenic material were chosen for microsensors measurements and FISH.

**Microsensor measurements.** To allow measurements during reactor operation, Kaldnes elements with biofilm were transferred during the initial filling period from the reactor to a separate 750 cm<sup>3</sup> flow chamber coupled to the recirculation of the reactor. Microsensors were inserted through small holes in the top lid, that were closed with stoppers during the non-

aerated period. Vertical concentration microprofiles were measured in the biofilm for oxygen using Clark type microsensors (45), and for ammonium, nitrite and nitrate using potentiometric ion-selective microelectrodes of the LIX type (15) as described previously. At least 20 profiles were measured for each parameter at different times covering the whole course of a treatment cycle. Measurements were distributed over 4 cycles to check for the similarity of conditions from different days of operation.

**Rate calculations.** Due to the periodic changes of the process conditions, the microprofiles measured in situ do not represent a steady state situation. Therefore, in the case of nitrate, profiles were corrected to allow the application of a one-dimensional diffusion-reaction model for calculation of specific volumetric rates of net consumption or production. In each nitrate profile, the first value measured in the bulk water was set to  $t = 0$ . Then for each depth the concentration change over time was calculated from two subsequent profiles. The resulting slope was used to correct the time-dependent change of concentration points at  $t > 0$  in each profile by linear interpolation. In that way, every profile is corrected for the dynamics of concentration changes leading to the elimination of transiency. The described correction procedure influenced absolute values of concentration in the deeper biofilm, but did not change the shape of the profiles. The correction of profile data was not applied to oxygen profiles because their appearance and the stability of bulk values throughout the oxic period of the process indicated a clear steady state situation with respect to oxygen.

Volumetric nitrification rates were calculated by applying a one-dimensional diffusion-reaction model to the corrected data. Each profile results from a combination of production (P), consumption (C), and diffusive transport as described by Ficks second law of one-dimensional diffusion, which, under steady state conditions ( $\partial c(z,t)/\partial t = 0$ ), can be written as

$$P - C = -D_s \cdot \partial^2 c(z,t) / \partial z^2$$

( $D_s$ : effective diffusion coefficient,  $c$ : solute concentration,  $z$ : depth, and  $t$ : time). Assuming a zero order reaction, volumetric net production was subsequently calculated by quadratic regression for each depth (38).

**DNA extraction.** DNA was extracted from native biofilm samples stored at  $-70^\circ\text{C}$  with the FastDNA-Extraction kit for soil (BIO 101, Carlsbad, CA, USA), as described in the manufacturer's instructions. The quality of DNA was checked by agarose gel electrophoresis (1%, wt/vol).

**16S rDNA analysis.** A 1 kb fragment of the 16S rDNA gene was amplified taking the complement of probe NOLI191 (43) as a forward and the unlabeled probe Nso1225 (35) as

reverse primer. The following reaction mixture was used: 50 pmol of each primer, 2.5  $\mu$ mol of each dNTP, 1  $\times$  PCR buffer, 1 U of SuperTaq DNA polymerase (HT Biotechnology, Cambridge, UK), 50 to 100 ng template DNA, and adjusted to 100  $\mu$ l with sterile water. PCR was performed with an Eppendorf Mastercycler (Eppendorf, Hamburg, Germany) in 35 cycles with hot start. The annealing temperature of 56°C for the primer set was determined in previous PCR runs with different temperature. After checking an aliquot of the PCR product by agarose gel electrophoresis, the DNA was directly ligated into the pGEM-T vector (Promega, Mannheim, Germany) according to the manufacturers instructions, and subsequently transformed to competent high efficiency *E. coli* cells (strain JM109; Promega, Mannheim, Germany). White and blue screening was used to screen for recombinant transformants. Inserts of positive clones were analyzed for redundancy by use of amplified rDNA restriction analysis (ARDRA) (44). One representative clone was sequenced for each distinct fragmentation pattern by Taq Cycle sequencing with the PCR primers or primers M13uni and M13rev on a model ABI377 sequencer (PE Corporation, Norwalk, CT, USA). The sequences were checked for chimera formation with the CHECK\_CHIMERA software of the Ribosomal Database Project (32). Sequences were aligned and analyzed by use of the ARB software package (55) based on the last release of the 16S rDNA sequence database of December 1998 and individually added sequences of recent publications. Trees were calculated for the clones and selected related sequences following the suggestions of Ludwig et al. (31). For tree calculation, maximum parsimony, distance matrix, and maximum likelihood methods were used, and the results combined in a consensus tree.

**Probe design.** Based on the newly retrieved and published sequences of the *Nitrosomonas oligotropha* lineage (40) a probe was designed using the PROBE\_DESIGN tool of ARB. The dissociation temperature of the probe was determined by hybridization with a pure culture of *Nitrosomonas ureae* isolate Nm10 at different formamide concentrations, ranging from 0 to 60% formamide. Analysis was done by confocal laser scanning microscopy (CLSM), and image analysis as described elsewhere (13). The specificity of the probe was checked against the ARB database and experimentally tested at the optimal hybridization conditions using the strains listed in Table 1.

**FISH.** Complete substratum elements with adhering biofilm were fixed with fresh 4% paraformaldehyde solution and alternatively with ethanol, washed with PBS, and stored in PBS/ethanol (1:1) at -20°C until further processing (1, 33). After freezing and removal of the plastic material, radial biofilm sections of 14  $\mu$ m thickness were prepared at -18°C, immobilized on gelatine coated microscopic slides and dehydrated in an ethanol series (50). In situ

hybridizations of cells in the biofilm were performed with fluorescently labeled, rRNA-targeted oligonucleotide probes according to Manz *et al.* (33). Probes and conditions are listed in Table 2. Probes labeled with the sulfoindocyanine dyes Cy3 and Cy5 were obtained from Interactiva (Ulm, Germany) and Biometra (Göttingen, Germany). In cases, where stringency conditions did not allow simultaneous hybridization with several probes, multiple probe hybridization was performed in subsequent steps by first hybridizing with the probe of higher stringency (59). The biofilm was additionally stained with DAPI after the hybridization step with a solution of 1 mg L<sup>-1</sup> for 10 minutes, or 100 mg L<sup>-1</sup> for 10 s for the purpose of polyphosphate staining, respectively (23). Samples were analyzed by standard epifluorescence microscopy on a Zeiss Axioplan II microscope and by CLSM on a Zeiss LSM 510 microscope (Carl Zeiss, Jena, Germany).

TABLE 1. Organisms used for determination of T<sub>d</sub>, their sequence at the target region, and hybridization results with probe Nmo218.

Organism/Probe	Sequence	FISH result with probe Nmo218
Probe sequence Nmo218 (3' to 5')	TACGAAAACCTCGCCGGC	
Target sequence (5' to 3')	AUGC UUUGGAGCGGCCG	
<i>Nitrosomonas ureae</i> Nm10 <sup>a</sup>	.....	+
<i>Nitrosomonas cryotolerans</i> Nm55 <sup>a</sup>	G.....	+
<i>Nitrosomonas aestuarii</i> Nm36 <sup>a</sup>	G.....	+
<i>Pseudomonas lemoignei</i> DSM 7445 <sup>b</sup>	....A.....	-
<i>Nitrosomonas communis</i> Nm2 <sup>a</sup>	G.....A.....	-
<i>Nitrosococcus mobilis</i> Nc2 <sup>a</sup>	GC.....	-

<sup>a</sup> Donated as fixed pure cultures from G. Timmermann, University of Hamburg, Germany.

<sup>b</sup> Active culture received from the German Culture Collection (DSMZ) and fixed as described in the text.

**Quantification of AOB and NOB.** Total AOB abundance was quantified by microscopical counting of cells hybridized with probes Nso1225 and Nso190 in several fields of view along a 50 µm thick horizontal layer up to a biofilm depth of 600 µm. Distinct populations of AOB were counted after hybridization with probes NEU and NOLI191. Quantification of NOB was done by confocal laser scanning microscopy as previously described (48), i.e., optical sections of a defined thickness of 0.6 µm were scanned, and, by determining the signal area and subsequent multiplication with a volume-specific cell abundance, the cell number for a given volume was calculated. Thorough calibration for NOB quantification was performed by counting DAPI stained cells in various scanned fields of view (n = 30), leading to volumetric indices with a 95% confidence interval of +/- 7%. Results with all probes used for

quantification were corrected for nonspecific binding by results with probe NON338 as a negative control.

For quantitative population analysis with FISH means as well as medians were calculated to describe the distribution of the AOB and NOB populations.

TABLE 2. Oligonucleotide probes and hybridization conditions used in this study.

Probe	Probe Sequence (5' to 3')	Target site <sup>a</sup>	Target organism(s)	FA [%] <sup>b</sup>	NaCl [mM] <sup>c</sup>	Reference
EUB338	GCTGCCTCCGTTAGGAGT	16S (338-355)	Domain <i>Bacteria</i>	20	225	(1)
NON338	ACTCCTACGGGAGGCAGC	16S (338-355)	Complementary to EUB338	20	225	(33)
ALF968	GGTAAGGTTCTGGCGTT	16S (968-985)	Most $\alpha$ -proteobacteria and other bacteria	35	80	(37)
ALF1b	CGTTGGTCTGAGCCAG	16S (19-35)	Most $\alpha$ -proteobacteria and other bacteria	20	225	(33)
ALF4-1322	TCCGCCTTCATGCTCTCG	16S (1322-1339)	Subgroup 4 of $\alpha$ -proteobacteria	40	56	(37)
RRP1088	CGTTGCCGGACTTAACC	16S (1088-1104)	Genera <i>Rhodobacter</i> , <i>Rhodovulum</i> , <i>Roseobacter</i> , <i>Paracoccus</i> and other bacteria	0	900	(37)
BET42a <sup>d</sup>	GCCTCCCACTTCGTTT	23S (1027-1043)	$\beta$ -Proteobacteria	35	80	(33)
HGC69a	TATAGTTACGACCGCGT	23S (1901-1918)	Gram-positive bacteria with high GC content	20	225	(46)
HGC1351	CAGCGTGTCTGATCTCG	16S (1351-1368)	Gram-positive bacteria with high GC content	30	112	(16)
GAM42a <sup>d</sup>	GCCTCCCACTTCGTTT	23S (1027-1043)	$\gamma$ -Proteobacteria	35	80	(33)
Nso1225	CGCCATTGTATTACGTGTGA	16S (1225-1244)	Ammonia-oxidizing $\beta$ -proteobacteria	35	80	(35)
Nso190	CGATCCCGCTGTTTCTCC	16S (190-208)	Ammonia-oxidizing $\beta$ -proteobacteria	55	20	(35)
Nsm156	TATTAGCACATCTTCGAT	16S (156-174)	Various <i>Nitrosomonas</i> spp.	5	636	(35)
Nsv443	CCGTGACCGTTCGTTCCG	16S (444-462)	<i>Nitrospira</i> spp.	30	112	(35)
NmII	TTAAGACACGTTCCGATGTA	16S (120-139)	<i>Nitrosomonas communis</i> -lineage	25	159	(40)
NmIV	TCTCACCTCTCAGCGAGCT	16S (1004-1023)	<i>Nitrosomonas cryotolerans</i> -lineage	35	80	(40)
NEU <sup>d</sup>	CCCTCTGCTGCCTCTA	16S (653-670)	Halophilic and halotolerant members of the genus <i>Nitrosomonas</i>	40	56	(61)
Nse1472 <sup>e</sup>	ACCCAGTCATGACCCCC	16S (1472-1489)	<i>N. europaea</i>	50	28	(22)
NmV	TCCTCAGAGACTACGGGG	16S (174-191)	<i>Nitrosococcus mobilis</i> lineage	35	80	(40)
NOL1191	CGATCCCACTTTCCCTC	16S (191-208)	Various members of the <i>Nitrosomonas oligotropha</i> lineage	30	112	(43)
cNOL1 <sup>f</sup>	CGATCCCACTTTCCCC	16S (191-208)				This study
Nmo218	CGCGCTCCAAAAGCAT	16S (218-235)	<i>Nitrosomonas oligotropha</i> lineage	35	80	This study
NIT3 <sup>g</sup>	CGTGTCTCCATGCTCCG	16S (1035-1048)	<i>Nitrobacter</i> spp.	40	56	(62)
NSR826	GTAACCCGCGACACTTA	16S (826-843)	Various <i>Nitrospira</i> spp.	20	225	(49)
NSR1156	CCGTTCTCTCTGGGAGT	16S (1156-1173)	Various <i>Nitrospira</i> spp. <sup>h</sup>	30	112	(49)
Nspa712 <sup>d, i</sup>	CGCCTTCGCCACCGGCTTCC	16S (712-732)	Phylum <i>Nitrospira</i>	35	80	(14)
Nspa662 <sup>d, i</sup>	GGAAATCCGCGCTCCCTT	16S (662-679)	Genus <i>Nitrospira</i>	35	80	(14)

<sup>a</sup> rRNA position according to *E. coli* numbering (9).

<sup>b</sup> Percentage of formamide in the hybridization buffer.

<sup>c</sup> Concentration of sodium chloride in the washing buffer.

<sup>d</sup> Used together with equimolar amount of unlabeled competitor oligonucleotide as indicated in the reference.

<sup>e</sup> Referred to as S<sup>+</sup>-Nse-1472-a-A-18 in the reference.

<sup>f</sup> Unlabeled competitor oligonucleotide applied in equimolar amount to discriminate against weak mismatches in *Thiobacillus thioparvus* and two *Azarcus* spp. sequences

<sup>g</sup> Excluding clones described by Burell et al. (10)

<sup>h</sup> Referred to as S<sup>+</sup>-Nspa-0712-a-A-21 and S-G-Nspa-0662-a-A-18, respectively, in the reference

**Analysis of *amoA* sequences.** To supplement results from FISH and the specific 16S rDNA library, comparative sequence analysis of biofilm derived 491 bp fragments of the ammonia monooxygenase gene (*amoA*) was performed as previously described (42). Amplificates of *amoA* were separated according to their GC content using agarose gel retardation as described by Schmid et al. (47).

**Nucleotide sequence accession numbers.** The 16S rDNA partial sequences obtained in this study are available from the EMBL nucleotide sequence database under accession numbers AJ297415 to AJ297419. The *amoA* partial sequences appear under the accession numbers AF293065 to AF293075 and AY007575.

## RESULTS

**Functional analysis.** Concentrations of the solutes measured by microsensors in the bulk liquid of the measuring setup closely reflected the bulk liquid composition in the reactor as determined independently by online monitoring (data not shown).

During the nonaerated period, oxygen could neither be detected in the bulk water nor in the biofilm at any time. During the aerated period of the process the biofilm was supplied with oxygen in amounts of  $227.8 \pm 5.4 \mu\text{M}$  (mean  $\pm$  SD,  $n = 16$ ) corresponding to  $80.2 \pm 1.9 \%$  air saturation. Oxygen penetration into the biofilm was limited to a depth of  $200 \mu\text{m}$  (Fig. 1), leaving substantial parts of the biofilm, anoxic during the whole treatment. The average areal oxygen uptake remained stable throughout the oxic period at  $0.84 \pm 0.05 \mu\text{mol cm}^{-2} \text{h}^{-1}$  (mean  $\pm$  SD,  $n = 16$ ). Neither the penetration depth nor the slope through the diffusive boundary layer were significantly altered during the oxic period (Fig. 1).

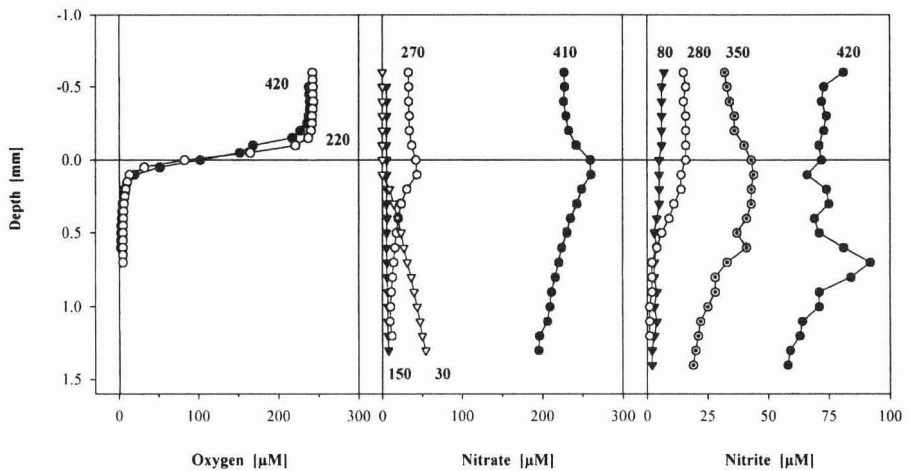


FIG. 1. Representative examples of vertical concentration microprofiles of oxygen, nitrate, and nitrite measured in the biofilm at different times of the reactor cycle. Numbers refer to the time in minutes after start of the treatment cycle (start of aeration:  $t = 180 \text{ min}$ ).

With ammonium, nitrate, and nitrite, absolute concentrations showed a certain variability, but the shape and time course of profiles were similar between different cycles. A strong initial decrease of ammonium directly after filling from  $2300 \mu\text{M}$  ( $t = 25 \text{ min}$ ) to  $950 \mu\text{M}$  ( $t = 60 \text{ min}$ ) could be observed in the biofilm analogous to the decline within the bulk water in the first 60 min (profiles not shown). Later, the concentration of ammonium decreased less but continuously up to the end of the treatment cycle to a value of  $800 \mu\text{M}$ . The concentration

in the biofilm followed this pattern. As no gradients of ammonium were observed above or within the biofilm, ammonium uptake of the whole biofilm or of any specific layer could not be quantified.

Production of nitrate during oxic conditions was restricted to a narrow surface layer of about 200  $\mu\text{m}$ , causing an accumulation of nitrate in the bulk water up to 230  $\mu\text{M}$  in the final period of the treatment (Fig. 1). The highest concentration of nitrate measured in the productive layer was 260  $\mu\text{M}$ . During the following nonaerated period (after draining and refilling the system), remaining nitrate was detected up to a concentration of 200  $\mu\text{M}$  in the deeper biofilm zones, but it continuously decreased during the anoxic period. At the beginning of the aeration ( $t = 180$  min), no nitrate from the previous treatment cycle was left in the biofilm (Fig. 1). The shape of nitrate profiles supported a denitrifying activity in the deeper biofilm layer. Nitrite accumulated during aeration up to 75  $\mu\text{M}$ . In the second half of the aerated treatment period, even a stronger local production of nitrite occurred in the deeper biofilm layers in a depth of 600 to 700  $\mu\text{m}$ , probably due to denitrification, with concentrations of more than 90  $\mu\text{M}$  (Fig. 1).

During the aerated period, there was a conspicuous delay in the first occurrence of both nitrite and nitrate compared to the onset of aeration. Detectable amounts of both solutes ( $> 1$   $\mu\text{M}$ ) first were measured at  $t = 270$  min, i.e. 90 min after onset of aeration.

A nitrogen balance based on nitrification products (300  $\mu\text{M}$ ), remaining ammonium (800  $\mu\text{M}$ ), and an assumed stripping and incorporation into bacterial biomass of 25% (61) indicates an unresolved N loss of about one third.

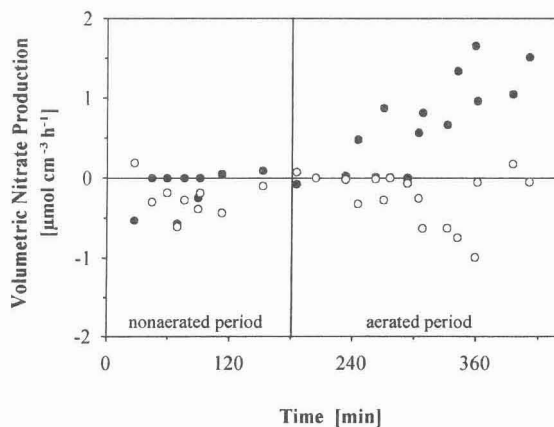
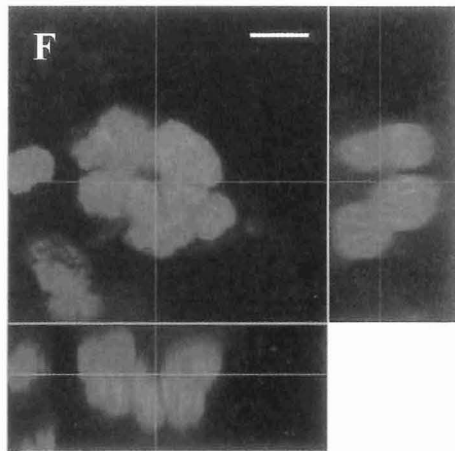
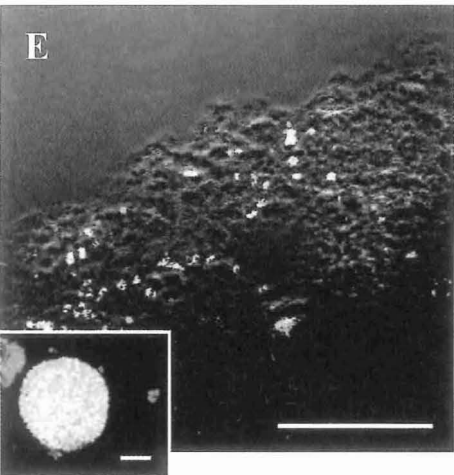
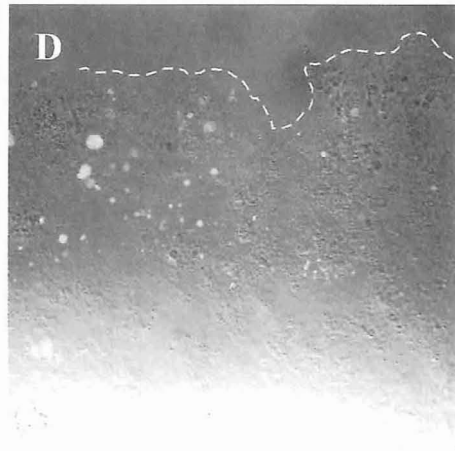
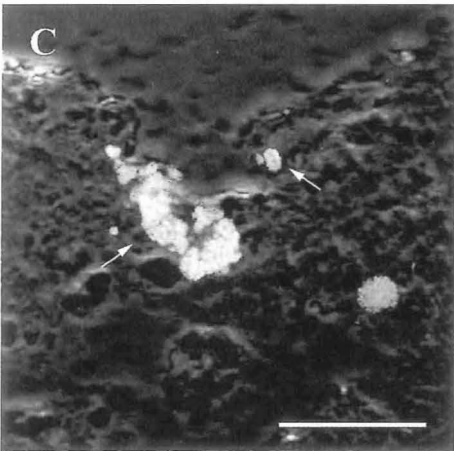
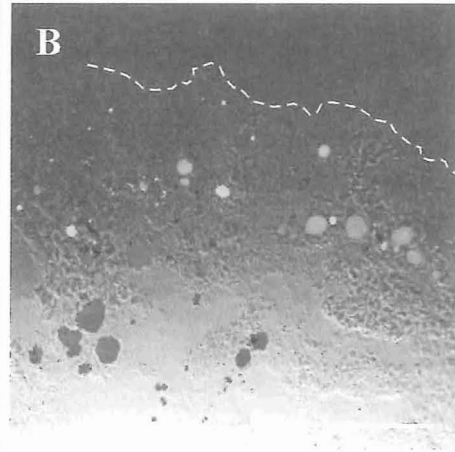
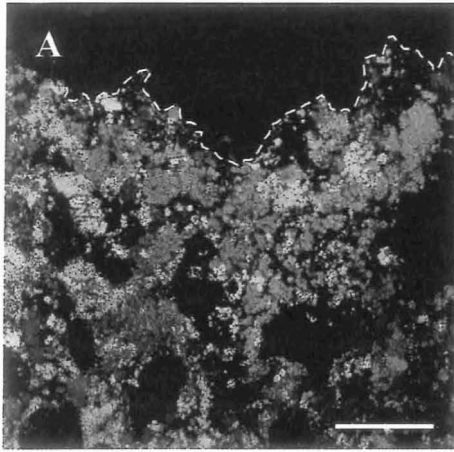


FIG. 2. Volumetric net production and consumption of nitrate at the biofilm surface [0 to 200  $\mu\text{m}$  (●)] and in the deeper biofilm [300 to 600  $\mu\text{m}$  (○)] during the reactor cycle. Data points originate from measurements of nitrate microprofiles of four different batch runs. For details of calculation see text.

**Calculation of nitrate production.** Volumetric nitrate production rates were separately estimated for the productive surface (0 to 200  $\mu\text{m}$  depth) and the deeper biofilm (300 to 600  $\mu\text{m}$ ) from profile data measured in 4 different batch runs. The deeper layer showed some denitrifying activity up to about  $1.0 \mu\text{mol cm}^{-3} \text{h}^{-1}$  at  $t = 360 \text{ min}$ , evolving together with nitrifying activity in the upper layer. The nitrate production in the surface layer during aeration reached maximum estimated rates of  $1.7 \mu\text{mol cm}^{-3} \text{h}^{-1}$  (corresponding to  $0.03 \mu\text{mol cm}^{-2} \text{h}^{-1}$ ) and, thus, accounted for about 7% of the oxygen uptake at the end of the process (Fig. 2).

**Broad-scale community structure.** Among all phylogenetic groups tested, four groups dominated the biofilm community as shown by FISH: (i) members of the gram-positive bacteria with high DNA G+C content (GPBHGC), mainly coccoid cells forming loose aggregates, (ii) members of the  $\beta$ -proteobacteria, forming dense layers at the very surface and dense globular aggregates mostly located within the upper 200  $\mu\text{m}$ , (iii) a population morphologically similar to the GPBHGC, with cells typically arranged in tetrads, that hybridized with probes ALF968, ALF1b, and GAM42a but not with probes for subgroups of the  $\alpha$ -proteobacteria (Fig. 3A), leaving their phylogenetic affiliation as yet unresolved, and (iv) members of the phylum *Nitrospira* (see below). Other phylogenetic groups together did not account for more than 20% of the microbial community in the biofilm (data not shown). The vast majority of all cells was located in the upper 300  $\mu\text{m}$  of the biofilm whereas in the deeper, permanently anoxic layers only few cell aggregates could be detected occasionally.

FIG. 3. Confocal laser-scanning micrographs of vertical thin sections of biofilm as hybridized with different fluorescent oligonucleotide probes. (A) Overview of the biofilm surface hybridized with ALF968 and HGC1351 (coloured in green and red, respectively). (B) Aggregates of  $\beta$ -subclass AOB as hybridized with Nso1225 (green) and NOB of the genus *Nitrospira* (Ntspa662; red). (C) Clustered aggregates (arrows) of members of the *N. communis* lineage (NmII, red) among the population  $\beta$ -subclass AOB (Nso1225, green). Colocalization of the two probes results in a yellow colour. (D) Aggregates of members of the *N. europaea* lineage as hybridized with probe NEU (green) and of the *N. oligotropha* lineage as hybridized with probe NOLI191 (red). (E) Colocalization of signals after hybridization with probes specific for the  $\beta$ -subclass AOB (Nso1225, green) and the *N. oligotropha* lineage (Nmo218, red); the insert shows a big aggregate as hybridized with probes Nso1225 (green) and NOLI191 (red). (F) Orthogonal representation of a dense assemblage of *Nitrospira* sp. as hybridized with probe Ntspa662. Scale bars are 50  $\mu\text{m}$  (A, B, D, and E), 25  $\mu\text{m}$  (C), and 5  $\mu\text{m}$  (insert in panels E, and F), respectively. Dashed lines indicate the surface of the biofilm exposed to the wastewater.



Additional staining with DAPI in high concentrations, indicating polyanionic inclusions by yellow fluorescence (23), was exclusively colocalized with hybridization signals for GPBHGC. However, only a fraction of the GPBHGC population was stained yellow with DAPI.

**AOB community structure.** A common problem for the quantification of nitrifying bacteria is the formation of dense aggregates resulting in a typical patchy distribution of AOB and NOB (Fig. 3). Therefore, neither normal distribution of values nor homogeneity of variances is given throughout the biofilm. For that reason, the median may be a better representative of cell densities than the mean, and will be given in the following sections. To allow comparison with other studies, however, both means and medians are displayed in Fig. 4.

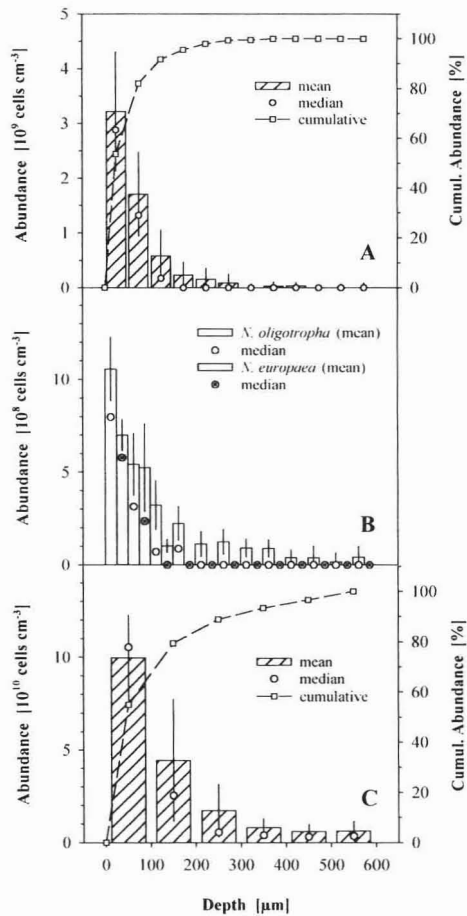


FIG. 4. Depth distribution of  $\beta$ -subclass AOB (A), of populations affiliating to different lineages of the genus *Nitrosomonas* (B), and of the NOB *Nitrospira* spp. (C) in the investigated biofilm. Numbers are given as volume-specific abundances. Cumul, cumulative. Note the different scales of the ordinates.

The globular aggregates hybridizing with probe BET42a were shown to belong to the AOB of  $\beta$ -proteobacteria by FISH with probes Nso1225 and Nso190 (Fig. 3B). The abundance of AOB was highest at the biofilm surface (Nso1225:  $2.9 \times 10^9 \text{ cm}^{-3}$ ; Nso190:  $2.0 \times 10^9 \text{ cm}^{-3}$ ), and declined below  $1 \times 10^8 \text{ cm}^{-3}$  within the first 200  $\mu\text{m}$ . A cumulative mean of 95% of all AOB could be detected within the first 200  $\mu\text{m}$  (Fig. 4A). A few single aggregates of  $\beta$ -ammonia oxidizers occurred in the deeper biofilm as well, but the abundance in these layers on average was very low. Hybridization with probes Nsm156 and Nsv443 revealed that the complete AOB community consisted of members of the genus *Nitrosomonas*. Within this genus, three different subgroups of AOB were detected. The smallest fraction (which was not further quantified) belonged to the *Nitrosomonas communis* lineage (40) of  $\beta$ -subclass AOB as identified by hybridization with probes Nso1225 and NmII (Fig. 3C). They formed small aggregates and were restricted to the upper 100  $\mu\text{m}$ . The two dominating subpopulations showed distinct distribution patterns. One population belonged to the *N. europaea* lineage of  $\beta$ -subclass AOB (40) as identified by hybridization with probes Nso1225, Nsm156, and NEU (Fig. 3D). Hybridization with Nse1472 or NmV resulted in no signals, indicating that the population is not identical with *N. europaea* or *Nitrosococcus mobilis*. The second population hybridized with probes Nso1225 and NOLI191 (Fig. 3D, E), a probe that had been designed for the *N. oligotropha* lineage (40) based solely on the sequence of *N. ureae* (43). Both groups together accounted for 55 up to 100% of  $\beta$ -subclass AOB hybridizing with probe Nso1225 in the upper 200  $\mu\text{m}$  of the biofilm. At the surface, 22% and 33% of Nso1225-positive cells hybridized with probes NEU and NOLI191, respectively. In a depth of 200  $\mu\text{m}$ , about 90% of Nso1225 positive cells hybridized with probe NOLI191, whereas the abundance of the *N. europaea* lineage declined to less than 10% (Fig. 4B). No signals were detected after hybridizations with probes NmIV indicative for *Nitrosomonas cryotolerans*.

**AOB-specific PCR.** Because hybridization with one single probe is sometimes not sufficient to prove identity of a given cell (2), a specific PCR and cloning strategy was applied to support the occurrence of populations affiliated with the *N. oligotropha* lineage within the biofilm. From the 26 clones analyzed by ARDRA, 10 different restriction patterns were obtained. Three of the patterns, representing a total of 13 clones, were indicative for sequences most similar to *Nitrosomonas* sp. isolate JL21 (56), a member of the *N. oligotropha* lineage (Fig. 5). Two patterns, representing a total of 8 clones, belonged to sequences most similar to *Nitrosomonas communis* Nm2. The remaining 5 clones with different ARDRA patterns represented single sequences not related to the genus *Nitrosomonas*. The amplification of

these sequences and of the ones similar to *Nitrosomonas communis* was due to insufficient primer discrimination under the conditions chosen.

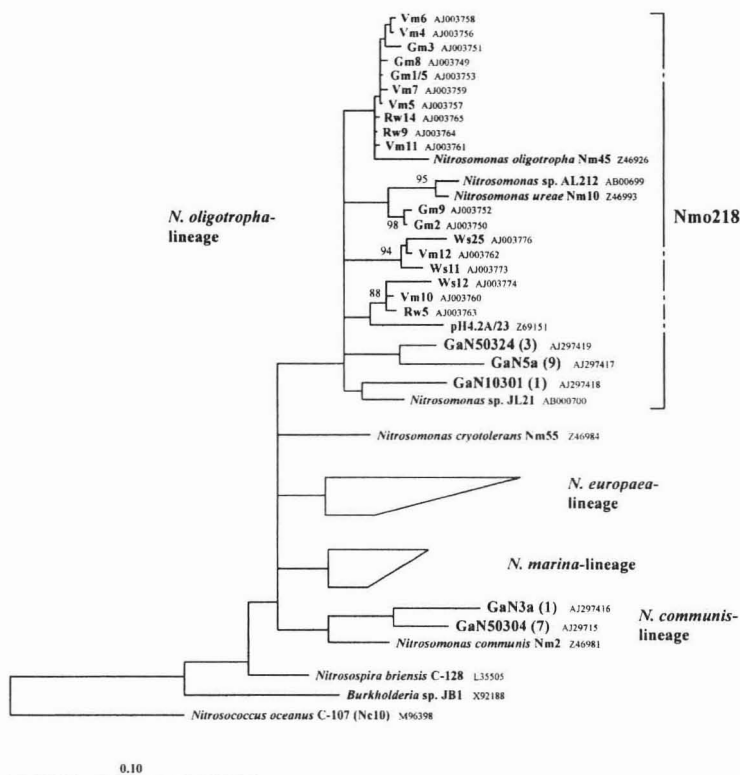


FIG. 5. Phylogenetic tree of the genus *Nitrosomonas* inferred from comparative analysis of 16S rDNA sequence data. Accession numbers of the published sequences used are given in the tree. Sequences with accession no. AB000701, AB000702, AJ005546, M96399, M96402, M96403, and Z46987 were used as representatives for the *N. europaea* lineage, and sequences with accession no. AJ003777, M96400, Z46990, Z69091, and Z69097 represent the *N. marina* lineage. The number of clones with identical ARDRA patterns for each sequence are given in brackets. Phylogenetic reconstruction is based on a maximum likelihood tree calculated from 950 informative positions with a genus-specific 50% positional variability filter. Tree topology was tested using distance matrix and maximum parsimony methods, and a consensus tree was drawn. Multifurcations connect branches for which a relative order could not unambiguously be determined with the different treeing methods used. Bootstrap values (100 cycles) refer to the maximum parsimony tree. Values smaller than 80% were omitted. The sequence of *N. oligotropha* isolate Nm45 was added to the consensus tree using the ARB maximum parsimony method without changing the tree topology. The bar represents 10% estimated sequence divergence.

**Design and application of Probe Nmo218.** The sequence of probe NOLI191 differs from the target site of most of the recently reported 16S rRNA sequences of the *N. oligotropha* lineage (e.g., (42, 52, 56). Furthermore, the probe hybridizes to organisms (e.g., *Pseudomonas lemoignei*) not belonging to the intended target group. Therefore, we designed probe Nmo218 encompassing the whole *N. oligotropha* lineage (Fig. 5). Probe sequence and binding sites of

target and non-target organisms are displayed in Table 1. The dissociation temperature of the probe was  $40.1 \pm 1.7^\circ\text{C}$ , optimal formamide concentration in the hybridization buffer was 35%. When applied under these conditions, probe Nmo218 did not hybridize with any negative controls, except for *Nitrosomonas cryotolerans* and *N. aestuarii* (Table 1). (The sequences of 5 clones with identical binding site to *N. cryotolerans* or *N. aestuarii* might also not be discriminated). The occurrence of *N. cryotolerans* can, however, be ruled out by parallel use of probe NmIV. Hybridization of probe Nmo218 to the biofilm resulted in a similar picture as with probe NOLI191 (Fig. 3D and E). However, simultaneous hybridization with both probes revealed a certain amount of organisms only hybridizing with either of both probes. Cells of *N. aestuarii* hybridized with probe Nmo218 (Table 1) but not with probe NOLI191. Consequently, cells showing this hybridization pattern might be related to *N. aestuarii*.

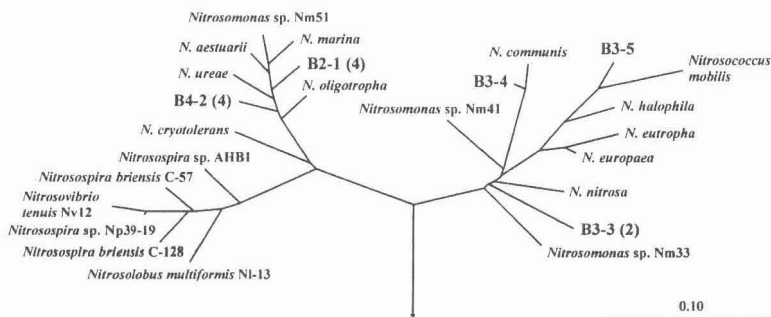


FIG 6. Phylogenetic FITCH-Margoliash *amoA* tree [using global rearrangement and randomized input order (7 jumbles)] showing the position of the 12 recovered biofilm sequences in relation to described  $\beta$ -subclass AOB (42). The bar indicates 10% estimated sequence divergence. The root was determined using the *amoA* sequences of  $\gamma$ -subclass AOB (42). Cloned *amoA* sequences with amino acid similarities  $> 99\%$  are represented by a single clone - the number in brackets indicates the number of clones for each representative. Clones labeled with the prefix B2, B3, and B4, respectively, were obtained from different gel retardation bands.

**AOB diversity assessed by comparative *amoA* sequence analysis.** Specific amplification of the *amoA* gene fragments from extracted biofilm DNA and subsequent separation by gel retardation resulted in three clearly visible *amoA* bands. All bands were excised, and separately cloned and sequenced. In total, 12 *amoA* clones (four from each band) were analyzed which represented five phylogenetically distinct  $\beta$ -subclass AOB (Fig. 6). Two clusters (representing two different bands), each containing four *amoA* sequences, were found within the *Nitrosomonas marina*-*N. oligotropha* lineages (which can not clearly be distinguished using *amoA* sequences) (42). The third band contained a higher diversity of *amoA* sequences. One *amoA* clone was closely related to *Nitrosomonas communis*. Another clone was affiliated with

*Nitrosococcus mobilis* which could not be detected in the biofilm by FISH. The two remaining *amoA* clones obtained from the third band clustered together and formed an independent lineage not closely related to any described AOB.

**NOB community structure.** The only NOB detected in the system were of the genus *Nitrospira* as identified by hybridization with probes Ntspa712, Ntspa662, and NSR826 (Fig. 3B and 3F). Low numbers of cells hybridized also with probe NSR1156. The abundance of *Nitrospira* spp. in the upper 100  $\mu\text{m}$  of the biofilm was  $1.1 \times 10^{11} \text{ cm}^{-3}$ , and therefore about 30 times higher than the abundance of  $\beta$ -subclass AOB as quantified with probe Nso1225. In comparison to the AOB, the vertical distribution was broadened towards depth. Within the section investigated, a 95% limit in cumulative (mean) abundance was reached not before 400  $\mu\text{m}$  depth, and numbers were high even in deeper layers of the biofilm (Fig. 4C).

**Cell-specific nitrification rates.** The average cell density of NOB in the upper 200  $\mu\text{m}$  of the biofilm where nitrification was mainly performed was  $6.6 \times 10^{10} \text{ cm}^{-3}$ . As nitrate production in this layer during aeration in average was  $0.7 \mu\text{mol cm}^{-3} \text{ h}^{-1}$ , conversion rates were about  $0.01 \text{ fmol nitrite cell}^{-1} \text{ h}^{-1}$  for the final aerated period. Maximum rates were  $0.025 \text{ fmol nitrite cell}^{-1} \text{ h}^{-1}$ . Cell-specific ammonia oxidation rates can only be roughly estimated based on nitrate production rates. With the average abundance of AOB of  $1.09 \times 10^9 \text{ cm}^{-3}$  in the upper 200  $\mu\text{m}$ , mean conversion rates were at least  $0.65 \text{ fmol ammonium cell}^{-1} \text{ h}^{-1}$  (maximum:  $1.5 \text{ fmol ammonium cell}^{-1} \text{ h}^{-1}$ ). However, because of the accumulation of nitrite within the nitrification zone, this number clearly is an underestimate.

## DISCUSSION

**Biofilm activity and community structure.** In the studied biofilm, biological phosphorus removal is combined with nitrogen removal via nitrification and denitrification. Nitrification is typically performed by distinct phylogenetic groups and will be discussed later. For biological P removal, involvement of various groups has been suggested, e.g., GPBHG (12, 60), members of the genus *Rhodocyclus* (7, 8, 21), or a mixture of multiple species (34). The high abundance of GPBHG and the detection of DAPI-stainable inclusions indicative for polyphosphate (23) in part of this population strongly promotes the first hypothesis for our system. However, the fixation procedure used might have led to the disappearance of polyphosphate granules (21), and therefore PAO, especially among Gram negative bacteria, might have been overlooked.

Denitrification can not at all be assigned to a certain microbial population nor is it restricted to a certain zone of the biofilm. During the anoxic period, the surface layers denitrify nitrate that has been accumulated during the oxic period of the preceding cycle (Fig. 1 and 2), and by that contribute about 20% to the total N loss. During the oxic period, the deeper parts of the biofilm remain anoxic and are provided with nitrate via nitrification (Fig. 1). The contribution of denitrification in the 300 to 600  $\mu\text{m}$  deep biofilm during the oxic period to total N loss is about 15%. Because there are reports about denitrifying PAO (28, 58), and because GPBHCG as potential PAO were found in close proximity to nitrifying bacteria, the source of nitrate, involvement of PAO into denitrification appears to be possible. However, this cannot be proven based upon our data.

**Competition for oxygen.** Nitrification as well as phosphate uptake both require oxygen. Therefore, competition for oxygen is to be expected between the respective microbial populations during the aerated period. Microsensor data indicate that the nitrifying bacteria were oxygen limited. Oxygen penetration was low, whereas ammonium was present in excess during the whole process. The distribution of AOB and NOB in general corresponds to the oxygen penetration depth, supporting findings of earlier studies (39, 50). The delayed onset of nitrification after the start of the aeration, and the accumulation of nitrite in spite of the high abundance of NOB very likely reflects limited supply of oxygen, too. Due to their high  $K_m$  for oxygen, AOB as well as NOB are poor competitors compared to heterotrophic bacteria (17, 41, 57). Thus, during the initial aerated period, oxygen is taken up preferentially by heterotrophs as the PAOs. As the phosphate uptake rate declines with the ongoing aeration period (data not shown), the stoichiometric oxygen demand of PAO metabolism decreases as well (51). Consequently, during the course of the aerated period, phosphate accumulation is most likely replaced by nitrification in terms of oxygen consumption.

**Nitrification rates.** The handling of concentration data to estimate volumetric nitrate production rates (see Materials and Methods section) is based on two assumptions: (i) low lateral heterogeneity of the concentration in the biofilm at a certain time, and (ii) slow dynamics of the concentration changes due to activity compared to those due to diffusion (i.e., a *pseudo* steady state situation). Structural analysis showed a certain lateral inhomogeneity based mostly on the clustering of nitrifiers (Fig 3B) but inhomogeneity is low in horizontal direction, and the resolution of the measurements was not in the range of the cluster size. Therefore, the first assumption is not violated. For a similar system (36) it was shown that the time required to reach equilibrium state was 1.8 min in a biofilm of 500  $\mu\text{m}$  thickness. This is quite short compared to the overall cycle dynamics observed here. Nevertheless, the second

assumption may introduce some error, especially in highly dynamic layers. The rates determined here should therefore be regarded as best estimates.

Both the estimated cell-specific in situ ammonia oxidation and nitrate production rate are on the order of magnitude of those calculated for aggregates of a nitrifying fluidized bed reactor based on microsensor measurements (48), and the ammonia oxidation rate estimated by a process mass balance of a sewage treatment plant (61). Unfortunately, the resolution of our measurements was too low to distinguish ammonia oxidation rates between the surface layer (with the mixed nitrifying community) and the deeper layer (with the *N. oligotropha*-like population). Also, different activities of each of the individual AOB populations in the surface layer, or of individual cells within a monospecies cluster can not be resolved. Therefore, it has to be noted that the cell-specific ammonia oxidation rate calculated here represents an average value for a diverse assemblage of AOB consisting of at least three different populations.

**Community structure of AOB.** The combined approach of FISH, 16S rDNA and *amoA* analysis led to the unexpected but consistent result of several different AOB populations occurring in close spatial vicinity. In contrast, previous studies in biofilms and activated sludge usually reported one single population dominating the system, e.g., populations related to *N. europaea* (39, 50), *Nitrosococcus mobilis* (22), or members of the genus *Nitrosospira* (39, 49). This raises the question of what mechanisms allow for the coexistence of the different AOB populations in the biofilm studied here.

*N. communis*-like AOB were only found within the first 100  $\mu\text{m}$  at the biofilm surface, and only in low abundance. Isolates of this lineage originally have been obtained from soils (24), and were recently also detected in activated sludge and biofilm systems (42). Unfortunately, the lack of ecophysiological data about *N. communis*, and its exclusive occurrence in the same zone together with both members of the *N. europaea*- and *N. oligotropha*-like AOB leave the specific adaptation of *N. communis*-like AOB to our system unresolved at present.

The second population was identified as members of the *N. europaea* lineage, however, not being identical with *N. europaea* itself. The low number of *amoA* sequences analyzed allows for some hidden diversity, as several clones might be represented by one band in the gel retardation. The *N. europaea*-like population detected by FISH might thus not be represented by any *amoA* clone. Members of this phylogenetic cluster, as e.g., *N. europaea* and *N. eutropha* are typically isolated from activated sludge systems (24), and the maximum substrate conversion rates for *N. europaea* are high compared to other strains of AOB (41). Pure culture and chemostat experiments revealed low substrate affinities for *N. europaea* with  $K_m$  ( $\text{NH}_4^+$ )

values in the range of 0.4 to 7 mM (41), and 0.88 to 1.96 mM (29), respectively. The same is true for oxygen affinity, with  $K_m$  ( $O_2$ ) values between 6.9 and 17.4  $\mu\text{M}$  (29). While ammonium concentrations in the biofilm exceeded most of the reported  $K_m$  values, oxygen limitation for *N. europaea*-like AOB is obvious. Between a depth of 100 and 200  $\mu\text{m}$ , the oxygen concentration decreases from  $33.8 \pm 5.45 \mu\text{M}$  to  $7.0 \pm 1.01 \mu\text{M}$  (means  $\pm$  SD,  $n = 15$ ). Consequently, *N. europaea*-like AOB virtually disappear within these layers (Fig. 4B). Here, the biofilm is dominated by *N. oligotropha*-like AOB with an abundance of  $1 \times 10^8$  to  $2 \times 10^8$  cells  $\text{cm}^{-3}$  down to a depth of 400  $\mu\text{m}$ . Based on 16S rDNA sequence analysis, members of the *N. oligotropha* lineage [also referred to as *Nitrosomonas* cluster 6a (26, 54)] have recently been detected in freshwater and brackish environments (52, 53), terrestrial habitats (26, 54), and activated sludge (42, 56). This suggests high physiological versatility and ecological importance. Isolates of this lineage are sensitive to ammonium concentrations exceeding 10 to 60 mM (24, 53, 56), show low  $K_m$  ( $\text{NH}_4^+ + \text{NH}_3$ ) values, and possess urease activity (53). These features support adaptation of the *N. oligotropha* lineage to low substrate concentrations. Although no kinetic data with respect to oxygen are available, this might also imply high affinity towards oxygen. Lower  $K_m$  ( $O_2$ ) values of the *N. oligotropha*-like AOB than the values reported for *N. europaea*-related AOB could be responsible for the outcompetition of the latter at the oxic/anoxic transition zone in the biofilm. At the biofilm surface, however, both populations were found to coexist in almost equal abundance. Assuming higher maximum substrate conversion rates for *N. europaea*-like AOB (41), they should be able to outcompete other AOB in this zone. For explanation of the co-occurrence, the dynamics of the system have to be taken into account, i.e. the metabolic activity of the populations might be separated in time. In the initial aeration period, in particular *N. oligotropha*-like AOB might be active because their higher oxygen affinity as suggested above allows competition for oxygen with the highly active heterotrophic PAO. In the late oxic period, when oxygen uptake of the heterotrophic PAO decreases, *N. europaea*-like AOB could become more active. Their relatively high maximum substrate conversion rate might compensate for their time-limited activity and contribute to the successful establishment of this population in the biofilm. It has been shown for biofilm populations of AOB that the abundance is likely not to be affected by short starvation periods, i.e. a few days. Furthermore, recovery for both, growth and activity of AOB from starvation is very rapid. This effect is likely to be coupled to high densities of AOB, as found in biofilms, and is probably due to cell-cell signalling (4). The high cell density and occurrence in dense clusters we found is in agreement with this hypo-

thesis. Based on this strategy, it can be argued that even merely short-term activity would allow AOB to persist in the biofilm.

In addition, there are reports about an anoxic type of metabolism in *N. europaea* and *N. eutropha* using electron acceptors other than oxygen (6). The ability to survive or even thrive during anoxic conditions is, however, likely to differ among the three AOB populations. Therefore, the nonaerated period of the reactor cycle might be another factor to support a mixed community of AOB. However, alternative hypotheses explaining the coexistence are possible. Detection of AOB populations in situ does not prove their recent activity (61). It can be speculated that the ability to maintain the ribosome content during inactive periods might be stronger in the *N. oligotropha* compared to the *N. europaea* lineage. This would cause *N. europaea*-like AOB to become more rapidly undetected by FISH in deeper layers of the biofilm compared to *N. oligotropha*. Currently, we have no evidence in favor of this hypothesis, but future studies including the detection of local activity, e.g., by use of microautoradiography (30) might help to support or reject this hypothesis. By *amoA* analysis, three more clones could be identified, related to *Nitrosococcus mobilis* (B3-5), and not closely affiliated to any isolated *Nitrosomonas* strain (B3-3). As both populations could not be identified by FISH, we assume that these populations were either low in numbers or in a dormant state.

**NOB population.** Using different probes for NOB, the existence of a certain population of *Nitrospira* spp. could be proven, whereas *Nitrobacter* spp. was not detected. This is in agreement with several other culture-independent studies of engineered systems (10, 22, 39, 48, 49, 62). Analysis of the probe match pattern in the current data set by the software package ARB (Technical University Munich, Munich, Germany) showed that it fits to a cluster of closely related sequences in the genus *Nitrospira* (strains with the accession numbers Y14636 to Y14643), retrieved from a nitrite-oxidizing sequencing batch reactor by Burrell et al. (10). The NOB population in our system is thus likely to be affiliated with this particular cluster of the genus *Nitrospira*. It might be speculated whether this cluster possesses common functional features leading to a competitive advantage under the periodically changing conditions typical for sequencing batch reactors. The cell densities of *Nitrospira* spp. found in this study are in the order of magnitude as those reported from a purely nitrifying fluidized bed reactor (48). However, the abundance is one order of magnitude higher than that of the AOB. The question remains, how such a high abundance is supported, when the substrate turnover is speculated to be low (48).

## CONCLUSION

By the combination of microsensor measurements with molecular methods it was possible to resolve the structure and activity of the nitrifying community in a complex, P-removing biofilm. First insights were obtained in the mechanism that allows for the co-existence of different populations of AOB in the same biofilm, i.e., separation of their distribution in space and separation of their activity in time. The design of probe Nmo218 specific for the *N. oligotropha* lineage enables in situ detection and quantification of *N. oligotropha*-like AOB in future studies to collect more information about their natural abundance and ecology.

## ACKNOWLEDGEMENTS

This study was supported by the German Research Foundation (SFB 411, Project A1 - Research Center for Fundamental Studies of Aerobic Biological Wastewater Treatment, Munich), and by the Max Planck Society.

We are indebted to Patrik Arnz for the maintenance of the reactor, and Jakob Pernthaler for image analysis for melting temperature determination. Gabriele Eickert, Anja Eggers, and Vera Hübner are acknowledged for the preparation of oxygen microelectrodes, and Dirk de Beer and Olivier Pringault for valuable comments on the handling of microsensor data. Harold L. Drake is acknowledged for his support.

## REFERENCES

1. **Amann, R. I., B. J. Binder, R. J. Olson, S. W. Chisholm, R. Devereux, and D. A. Stahl.** 1990. Combination of 16S rRNA-targeted oligonucleotide probes with flow cytometry for analyzing mixed microbial populations. *Appl. Environ. Microbiol.* **56**:1919-1925.
2. **Amann, R. I., W. Ludwig, and K.-H. Schleifer.** 1995. Phylogenetic identification and *in situ* detection of individual microbial cells without cultivation. *Microbiol. Rev.* **59**:143-169.
3. **Arnz, P., E. Arnold, and P. A. Wilderer.** 2001. Enhanced biological phosphorus removal in a semi full-scale SBBR. *Water Sci. Technol.* **43**:167-174.
4. **Batchelor, S. E., M. Cooper, S. R. Chhabra, L. A. Glover, G. S. A. B. Stewart, P. Williams, and J. I. Prosser.** 1997. Cell density-regulated recovery of starved biofilm populations of ammonia-oxidizing bacteria. *Appl. Environ. Microbiol.* **63**:2281-2286.
5. **Bitton, G.** 1999. *Wastewater Microbiology*, 2nd ed. Wiley-Liss, New York.

6. **Bock, E., I. Schmidt, R. Stüven, and D. Zart.** 1995. Nitrogen loss caused by denitrifying *Nitrosomonas* cells using ammonium or hydrogen as electron donors and nitrite as electron acceptor. *Arch. Microbiol.* **163**:16-20.
7. **Bond, P. L., P. Hugenholtz, J. Keller, and L. L. Blackall.** 1995. Bacterial community structures of phosphate-removing and non-phosphate-removing activated sludges from sequencing batch reactors. *Appl. Environ. Microbiol.* **61**:1910-1916.
8. **Bond, R. L., R. Erhart, M. Wagner, J. Keller, and L. L. Blackall.** 1999. Identification of some of the major groups of bacteria in efficient and nonefficient biological phosphorus removal activated sludge systems. *Appl. Environ. Microbiol.* **65**:4077-4084.
9. **Brosius, J., T. J. Dull, D. D. Sleeter, and H. F. Noller.** 1981. Gene organization and primary structure of a ribosomal RNA operon from *Escherichia coli*. *J. Mol. Biol.* **148**:107-127.
10. **Burrell, P., J. Keller, and L. Blackall.** 1998. Microbiology of a nitrite-oxidizing bioreactor. *Appl. Environ. Microbiol.* **64**:1878-1883.
11. **Characklis, W. G., and P. A. Wilderer.** 1989. *Structure and Function of Biofilms*, John Wiley & Sons, Chichester, UK.
12. **Christensson, M., L. L. Blackall, and T. Welander.** 1998. Metabolic transformations and characterisation of the sludge community in an enhanced biological phosphorus removal system. *Appl. Microbiol. Biotechnol.* **49**:226-234.
13. **Daims, H., A. Brühl, R. Amann, K.-H. Schleifer, and M. Wagner.** 1999. The domain-specific probe EUB338 is insufficient for the detection of all *Bacteria*: Development and evaluation of a more comprehensive probe set. *Syst. Appl. Microbiol.* **22**:434-444.
14. **Daims, H., P. Nielsen, J. L. Nielsen, S. Juretschko, and M. Wagner.** 2000. Novel *Nitrospira*-like bacteria as dominant nitrite-oxidizers in biofilms from wastewater treatment plants: diversity and *in situ* physiology. *Water Sci. Technol.* **41**:85-90.
15. **de Beer, D., A. Schramm, C. M. Santegoeds, and M. Kühl.** 1997. A nitrite microsensor for profiling environmental biofilms. *Appl. Environ. Microbiol.* **63**:973-977.
16. **Erhart, R.** 1997. *In situ* Analyse mikrobieller Biozönosen in Abwasserreinigungsanlagen. PhD thesis. Technical University Munich, Munich, Germany.
17. **Focht, D. D., and W. Verstraete.** 1977. Biochemical ecology of nitrification and denitrification. *Adv. Microb. Ecol.* **1**:135-214.
18. **González-Martínez, S., and P. A. Wilderer.** 1991. Phosphate removal in a biofilm reactor. *Water Sci. Technol.* **23**:1405-1415.
19. **Hanaki, K., C. Wanatwin, and S. Ohgaki.** 1990. Effects of the activity of heterotrophs on nitrification in a suspended-growth reactor. *Water Res.* **24**:289-296.
20. **Hartmann, L.** 1999. Historical development of wastewater treatment process, p. 5-16. *In* H.-J. Rehm, G. Reed, A. Pühler, and P. Stadler (ed.), *Biotechnology*, 2nd ed., vol. 11a. Wiley VCH, Weinheim New York.
21. **Hesselmann, R. P. X., C. Werlen, D. Hahn, J. R. van der Meer, and A. J. B. Zehnder.** 1999. Enrichment, phylogenetic analysis and detection of a bacterium that performs enhanced biological phosphate removal in activated sludge. *Syst. Appl. Microbiol.* **22**:454-465.

22. **Juretschko, S., G. Timmermann, M. Schmid, K.-H. Schleifer, A. Pommerening-Röser, H. P. Koops, and M. Wagner.** 1998. Combined molecular and conventional analysis of nitrifying bacterium diversity in activated sludge: *Nitrosococcus mobilis* and *Nitrospira*-like bacteria as dominant populations. *Appl. Environ. Microbiol.* **64**:3042-3051.
23. **Kawaharasaki, M., H. Tanaka, T. Kanagawa, and K. Nakamura.** 1999. In situ identification of polyphosphate-accumulating bacteria in activated sludge by dual staining with rRNA-targeted oligonucleotide probes and 4',6-Diamidino-2-phenylindol (DAPI) at a polyphosphate-probing concentration. *Water Res.* **33**:257-265.
24. **Koops, H. P., B. Böttcher, U. C. Möller, A. Pommerening-Röser, and G. Stehr.** 1991. Classification of eight new species of ammonia-oxidizing bacteria: *Nitrosomonas communis* sp. nov., *Nitrosomonas ureae* sp. nov., *Nitrosomonas aestuarii* sp. nov., *Nitrosomonas marina* sp. nov., *Nitrosomonas nitrosa* sp. nov., *Nitrosomonas eutropha* sp. nov., *Nitrosomonas oligotropha* sp. nov., *Nitrosomonas halophila* sp. nov. *J. Gen. Microbiol.* **137**:1689-1699.
25. **Koops, H.-P., and U. C. Möller.** 1992. The lithotrophic ammonia-oxidizing bacteria, p. 2625-2637. In A. Balows, Trüper, HG, Dworkin, M, Harder, W, Schleifer, K-H (ed.), *The Prokaryotes (A Handbook of the Biology of Bacteria: Ecophysiology, Isolation, Identification, Applications)*, 2nd ed, vol. 3. Springer, New York Berlin Heidelberg.
26. **Kowalchuk, G. A., A. W. Stienstra, H. J. Heilig, J. R. Stephen, and J. W. Woldendorp.** 2000. Molecular analysis of ammonia-oxidising bacteria in soil of successional grasslands of the Drentsche A (The Netherlands). *FEMS Microbiol. Ecol.* **31**:207-215.
27. **Kuba, T., M. C. M. van Loosdrecht, and J. J. Heijnen.** 1996. Phosphorus and nitrogen removal with minimal COD requirement by integration of denitrifying dephosphatation and nitrification in a two-sludge system. *Water Res.* **30**:1702-1710.
28. **Kuba, T., A. Wachtmeister, M. C. M. van Loosdrecht, and J. J. Heijnen.** 1994. Effect of nitrate on phosphorus release in biological phosphorus removal systems. *Water Sci. Technol.* **30**:263-269.
29. **Laanbroek, H. J., P. L. E. Bodelier, and S. Gerards.** 1994. Oxygen consumption kinetics of *Nitrosomonas europaea* and *Nitrobacter hamburgensis* grown in mixed continuous cultures at different oxygen concentrations. *Arch. Microbiol.* **161**:156-162.
30. **Lee, N., P. H. Nielsen, K. H. Andreasen, S. Juretschko, J. L. Nielsen, K.-H. Schleifer, and M. Wagner.** 1999. Combination of fluorescent in situ hybridization and microautoradiography - a new tool for structure-function analyses in microbial ecology. *Appl. Environ. Microbiol.* **65**:1289-1297.
31. **Ludwig, W., O. Strunk, S. Klugbauer, N. Klugbauer, M. Weizenegger, J. Neumaier, M. Bachleitner, and K.-H. Schleifer.** 1998. Bacterial phylogeny based on comparative sequence analysis. *Electrophoresis.* **19**:554-568.
32. **Maidak, B. L., J. R. Cole, C. T. Parker, G. M. Garrity, N. Larsen, B. Li, T. G. Lilburn, M. J. McCaughey, G. J. Olsen, R. Overbeek, S. Pramanik, T. M. Schmidt, T. J. M., and C. R. Woese.** 1999. A new version of the RDP (Ribosomal Database Project). *Nucleic Acids Res.* **27**:171-173.
33. **Manz, W., R. Amann, W. Ludwig, M. Wagner, and K.-H. Schleifer.** 1992. Phylogenetic oligodeoxynucleotide probes for the major subclasses of proteobacteria: problems and solutions. *Syst. Appl. Microbiol.* **15**:593-600.

34. **Mino, T., M. C. M. van Loosdrecht, and J. J. Heijnen.** 1998. Microbiology and biochemistry of the enhanced biological phosphate removal process. *Water Res.* **32**:3193-3207.
35. **Mobarry, B. K., M. Wagner, V. Urbain, B. E. Rittmann, and D. A. Stahl.** 1996. Phylogenetic probes for analyzing abundance and spatial organization of nitrifying bacteria. *Appl. Environ. Microbiol.* **62**:2156-2162.
36. **Morgenroth, E.** 1998. Enhanced Biological Phosphorus Removal in Biofilm Reactors. PhD thesis. Technical University Munich, Munich, Germany.
37. **Neef, A.** 1997. Anwendung der *in situ*-Einzelzell-Identifizierung von Bakterien zur Populationsanalyse in komplexen mikrobiellen Biozönosen. PhD thesis. Technical University Munich, Munich, Germany.
38. **Nielsen, L. P., P. B. Christensen, N. P. Revsbech, and J. Sørensen.** 1990. Denitrification and oxygen respiration in biofilms studied with a microsensor for nitrous oxide and oxygen. *Microb. Ecol.* **19**:63-72.
39. **Okabe, S., H. Satoh, and Y. Watanabe.** 1999. In situ analysis of nitrifying biofilms as determined by in situ hybridization and the use of microelectrodes. *Appl. Environ. Microbiol.* **65**:3182-3191.
40. **Pommerening-Röser, A., G. Rath, and H. P. Koops.** 1996. Phylogenetic diversity within the genus *Nitrosomonas*. *Syst. Appl. Microbiol.* **19**:344-351.
41. **Prosser, J. I.** 1989. Autotrophic nitrification in bacteria. *Adv. Microb. Physiol.* **30**:125-181.
42. **Purkhold, U., A. Pommerening-Röser, S. Juretschko, M. C. Schmid, H.-P. Koops, and M. Wagner.** 2000. Phylogeny of all recognized species of ammonia-oxidizers based on comparative 16S rRNA and *amoA* sequence analysis: Implications for molecular diversity surveys. *Appl. Environ. Microbiol.* **66**:5368-5382.
43. **Rath, G.** 1996. Entwicklung eines Nachweissystems zur *in situ*-Analyse nitrifizierender Bakterienpopulationen auf der Basis spezifischer 16S rRNA-Gensequenzen. PhD thesis. University of Hamburg, Hamburg, Germany.
44. **Ravenschlag, K., K. Sahm, J. Pernthaler, and R. Amann.** 1999. High bacterial diversity in permanently cold marine sediments. *Appl. Environ. Microbiol.* **65**:3982-3989.
45. **Revsbech, N. P.** 1989. An oxygen microelectrode with a guard cathode. *Limnol. Oceanogr.* **34**:474-478.
46. **Roller, C., M. Wagner, R. Amann, W. Ludwig, and K.-H. Schleifer.** 1994. *In situ* probing of Gram-positive bacteria with high DNA G+C content using 23S rRNA-targeted oligonucleotides. *Microbiology.* **140**:2849-2858.
47. **Schmid, M., U. Twachtmann, M. Klein, M. Strous, S. Juretschko, M. S. M. Jetten, J. W. Metzger, K.-H. Schleifer, and M. Wagner.** 2000. Molecular evidence for genus level diversity of bacteria capable of catalyzing anaerobic ammonium oxidation. *Syst. Appl. Microbiol.* **23**:93-106.
48. **Schramm, A., D. de Beer, J. C. van den Heuvel, S. Ottengraf, and R. Amann.** 1999. Microscale distribution of populations and activities of *Nitrosospira* and *Nitrospira* spp. along a macroscale gradient in a nitrifying bioreactor: Quantification by in situ hybridization and the use of microsensors. *Appl. Environ. Microbiol.* **65**:3690-3696.
49. **Schramm, A., D. de Beer, M. Wagner, and R. Amann.** 1998. Identification and activities in situ of *Nitrosospira* and *Nitrospira* spp. as dominant populations in a nitrifying fluidized bed reactor. *Appl. Environ. Microbiol.* **64**:3480-3485.

50. Schramm, A., L. H. Larsen, N. P. Revsbech, N. B. Ramsing, R. Amann, and K.-H. Schleifer. 1996. Structure and function of a nitrifying biofilm as determined by in situ hybridization and the use of microelectrodes. *Appl. Environ. Microbiol.* **62**:4641-4647.
51. Smolders, G. J. F., J. van der Meij, M. C. M. van Loosdrecht, and J. J. Heijnen. 1994. Stoichiometric model of the aerobic metabolism of the biological phosphorus removal process. *Biotechnol. Bioeng.* **44**:837-848.
52. Speksnijder, A., G. Kowalchuk, K. Roest, and H. Laanbroek. 1998. Recovery of a *Nitrosomonas*-like 16S rDNA sequence group from freshwater habitats. *Syst. Appl. Microbiol.* **21**:321-330.
53. Stehr, G., B. Böttcher, P. Dittberner, G. Rath, and H. P. Koops. 1995. The ammonia-oxidizing nitrifying population of the river Elbe estuary. *FEMS Microbiol. Ecol.* **17**:177-186.
54. Stephen, J. R., A. E. McCaig, Z. Smith, J. I. Prosser, and T. M. Embley. 1996. Molecular diversity of soil and marine 16S rRNA gene sequences related to  $\beta$ -subgroup ammonia-oxidizing bacteria. *Appl. Environ. Microbiol.* **62**:4147-4154.
55. Strunk, O., O. Gross, B. Reichel, M. May, S. Hermann, N. Stuckmann, B. Nonhoff, M. Lenke, A. Ginhart, A. Vilbig, T. Ludwig, A. Bode, K.-H. Schleifer, and W. Ludwig. 1996. ARB: a software environment for sequence data. Department of Microbiology, Technical University Munich, Munich, Germany.
56. Suwa, Y., T. Sumino, and K. Noto. 1997. Phylogenetic relationships of activated sludge isolates of ammonia oxidizers with different sensitivities to ammonium sulfate. *J. Gen. Appl. Microbiol.* **43**:373-379.
57. van Niel, E. W. J., L. A. Robertson, and J. G. Kuenen. 1993. A mathematical description of the behaviour of mixed chemostat cultures of an autotrophic nitrifier and a heterotrophic nitrifier/aerobic denitrifier; a comparison with experimental data. *FEMS Microbiol. Ecol.* **102**:99-108.
58. Vlekke, G. J. F. M., Y. Comeau, and W. K. Oldham. 1988. Biological phosphate removal from wastewater with oxygen or nitrate in sequencing batch reactors. *Environ. Technol. Lett.* **9**:791-796.
59. Wagner, M., R. Amann, P. Kämpfer, B. Assmus, A. Hartmann, P. Hutzler, N. Springer, and K.-H. Schleifer. 1994. Identification and *in situ* detection of gram-negative filamentous bacteria in activated sludge. *Syst. Appl. Microbiol.* **17**:405-417.
60. Wagner, M., R. Erhart, W. Manz, R. Amann, H. Lemmer, D. Wedi, and K.-H. Schleifer. 1994. Development of an rRNA-targeted oligonucleotide probe specific for the genus *Acinetobacter* and its application for in situ monitoring in activated sludge. *Appl. Environ. Microbiol.* **60**:792-800.
61. Wagner, M., G. Rath, R. Amann, H. P. Koops, and K.-H. Schleifer. 1995. *In situ* identification of ammonia-oxidizing bacteria. *Syst. Appl. Microbiol.* **18**:251-264.
62. Wagner, M., G. Rath, H. P. Koops, J. Flood, and R. Amann. 1996. *In situ* analysis of nitrifying bacteria in sewage treatment plants. *Water Sci. Technol.* **34**:237-244.



## **Chapter 5**

# **Structure and Activity of Multiple Nitrifying Bacterial Populations Coexisting in a Biofilm**

A. Gieseke, L. Bjerrum, M. Wagner, and R. Amann



## Structure and Activity of Multiple Nitrifying Bacterial Populations Coexisting in a Biofilm

Armin Gieseke<sup>1\*</sup>, Lotte Bjerrum<sup>2</sup>, Michael Wagner<sup>2</sup>, and Rudolf Amann<sup>1</sup>

<sup>1</sup>Molecular Ecology Group, Max Planck Institute for Marine Microbiology, D-28359 Bremen, Germany

<sup>2</sup>Department of Microbiology, Technische Universität München, D-85350 Freising, Germany

A biofilm from a nitrifying pilot-scale sequencing batch reactor was investigated for the effects of varying process conditions on its microscale activity. Biofilm was incubated at high and low ammonium concentrations reflecting the initial and final situation during a treatment cycle, respectively. Additionally, different oxygen regimes were applied to simulate local oxygen depletion in the fixed bed. Microsensors were used to measure conversion of oxygen, substrates and products of nitrification within the biofilm. Under high ammonium conditions, release of nitrite and nitrate did not account for ammonium uptake. This net N loss was much lower under low ammonium conditions. Additionally, inhibition of nitrite-oxidizing bacteria (NOB), but not of ammonia-oxidizing bacteria (AOB) by free ammonia was likely to occur under the initial high ammonium conditions. Phylogenetic diversity, spatial distribution, and abundance of nitrifying bacteria in biofilm samples was analyzed by fluorescence *in situ* hybridization (FISH). At least 6 different nitrifying populations were found in the biofilm. *Nitrosococcus mobilis* formed microcolonies locally embedded within *N. europaea/eutropha* aggregates. The latter population dominated the AOB community. A third less abundant AOB population was affiliated to the *N. oligotropha* lineage. NOB of the genera *Nitrobacter* and *Nitrospira*, the latter with at least two distinct populations, occurred in the biofilm and showed a large scale heterogeneity in their distribution. *Nitrospira* spp. mostly predominated in the deeper inactive biofilm layers, where it might rather persist than thrive and act as seedling when detached. The nitrifying populations were not stratified, but rather heterogeneously distributed. Thus, correlation to functional changes as revealed by the microsensor experiments was limited. Assignment of specific niches to individual populations in such complex systems might afford additional methods.

## INTRODUCTION

Increasing requirements for the removal of secondary pollutants of wastewater, i.e., chemically bound nitrogen and phosphorus, have led to the development of treatment strategies that are efficient as well as flexible. One such technique is the sequencing batch reactor (SBR)

technology, where different treatment steps proceed in a temporal rather than a spatial sequence (26), allowing a very compact design. SBR processes are characterized by three periods: filling, recirculation, and draining (26). The recirculation period can be subdivided into periods with different conditions (e.g., nonaerated-aerated) depending on the process to be achieved. SBR systems are either activated sludge-based or biofilm-based (sequencing batch biofilm reactor, SBBR). As the treatment is discontinuous, the microorganisms in SBRs are subjected to different yet periodically recurrent environmental changes, e.g., in substrate concentration. In SBBRs, additional concentration gradients of substrates and oxygen occur across the liquid-biofilm interface and within the biofilm, caused by, and influencing the activity of the microbial populations in the biofilm. Hence, it is to be expected, that this 4-dimensional heterogeneity generates multiple niches for various bacterial populations, even though the macroscopic function appears to be homogeneous. *In situ* studies on the microscale might help to understand the structure and function of the microbial community in such systems. Several studies have been performed on nitrifying biofilms combining FISH and microsensor analyses (28, 36-39). However, most of these biofilms originated from experimental systems with a low complexity in the composition and activity of the microbial community. In contrast, detailed studies on community composition and adaptation of different microbial populations in complex, applied systems such as SBBRs are rare. Recently, an *in situ* microscale study of nitrification in a phosphate-removing biofilm demonstrated the coexistence of several ammonia-oxidizing populations (15). It was hypothesized that their coexistence could be due to adaptation to different oxygen concentrations and separation of activity in time.

In the present study, we investigated the community structure and function of a biofilm from a nitrifying pilot-scale SBBR treating ammonium-rich reject water from sludge dewatering. The experiments addressed the questions of how nitrifying activity of the biofilm is affected on the microscale by typical changes occurring during a treatment cycle and how the individual populations contribute to it. For this purpose, biofilm samples from the reactor were incubated at different concentrations of ammonium, simulating the changes during a SBBR cycle, and at different concentrations of oxygen, simulating locally different conditions in the fixed bed. *In situ* measurements with microelectrodes were applied to follow the local activities. The community structure of nitrifying bacteria in the SBBR as revealed by previous investigations based on the full-cycle rRNA approach (11) and comparative *amoA* sequence analysis (31) indicated the presence of various populations of ammonia-oxidizing bacteria (AOB) as well as nitrite-oxidizing bacteria (NOB) of the genera *Nitrospira* and *Nitrobacter* in

this system. In the present study the structure of the nitrifying community in the SBBR biofilm was addressed by fluorescence *in situ* hybridization (FISH) to get insights into the spatial organization of the coexisting nitrifiers. The goal of this combined approach was to reveal the structural and functional niches of the coexisting populations of AOB and NOB under typical process conditions.

## MATERIAL AND METHODS

**Process scheme and sampling.** Biofilms originated from a pilot-scale facility at the municipal wastewater treatment plant in Ingolstadt (Germany). The reactor with a volume of 17 m<sup>3</sup> contained a fixed bed of expanded clay beads as substratum. It was operated in a sequencing batch mode for nitrification. The system was supplied with concentrated sewage originating from sludge dewatering of anaerobic digestion products. The sewage carried a high load of ammonium generated during anaerobic digestion, while most of the carbon compounds were not readily biodegradable. Details of reactor operation are given elsewhere (3). To enable sampling a sieve cage of about 400 cm<sup>3</sup> filled with different types of substratum elements was incubated 2 m below the surface of the fixed bed of the reactor for a period of 8 weeks. Substratum types consisted of expanded clay beads, polystyrene beads (Biostyr, Krüger, Søborg, DK), and Kaldnes polymer elements (Purac, Merseburg, Germany).

**Experiments and microprofiling.** For microsensor measurements, substratum elements with adhering biofilm were removed from the cage and carefully transferred to a measurement setup. The setup consisted of a 20 l aquarium serving as a medium reservoir and temperature buffer. Reject water, collected at the sampling site, prefiltered on 0.4 µm pore size filters and stored at 4°C, was used as a medium for the experiments. Ammonium concentration was adjusted by dilution where necessary. A flow cell of 100 x 50 x 50 mm, connected to tubes at both head planes was incubated in the reservoir, and medium was pumped through the flow cell via a small submersible pump with a flow rate of 1 cm s<sup>-1</sup>. The flow was laminarized by a sieve insert at the inlet. Substratum elements with adhering biofilm were placed in the flow cell and carefully attached to the bottom with small amounts of agar. Different degrees of oxygen saturation of the medium were achieved by aeration of the medium with air or a mix of air and nitrogen. A cover of hollow plastic spheres (Allplas, Capricorn Chemicals Corp., Secaucus, NJ, USA) on top of the medium in the reservoir was used to reduce evaporation and gas exchange between the medium and the air.

Four different experiments were performed. In experiments A to C, the ammonium concentration was kept at a saturating level of 2.3 to 3.2 mM, while the concentration of oxygen in the medium was adjusted to  $246.3 \pm 2.1 \mu\text{M}$  (experiment A),  $135 \pm 1.6 \mu\text{M}$  (B) and  $41.5 \pm 0.9 \mu\text{M}$  (C) oxygen, corresponding to about 100%, 50%, and 15% air saturation at a temperature of 25°C. In experiment D, the concentration of ammonium in the medium was decreased to 800  $\mu\text{M}$ , while the oxygen concentration was kept at air saturation ( $253.7 \pm 1.2 \mu\text{M}$ ). The functional response of the biofilm community to each experimental condition was measured by recording vertical microprofiles with microsensors for oxygen (33), and ion-selective microelectrodes for ammonium, nitrite, nitrate, and pH (12). In each experiment, solute concentrations in the biofilm were allowed to reach steady state for at least 2h before measurements were started. For practical reasons, all profiles were measured on biofilm grown on clay beads.

**Calculation of conversion rates.** Areal rates of oxygen and ammonium uptake, and release of nitrite and nitrate were calculated based on the slope of the concentration gradient of the respective solute through the diffusive boundary layer (DBL) above the biofilm (34). For each depth interval within the biofilm, volumetric conversion rates were calculated with a stepwise procedure as described elsewhere (13). As effective diffusion coefficients for oxygen, ammonium, nitrite, and nitrate, we applied values of  $2.18 \times 10^{-5} \text{ cm}^2 \text{ s}^{-1}$ ,  $1.78 \times 10^{-5} \text{ cm}^2 \text{ s}^{-1}$ ,  $1.67 \times 10^{-5} \text{ cm}^2 \text{ s}^{-1}$ , and  $1.73 \times 10^{-5} \text{ cm}^2 \text{ s}^{-1}$ , respectively. These values are based on the molecular diffusion coefficients  $D_0$  in water at 25°C (6, 22), and on a  $D_{\text{eff}}/D_0$  ratio of 0.9 (8).

**Oligonucleotide probe design.** A probe for a subgroup of *Nitrospira* spp. was designed based on available sequence data (accession no. Y14636 to Y14643). For probe design we used the ARB software package (Technical University Munich, Munich, Germany) with the recent 16S rDNA sequence dataset supplemented by publicly available and in-house sequences. The synthesized oligonucleotide was evaluated by use of biofilm sample material. A series of hybridization experiments were performed with increasing formamide concentrations in steps of 5% in the hybridization buffer starting from 0%. The samples were additionally hybridized with probes Ntspa712 and Ntspa662 as described below.

**FISH analysis.** The different types of substratum elements with adhering biofilm were fixed with fresh paraformaldehyde solution as described earlier (1, 23). The samples were stored at  $-18^\circ\text{C}$  in a 1:1 mixture of PBS/ethanol until further processing. Biofilms grown on polystyrene beads and on the Kaldnes elements were incubated in cryo embedding compound (OCT, Miles, Elkhart, IN, USA), and, after freezing at  $-30^\circ\text{C}$ , carefully removed from the substratum. Subsequently, sections perpendicular to the surface were prepared and immobi-

lized on gelatine-coated microscopic slides as reported earlier (39). As the clay beads had a rough surface with small ridges and cavities, biofilm was firmly attached and could not be removed quantitatively. Therefore, whole clay beads with adhering biofilm were subjected to FISH. Hybridization was performed according to procedures reported earlier (23) with a hierarchical set of labeled oligonucleotide probes (Table 1). Probes were labeled with the sulfoindocyanine dyes Cy3 and Cy5, and with 5,(6)-carboxyfluorescein (Fluos) and were obtained from Interactiva (Ulm, Germany). Simultaneous hybridization with several probes was performed in subsequent steps by first hybridizing with the probe of higher stringency (42). Hybridized samples were analyzed by use of a confocal laser scanning microscope (CLSM) Zeiss LSM 510 (Carl Zeiss, Jena, Germany). Material grown on whole clay beads was analyzed after FISH by scanning image stacks parallel to the surface on a CLSM. Due to the optical density of the biofilm, however, detection was restricted to a depth of 50  $\mu\text{m}$ .

TABLE 1. Oligonucleotide probes and hybridization conditions applied in this study.

Probe	Probe Sequence (5' to 3')	Target site <sup>a</sup>	Target organism(s)	FA [%] <sup>b</sup>	NaCl [mM] <sup>c</sup>	Reference
EUB338	GCTGCTCCCGTAGGAGT	16S (338-355)	Most but not all <i>Bacteria</i>	20	225	(1)
EUB338-II	GCAGCCACCCGTAGGTG	16S (338-355)	<i>Planctomycetes</i> , some members of candidate division OP11	20	225	(9)
EUB338-III	GCTGCCACCCGTAGGTG	16S (338-355)	<i>Verrucomicrobia</i> , some members of the green non-sulfur bacteria, some members of candidate division OP11	20	225	(9)
NON338	ACTCCTACGGGAGGAGC	16S (338-355)	Complementary to EUB338	20	225	(23)
BET42a <sup>d</sup>	GCCTCCGCACTTCGTTT	23S (1027-1043)	$\beta$ -Proteobacteria	35	80	(23)
Nso1225	CGCCATTGTATTACGGTGA	16S (1225-1244)	Ammonia-oxidizing $\beta$ -proteobacteria	35	80	(24)
Nsm156	TATTAGCACATCTTTCGAT	16S (156-174)	Various <i>Nitrosomonas</i> spp.	5	636	(24)
Nsv443	CGGTGACCGTTTCGTTCCG	16S (444-462)	<i>Nitrosospira</i> spp.	30	112	(24)
NEU <sup>e</sup>	CCCTCTGCTGCACTCTA	16S (653-670)	Halophilic and halotolerant members of the genus <i>Nitrosomonas</i> , <i>Nitrosococcus mobilis</i>	40	56	(43)
Nse1472 <sup>f</sup>	ACCCCACTCATGACCCCC	16S (1472-1489)	<i>Nitrosomonas europaea</i> , <i>N. europaea</i> , <i>N. halophila</i>	50	28	(19)
NmII	TTAAGACAGCTCCGATGTA	16S (120-139)	<i>Nitrosomonas communis</i> lineage	25	159	(29)
NmIV	TCTCACCTCTCAGCGGCT	16S (1004-1023)	<i>Nitrosomonas cryotolerans</i> lineage	35	80	(29)
NmV	TCTCAGAGACTACGGGG	16S (174-191)	<i>Nitrosococcus mobilis</i> lineage	35	80	(29)
NOLI191 <sup>g</sup>	CGATCCCCACTTTCCTC	16S (191-208)	Various members of the <i>Nitrosomonas oligotropha</i> lineage	30	112	(32)
Nmo218	CGGCCGCTCCAAAAGCAT	16S (218-235)	<i>Nitrosomonas oligotropha</i> lineage	35	80	(15)
NIT3 <sup>h</sup>	CCTGTGCTCCATGCTCCG	16S (1035-1048)	<i>Nitrobacter</i> spp.	40	56	(44)
NSR826	GTAAACCCGCGACACTTA	16S (826-843)	Various freshwater <i>Nitrosospira</i> spp.	20	225	(38)
NSR1156	CCCGTTCTCTGGGGAGT	16S (1156-1173)	Various freshwater <i>Nitrosospira</i> spp.	30	112	(38)
NSR1253	CCTCAGCGTTTCAGAGG	16S (1253-1270)	"SBBR" subgroup of <i>Nitrosospira</i> spp.	10	450	This study
Nspa712 <sup>i</sup>	CGCCTTCGCGACCGGCTTCC	16S (712-732)	Phylum <i>Nitrosospira</i>	35	80	(10)
Nspa662 <sup>j</sup>	GGAAATCCGGGCTCCCTCT	16S (662-679)	Genus <i>Nitrosospira</i>	35	80	(10)
S*-Amx-0820-a-A-22	AAAACCCCTCTACTTAGTGCCC	16S (820-841)	Anaerobic ammonium oxidizers	40	56	(35)

<sup>a</sup> rRNA position according to *E. coli* numbering (9)

<sup>b</sup> percentage of formamide in the hybridization buffer

<sup>c</sup> concentration of sodium chloride in the washing buffer

<sup>d</sup> used together with equimolar amount of unlabeled competitor oligonucleotide as indicated in the reference

<sup>e</sup> referred to as S\*-Nse-1472-a-A-18 in the reference

<sup>f</sup> used together with unlabeled competitor oligonucleotide as indicated in (15)

<sup>g</sup> referred to as S\*-Nspa-0712-a-A-21 and S-G-Nspa-0662-a-A-18, respectively, in the reference.

For quantitative description of the spatial arrangement of various populations, thin sections of biofilm grown on Kaldnes material were prepared as described and hybridized with probes for various AOB and NOB. Subsequently, adjacent fields of view were scanned from the surface to the substratum end of the biofilm by use of a CLSM. This was repeated several times with fields of view laterally adjacent to each other, and with multiple thin sections. After

thorough calibration and threshold definition (9), the number of pixels with a signal were determined for each image, and additionally related to the amount detected with the bacterial EUB338 probe set (9).

## RESULTS

**Functional response.** Optical inspection of the biofilm before and during the measurements showed that the biofilm was about 200 to 500  $\mu\text{m}$  thick and distributed in patches on the clay beads. Microsensor measurements revealed that the main processes were located in the upper 300  $\mu\text{m}$  of the biofilm. Thus, for practical reasons, profiling mostly did not exceed this depth.

The four experimental conditions produced clearly different responses in the consumption of oxygen and production of nitrite and nitrate. Figure 1 shows the averaged concentrations in the biofilm and the volumetric conversion rates for all three analytes. In experiments A to C, oxygen penetration was 75 to 100  $\mu\text{m}$ . Highest oxygen consumption took place near the surface, and decreased towards depth. This distribution of local rates was unaffected by oxygen concentrations in the bulk through experiments A to C. Total oxygen uptake of the biofilm, as represented by the flux across the DBL (Table 2) showed a positive correlation to bulk concentrations ( $R^2 = 0.971$ ). Experiment D did not differ significantly in terms of oxygen uptake compared to A (t test;  $\alpha = 0.05$ ). Penetration depth, however, was increased to about 250  $\mu\text{m}$  and oxygen accordingly was consumed to a certain extent in deeper layers. An amount of 59% of the volumetric consumption integrated over the whole depth occurred in the upper 100  $\mu\text{m}$ , whereas 31% were consumed in the 100 to 200  $\mu\text{m}$  layer. In comparison, in A, B and C, the surface layer consumed 94%, 96%, and 74% of the oxygen, respectively.

In contrast to the full scale reactor, no alkalinity was added to keep the pH constant. However, both bulk and biofilm pH were rather stable in experiments A and B (data not shown). In the bulk, the pH was at 8.4 and 8.2, respectively. Within the biofilm layer, it decreased to 8.1 and 7.9, respectively. In experiment D, the bulk pH was 7.8, and 7.2 in the biofilm, reflecting high ammonia oxidation activity

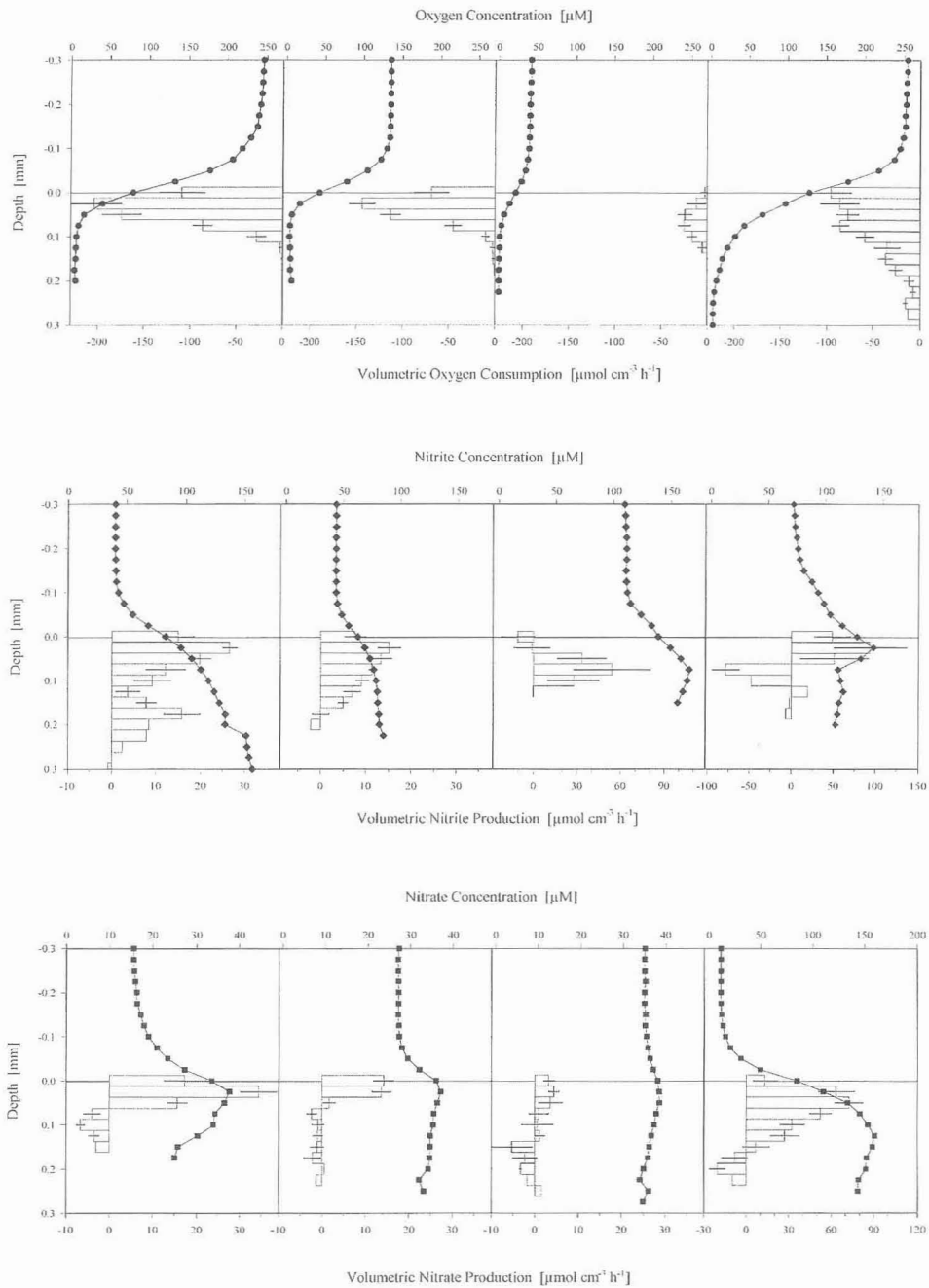


FIG. 1. Averaged microprofiles of oxygen (top), nitrite (middle), and nitrate (bottom) and the respective volumetric conversion rates within different biofilm layers (grey bars). Volumetric rates were calculated in a stepwise procedure for individual profiles as described in the text. Horizontal bars represent mean values ( $\pm$  SD, number of profiles given in Table 2). Negative values indicate consumption. The four columns refer to experiments A to D (from left to right).

In both experiments, A and B, production of nitrite occurred in the oxic part of the biofilm, and was highest near the surface. The production calculated for a depth below 125  $\mu\text{m}$  in A is caused by artefacts, i.e., irregularities of nitrite profiles in the anoxic part of the biofilm, as can be seen in the mean profile. Nitrite concentrations in the biofilm (Fig. 1) as well as the release of nitrite (Table 2) were lower in experiment B. In contrast, in experiment C, a measurable accumulation of nitrite occurred in the bulk medium, and the production appeared to be shifted to a narrow subsurface layer close to the limit of oxygen penetration. However, due to higher bulk concentrations of nitrite, the low apparent volumetric consumption at the surface might reflect rather the reduced concentration gradient than a lower local ammonia oxidation activity. Highest volumetric production rates within the biofilm exceeded those found in experiment A and B. As only a few profiles were available for C ( $n = 3$ ), the calculated efflux of nitrite, however, showed a high error and no significant difference could be demonstrated compared to A and B. This also held true for experiment D. Nitrite production occurred near the surface with increased volumetric rates compared to A and B. In a layer below 75  $\mu\text{m}$ , however, nitrite consumption was found in experiment D, but not in experiments A to C.

TABLE 2. Areal fluxes of measured solutes through the bulk liquid-biofilm interface. Negative values indicate uptake, positive values a release of the appropriate solute.

Experiment	Areal flux $J^a$ [ $\mu\text{mol cm}^{-2} \text{h}^{-1}$ ]			
	Oxygen	Ammonium	Nitrite	Nitrate
A	$-1.70 \pm 0.29$ (12)	$-1.70 \pm 0.29$ (12)	$0.39 \pm 0.08$ (4)	$0.14 \pm 0.06$ (12)
B	$-1.07 \pm 0.11$ (15)	$-1.04^b \pm 0.52$ (2)	$0.21^b \pm 0.03$ (6)	$0.16^b \pm 0.02$ (5)
C	$-0.28 \pm 0.07$ (6)	nd <sup>c</sup>	$0.55^b \pm 0.39$ (3)	$0.06^b \pm 0.02$ (6)
D	$-1.58 \pm 0.16$ (20)	$-1.58 \pm 0.16$ (20)	$0.57^b \pm 0.15$ (3)	$0.50^b \pm 0.08$ (9)

<sup>a</sup> Mean values  $\pm$  95% confidence limits; number of profiles indicated in brackets.

<sup>b</sup> Flux normalized by the ratio of bulk concentrations between the appropriate experiment and experiment A.

<sup>c</sup> Not determined.

Nitrate production in general was reduced with decreased oxygen concentration. High production was found in A in the upper 75  $\mu\text{m}$ , whereas some consumption occurred below that layer. Both, surface production as well as subsurface consumption were lower in experiment B, and even more in C. Comparison with nitrite production did not indicate a clear separation of both ammonia and nitrite oxidation. In experiment D, along with the deeper oxygen penetration observed, a much broader layer of 150  $\mu\text{m}$  contributed to nitrate production. Rates were highest in the layer 25 to 75  $\mu\text{m}$  below the surface, and twice as high as observed in A.

Both the higher rates and the broadened nitrate production zone contributed to a nearly four times higher nitrate efflux across the DBL compared to A (Table 2). Nitrate consumption in deeper layers was also increased, but shifted to a depth below 200  $\mu\text{m}$ .

Based on areal uptake rates, a budget could be calculated relating the ammonia and nitrite oxidation rates, and nitrification rates in total to the uptake of oxygen and ammonia (Table 3). When the oxygen concentration was reduced to the half (A to B) the ratio of oxygen consumed by ammonia oxidation did not appear to be affected. However, the amount of oxygen consumed by nitrite oxidation increased from 16% to 42% from experiment A to C. The ratio of oxygen consumed by ammonia oxidation could not reliably be determined in experiment C, because only a few nitrite profiles were measured in that experiment and the areal uptake rate consequently showed a high error. However, the oxygen consumption by ammonia oxidation was likely to be high. The results indicate a clear increase in the amount of oxygen consumed by nitrification in total throughout experiments A to C. Nevertheless, only part of the oxygen uptake could be explained by nitrification in experiments A and B. In detail, the distribution of local volumetric production rates (Fig. 1) for nitrite and nitrate suggests that the contribution of the surface layer to oxygen consumption decreased, whereas subsurface consumption became more important. Although less pronounced, the same effect occurred in the local oxygen consumption as seen in experiment C (Fig. 1). In contrast to A and B, the oxygen consumption could be fully explained with the amounts of nitrite and nitrate released in experiment D. Here, both processes contributed equally to oxygen consumption (Table 3).

TABLE 3. Amount of oxygen or ammonium consumed per nitrite or nitrate released, and sum of both (in %).

Experiment	Nitrite produced		Nitrate produced		Oxidized N produced	
	oxygen <sup>a</sup>	ammonium <sup>b</sup>	oxygen <sup>c</sup>	ammonium <sup>d</sup>	oxygen	ammonium
A	34	23	16	8	50	31
B	30	20	30	15	60	35
C	nd <sup>e</sup>	nd <sup>e</sup>	42	nd <sup>e</sup>	nd <sup>e</sup>	nd <sup>e</sup>
D	54	36	64	32	118	68

<sup>a</sup> Based on areal flux of oxygen and nitrite through the bulk liquid-biofilm interface.

<sup>b</sup> Based on areal flux of ammonium and nitrite through the bulk liquid-biofilm interface.

<sup>c</sup> Based on areal flux of oxygen and nitrate through the bulk liquid-biofilm interface.

<sup>d</sup> Based on areal flux of ammonium and nitrate through the bulk liquid-biofilm interface.

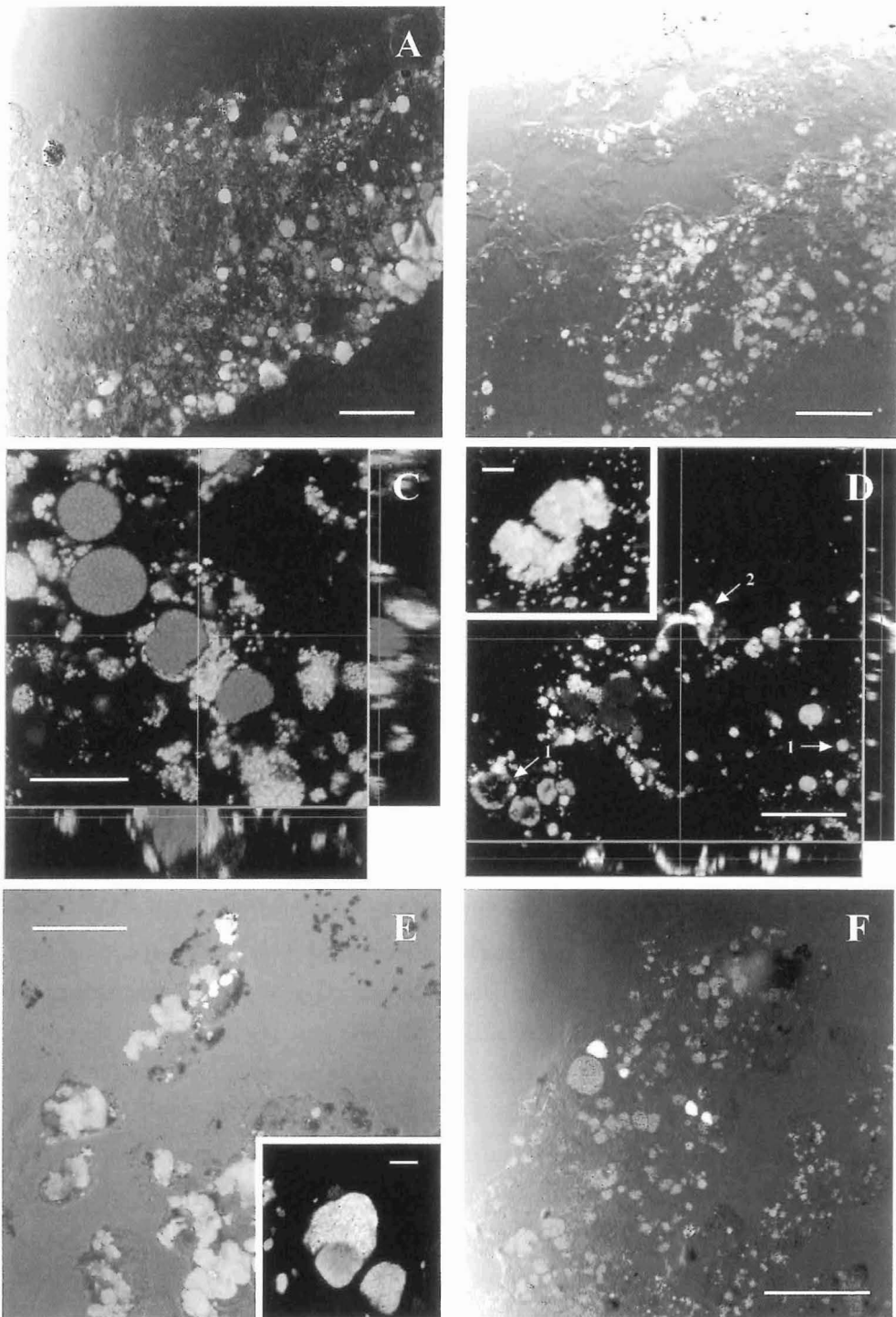
<sup>e</sup> Not determined.

Relating the uptake of ammonium to the release of nitrite and nitrate, it became evident that only 31% of the ammonium taken up ended up in oxidized products in A and B (Table 3),

i.e., a large amount of nitrite and less as nitrate. In contrast, the observed efficiency was much higher in D, where the products released accounted for 68% of the ammonium uptake, i.e., twice as much as in the experiments under reduced oxygen concentration.

**General community composition.** Hybridization of cross sections from material grown on Kaldnes elements and on polystyrene beads revealed the presence of at least 6 nitrifying populations (Fig. 2). Among the AOB, we found a population hybridizing with Nso1225, NEU, and Nse1472, indicative for *Nitrosomonas europaea* or *N. eutropha* (FIG. 2B to D). This affiliation was independently confirmed by a previous phylogenetic analysis of 16S rDNA clones retrieved from the same SBBR system (11). There, 33 clones could be assigned to the AOB of the beta subclass of *Proteobacteria* ( $\beta$ -AOB). All clones were highly related to each other and to *Nitrosomonas europaea* and contained the target sites of probes Nso1225, NEU, and Nse1472. A second population in the studied biofilm did not hybridize with probe Nso1225, but with probes NEU and NmV, indicating a population related to *Nitrosococcus mobilis* (Fig. 2C and D). A third AOB population gave positive signals with probe Nso1225, and probes NOLI191 and Nmo218, assigning it to the *Nitrosomonas oligotropha* lineage (29) (Fig. 2F). In the biofilm grown on the polymeric substrata, the *N. europaea/eutropha*-affiliated population was visually the most abundant followed by *Nitrosococcus mobilis*, while small clusters of the *N. oligotropha*-affiliated population occurred only sporadically. The same was found for the area of biofilm on complete clay beads accessed by CLSM.

FIG. 2. Confocal laser scanning micrographs of vertical biofilm thin sections hybridized with different probes. Probes were labeled with Cy3 (displayed as red), Cy5 (displayed as green), and Fluos (displayed as blue). The yellow colour originates from colocalization of probes labeled with Cy3 and Cy5, cyan to light green from colocalization of Cy5 and Fluos signals, and magenta from Cy3 and Fluos signals. (A) Localization of AOB and NOB populations as hybridized with NmV and Nso1225 (both red) targeting  $\beta$ -AOB, and Ntspa712 (green) targeting the phylum *Nitrospira* among *Bacteria* (EUB338, blue). (B) Organization of various AOB populations: *N. europaea/eutropha* (Nso1225 and NEU, cyan), *Nitrosococcus mobilis* (NEU and NmV, magenta), and a third population affiliated to the  $\beta$ -AOB (Nso1225, green). (C) Orthogonal reconstruction from an image stack of 14.4  $\mu\text{m}$  depth showing the association of *Nitrosococcus mobilis* (NmV, red) and *N. europaea/eutropha* (Nso1225, green). (D) Orthogonal reconstruction from an image stack of 18.7  $\mu\text{m}$  in thickness representing different sizes of *Nitrosococcus mobilis* aggregates (NEU, green, arrows 1) and hollow spherical spaces (arrow 2) of *N. europaea/eutropha* (NEU and Nse1472, yellow). Insert: Overlay of an image stack of 14.4  $\mu\text{m}$  thickness showing the close vicinity with direct cell contact of *Nitrosococcus mobilis* aggregates and *N. europaea/eutropha* cells. (E) Members of the genus *Nitrospira* (Ntspa662, green) and some aggregates of a *Nitrospira* subpopulation hybridized with probe NSR1253 (Ntspa662 and NSR1253, yellow). The image is a 2D projection of an image stack ( $z = 20 \mu\text{m}$ ). Insert: Close vicinity of NSR1253 positive (Ntspa662 and NSR1253, yellow) and negative subpopulations (Ntspa662, green) of *Nitrospira* spp. (F) Aggregates affiliated to the *N. oligotropha/N. ureae* lineage simultaneously hybridized with Nso1225 (green) and Nmo218 (red). Biofilm surface in A, B, D, and F is on the upper left side. The length of the scale bar is 50  $\mu\text{m}$  in A, B, and in D-F, 20  $\mu\text{m}$  in C, and 10  $\mu\text{m}$  in the inserts of D and E, respectively.



Among the NOB, one population was related to *Nitrobacter* spp., as hybridized with the probe NIT3. Furthermore, we could detect a population related to *Nitrospira* spp. by use of the probes Ntspa712 and Ntspa662, and NSR826, but not with NSR1156. The newly designed probe NSR1253 only hybridized with *Nitrospira*-like cells which could also be detected by probes Ntspa662, Ntspa712, and NSR826. At a formamide concentration higher than 10% in the hybridization buffer the signal intensity of probe NSR1253 decreased markedly. We thus suggest optimal stringency at 10% formamide. When analyzing simultaneous hybridization with probes Ntspa712 and NSR1253, only a small amount of cells showed a signal with the latter probe. Populations of NSR1253-positive and NSR1253-negative *Nitrospira* spp. were often found in close vicinity (Fig. 2E). Probe NSR1253 was also tested with sample material from another SBBR system (15). The biofilm in that system harbored a *Nitrospira* spp.-related population with the same hybridization pattern as the one reported here. However, in these samples the majority of *Nitrospira* spp. hybridized as well with probe NSR1253.

In addition, SBBR biofilm samples were hybridized with probe S-\*.-Amx-0820-a-A-22 specific for the two recently described candidatus genera of deep branching planctomycetes capable to anaerobically oxidize ammonium (35, 40). However, only very few cells with hybridization signals could be observed in the sample material.

Simultaneous hybridization with probes Nso1225, NmV, and Ntspa712, covering most of the nitrifiers in the system, and with the EUB338 probe mix, revealed that the majority of all microorganisms detected with the bacterial probe set were comprised with the selected probe set for nitrifying bacteria (Fig. 2A). This is consistent with previous quantitative community analysis in this system which demonstrated that 55% and 8% of the biovolume of all bacteria detectable by FISH could be assigned to AOB and NOB, respectively (11) (Fig. 2A).

**Spatial distribution of populations.** Reproducible patterns were found in the arrangement of some populations. Whereas the *N.europaeae/utropha*-affiliated population occurred in all layers of the biofilm, *Nitrosococcus mobilis*-related cells were not present near the surface (Fig 2B to D). Both NOB populations related to *Nitrospira* spp. and *Nitrobacter* spp., respectively, showed a very inhomogeneous spatial distribution. On polystyrene, we exclusively detected *Nitrospira* spp., which mostly occurred more or less close to the substratum (Fig. 2A). Single aggregates were also found distributed throughout the biofilm. In most sections from biofilm grown on Kaldnes substratum, *Nitrospira* spp. was dominant and *Nitrobacter* spp. was only rarely detected. In some sections, however, *Nitrobacter* spp. was found to be the dominant NOB population while numbers of *Nitrospira*-like cells were low (Fig. 3). These results indicate a heterogeneity on a larger scale. Due to the low depth penetration of CLSM,

however, no additional evidence could be provided by analysis of clay bead material. In the homogenized biofilm material, however, *Nitrospira* spp.-related cells were found predominantly.

The heterogeneous distribution of all populations within the biofilm was supported by quantitative 2-D analysis of confocal image series (Fig. 3). As AOB and NOB both occurred in clusters and more or less spread in the biofilm, the calculation of an average for a certain layer showed a large variation. For neither the AOB nor the NOB, a correlation of abundance with depth was found.

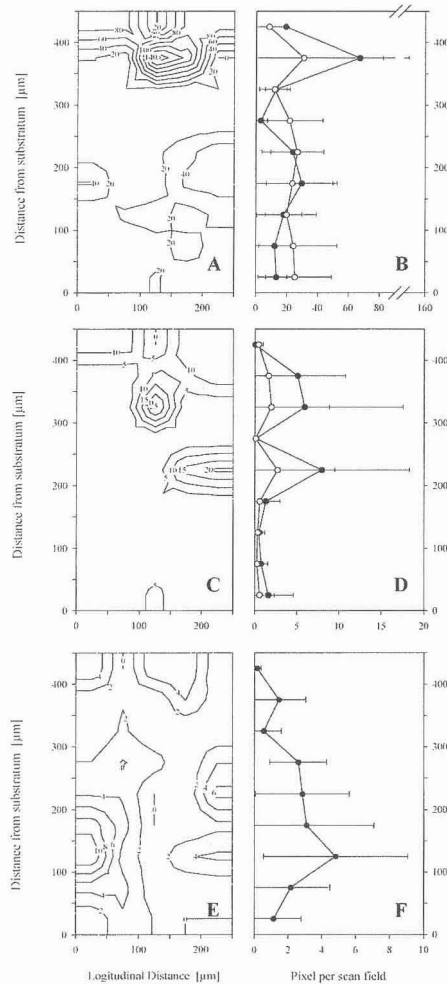


FIG. 3. Quantitative representation of the 2D heterogeneity of AOB as hybridized with a mix of Nso1225 and NEU (A, B), of *Nitrospira* spp. as hybridized with Nts662 (C, D), and of *Nitrobacter* spp. as hybridized with NIT3 (E, F). Diagrams A, C, and E show the amount of fluorescent pixels per scan field ( $50 \times 50 \mu\text{m}$ ) for a randomly chosen fields of view of  $250 \times 450 \mu\text{m}$ . The diagrams B, D, and F represent the means ( $\pm$  SD) for all the scan fields of one depth (in B and D:  $n = 15$ , in F:  $n = 5$ ).

A conspicuous observation were the very regular spherical clusters up to 18  $\mu\text{m}$  in size formed by *Nitrococcus mobilis* cells. While the smaller clusters were found in less densely populated areas of the biofilm, the larger ones were often densely surrounded by cells of the *N. europaea/eutropha*-affiliated population (Fig. 2C, D). Some of the largest *Nitrosococcus mobilis* clusters were hollow in the center (Fig. 2D). These compound structures were as well detected in biofilm grown on clay beads.

## DISCUSSION

**Experimental constraints.** Our experiments aimed at addressing both, the functional response on the community level as well as the adaptation of the individual populations to these situations. Therefore, we combined the experimental approach with structural investigations of the microbial populations. Compared to the other substrata, the biofilm grown on clay beads proved best suited for the microsensor experiments. It remained firmly attached to the substratum in the laminar flow applied, whereas on the other substratum types irregularities were observed and biofilm on bare surfaces tended to slough off. However, the rough surface of the clay beads hindered a proper and quantitative preparation for FISH. A certain amount of biofilm material remained attached in cavities and small ridges upon preparation. This problem was approached by comparing detailed analysis of the biofilm structure on the polymeric substratum types with hybridizations of biofilm on whole clay beads using CLSM. We found no evidence for differences in the structure of the upper 50  $\mu\text{m}$  of clay bead biofilm that were accessible with CLSM compared to vertical thin sections of the biofilm grown attached to polystyrene. The biofilm grown on Kaldnes appeared slightly more fluffy, presumably due to the sheltered conditions and reduced shear forces it had been subjected to. Homogenized biofilm material from different substratum types showed no apparent differences in the microbial composition of the biofilms. The results suggest that the biofilms from clay and polystyrene beads to a certain extent are comparable in spatial structure, microbial diversity, and relative abundances of the microbial populations. Therefore, we assume that a combination of our functional analysis with structural findings is acceptable although based in detail on different substratum types.

**Functional performance of the biofilm.** The overall activity of the biofilm, in terms of areal rates of oxygen and ammonium uptake into, and of nitrite and nitrate release from the biofilm was high. The uptake of oxygen and ammonium under conditions reflecting the be-

ginning of a cycle (experiment A) were one order of magnitude higher than those determined in flocs of an experimental nitrifying fluidized bed reactor (37), and of biofilms from a rotating disc reactor operated with domestic wastewater and synthetic medium (28), respectively. As the biofilm used here was typically subjected to much higher ammonium concentrations in the reactor (average: 32 mM; (3)), this might reflect the adaptation of the microbial community to the high ammonium loads.

The efflux of the products, nitrite and nitrate, did not account for the uptake of oxygen and ammonium in experiments A and B. This N loss was also observed on the reactor scale (3). In our experiments, the amount of oxidized N released corresponded to 31% and 38% of the ammonium uptake in A and B, respectively, but 68% in D. Which processes are responsible for this N loss? Nitrogen assimilation by nitrifiers can be estimated based on the N:C ratio of bacterial biomass and the carbon yield on ammonia or nitrite, respectively. Typical values for the N:C ratio [ $0.2 \text{ mol N (mol C)}^{-1}$ , (14)] and a maximum value for the carbon yield of nitrifiers [ $0.13 \text{ mol C/(mol N converted)}^{-1}$ , (30)], however, result in an assimilation ratio of only 2.6%, which does not explain the N loss as observed in A and B. Denitrifying processes, thus, very likely contributed to the N loss. Three denitrifying processes could have been responsible here: (i) conventional anaerobic denitrification in deeper parts of the biofilm, (ii) anaerobic ammonium oxidation [Anammox (18)] in the deeper biofilm layers, and (iii) denitrification by *N. europaea/eutropha* under oxygen-limitation (4). Reaction (i) is dependent on degradable organic carbon, which was present only in low amounts (3), but might have been provided by cell lysis within the biofilm. Due to the low cell numbers, (ii) does not seem to be of importance for this system. Sampling and investigation of biofilm by FISH, however, showed, that a population detectable with probe S-\*-Amx-0820-a-A-22 slowly increased in abundance several months after our experiments (41). Both, (i) and (ii) should be found in the anaerobic zones of the biofilm. According to local nitrate consumption rates, apparent denitrification in these layers, however, was low. Consequently, both processes might be of minor importance for the observed N loss. On the other hand, the *N. europaea/N. eutropha*-related population was very abundant, and denitrifying activity of these organisms with nitrite as electron acceptor has been demonstrated under oxygen limitation in cultures (4), as well as for sewage sludge (27). The *N. europaea/eutropha*-affiliated populations were found in close spatial vicinity to other AOB, which might be able to perform conventional ammonia oxidation. The resulting tight internal coupling of both processes would then explain the N loss without any distinct denitrifying zone. This explanation is in agreement with the observation that only part of the oxygen taken up from the biofilm is released in the form of oxidized N

products, especially during oxygen-limited conditions (Table 3). It can be suggested that local nitrite and nitrate production rates are higher than the apparent (gross) rates. Hence, we suggest a "nitrifier denitrification" (17) being likely to play a role during extended time periods of the treatment cycle, when oxygen is limited.

**Inhibition by free ammonia and free nitrous acid.** It is well documented that high concentrations of free ammonia (FA) and free nitrous acid (FNA) can hamper activity and growth of nitrifying bacteria (2, 16). Concentrations of 10 to 150 mg FA l<sup>-1</sup> were reported to be inhibitory to *Nitrosomonas* spp. whereas 0.1 to 1.0 mg FA l<sup>-1</sup> was found to inhibit *Nitrobacter* spp. (2). Free nitrous acid (FNA) inhibited *Nitrobacter* spp. at 0.22 to 2.8 mg FNA l<sup>-1</sup> (2). To test whether inhibition by FA could have caused the inefficient nitrification in experiments A to C compared to D, we calculated the concentrations of FA and FNA for the experimental conditions according to (2):

$$FA = 17/14 \times TA \times 10^{pH} / ([K_b / K_w] + 10^{pH}) \quad \text{with } K_b / K_w = \exp(6344/T) \quad \text{and}$$

$$FNA = 46/14 \times TN / (K_a \times 10^{pH}) \quad \text{with } K_a = \exp(-2300/T)$$

with  $TA$ : total ammonia in [mg N l<sup>-1</sup>];  $K_b$ ,  $K_w$ , and  $K_a$ : protolysis constants of ammonia, of water, and of nitrous acid equilibrium [-];  $T$ : temperature in [K];  $TN$ : nitrite concentration in [mg N l<sup>-1</sup>]. Under the bulk conditions in experiment A and B, i.e., pH = 8.2 to 8.4 and  $TA = 45$  mg N l<sup>-1</sup>, FA is 7.1 mg N l<sup>-1</sup>. This is in the range of inhibition for *Nitrobacter* spp. but not for *Nitrosomonas* spp. In the biofilm the conditions are more moderate (pH = 8.1;  $TA = 40.6$  mg N l<sup>-1</sup>) but still in the inhibiting range for *Nitrobacter* spp. FNA under our experimental conditions is low. Highest values were around  $1 \times 10^{-4}$  mg N l<sup>-1</sup> and, thus, are not critical. In experiment D, the pH in the biofilm was 7.2 and  $TA$  around 10 mg N l<sup>-1</sup>. The calculated FA is 0.1 mg N l<sup>-1</sup> coming close to the lower limit of the inhibitory range of *Nitrobacter* spp. In the full scale system pH is buffered at 7.5 but ammonia concentrations are much higher. Whether FA inhibits NOB of the genus *Nitrospira* is not known. It can be concluded that under the experimental as well as applied conditions inhibition of nitrite oxidation at least in *Nitrobacter* spp. occurs.

**Structure of the nitrifying community.** There are several reports from nitrifying biofilms that AOB and NOB occur more or less spatially segregated, either due to externally applied gradients (36), or as a result of lower growth rates and/or adaptation to lower oxygen concentrations as in the case of *Nitrospira* spp. (28). In these cases, solute gradients and spatial dis-

tribution of populations were correlated and revealed details on their specific *in situ* ecophysiology. However, quantitative evidence for a layered distribution of AOB and NOB populations is difficult to obtain, or limited, which might be due to the typically patchy distribution of both the AOB and the NOB populations (15, 24, 39). Our results from visual inspection of the biofilms grown on different substratum types suggest that the spatial arrangement is very heterogeneous. As an exception *Nitrospira* spp. populations tended to occupy preferentially the biofilm base but were also found in other parts of the biofilm. Attempts of quantification did not result in additional evidence on what rules the spatial distribution of the populations of AOB and NOB.

It can be speculated, that during the SBBR cycle, the periods of steady state with stable vertical gradients especially of oxygen are not long enough to support the generation of a layered arrangement. In contrast, we assume that the heterogeneity of the microenvironments is high, leading to this mixed spatial distribution.

**Coexistence of AOB populations.** Results of FISH clearly demonstrate the stable coexistence of three AOB populations. Assuming a niche separation, the populations have to apply different strategies to persist in the biofilm. The experimental results have shown that during most of the reactor cycle, the penetration of oxygen is low. Thus, populations near the surface might have an advantage in oxygen supply. On the other hand, regular backwashing will have a stronger impact on the biofilm surface than on the base, subsequently promoting the establishment of fast-growing populations. We found *N. europaea/eutropha* to be the dominant AOB in the system, which might be the result of two facts: (i) the growth rates of *N. europaea/eutropha* with up to  $0.088 \text{ h}^{-1}$  are relatively high compared to other AOB (30), and (ii) *N. europaea/eutropha* are potentially capable of using alternative electron acceptors like nitrite under oxygen limitation (4) as pointed out above. Both abilities would allow an adaptation to both the constraints of surface and deeper biofilm growth. The maximum growth rate of *Nitrosococcus mobilis*, the second most abundant AOB, is  $0.077$  to  $0.083 \text{ h}^{-1}$  (20) and, thus, nearly in the same range. With respect to the strategies of persistence of these two populations in the biofilm, the close vicinity of *Nitrosococcus mobilis* aggregates to or even embedding in *N. europaea/eutropha* colonies is interesting. Similar associations of two types of bacteria have been reported for syntrophic aggregates of methanogens and sulfate-reducing bacteria (5), for *Nitrosomonas* and *Nitrobacter* (24, 39), and for *Nitrosococcus mobilis* and *Nitrospira* (19). These types of associations, however, all consist of two functionally different bacterial populations and are very likely based on cooperation. What is the advantage of association for two populations, that are supposed to compete for the same compounds? Close

competition would clearly lead to the exclusion of one of the populations. It might be speculated, whether some partial cooperation exists: under oxygen limitation *N. europaea/eutropha* might perform ammonia oxidation with nitrite, which in turn is provided by *Nitrosococcus mobilis*. Evidence for this hypothesis is given by the fact, that these dense associations were not found at the very surface, but only inside the biofilm. Such a strategy would imply a higher oxygen affinity of *Nitrosococcus mobilis*. However, no data are available to support this hypothesis. Furthermore, although the concentration gradient over a distance of a few  $\mu\text{m}$  is low to nonexistent, the expected spatial arrangement in this case should be the inverse: *Nitrosococcus mobilis* at the outside where the oxygen concentration is higher, and *N. europaea/eutropha* in the center. This was not observed. Alternatively, these associations could have been formed passively by *N. europaea/eutropha* simply overgrowing *Nitrosococcus mobilis*, without completely blocking it off from oxygen supply. The existence of different types, free-growing, surrounded and large hollow aggregates (Fig. 2D), possibly indicates a succession starting with a few *Nitrosococcus mobilis* cells in areas with a low local cell density, which is then later surrounded by *N. europaea/eutropha*, and finally inactivated and degraded due to shortage in oxygen.

The detection of an *N. oligotropha*-related population is independently supported by a 16S rDNA analysis of the biofilm community in a previous study (11). It might thus be considered a stable member of the AOB community in this biofilm. According to results from a phosphate-removing SBBR with nitrifying activity (15), it was speculated, that a potentially higher oxygen affinity allows *N. oligotropha*-related organisms to coexist with other AOB populations in a biofilm. The heterogeneous biofilms studied here, however, are not suitable to support this hypothesis. It appears challenging to apply methods which are able to focus on the activity of a single population or even a single cell in the future to get deeper insights on this coexistence and potential cooperation.

**Diversity among nitrite-oxidizing bacteria.** The two phylogenetically unrelated but functionally similar NOB populations detected in the biofilm did not exclude each other from the system. Earlier studies suggest *Nitrobacter* spp. to be adapted to high substrate concentrations, in contrast to *Nitrospira* spp., which was found predominantly in a zone of lower substrate and oxygen concentrations in a membrane-grown biofilm (36). During the SBR cycle the concentration of ammonium covered a broad range, and might allow the persistence of both NOB by temporal activity. The heterogeneity in spatial distribution on a larger scale, however, was not addressed by our experiments.

After using different probes for the *Nitrospira* spp. population, we found a signal pattern identical to that of the NOB population reported from a phosphate removing SBBR (15), and from a SBR designed for nitrite oxidation (7). The probe match pattern exactly fit to a monophyletic cluster of *Nitrospira* [clone clade 2 in (7)]. The design and application of a new probe for this monophyletic group showed additional diversity: at least two different populations of this cluster were present in the investigated biofilm. As mentioned above, activity measurements on the single population or single cell level in future studies might be able to reveal the adaptations leading to the irregular distribution with even close vicinity of the two *Nitrospira* spp. populations to each other (Fig. 2E) and their role in such systems.

The observations on the bead-grown biofilm suggest the lower growth rate of *Nitrospira* to cause its predominant occurrence at the substratum side of the biofilm. Our experiments clearly demonstrated, that the biofilm base was free of oxygen throughout most of the cycle. Experiment D demonstrated that oxygen in this layer is not available until ammonium concentration has become low, i.e., under practical conditions for only a very short period. Nitrate profiles, on the other hand, did not suggest any nitrite-oxidizing activity near the substratum. Thus activity and subsequent growth is only possible for populations mixed into layers closer to the surface. The persistence strategy of the *Nitrospira* strains might therefore not only consist in a high affinity towards oxygen as suggested earlier (28, 36, 37), but the cells, while being inactive, maintain their ribosome content for a long period of inactivity (25) and could act as seedlings that immediately recover their activity in other places when detached. In principle, this might also apply for *Nitrospira* spp. in other SBR setups. Their existence in other (SBR type) systems and their ecophysiology is a potential topic of future studies.

## CONCLUSIONS

Nitrogen loss, assumingly caused by denitrification by *N. europaea/eutropha*, and inhibition of nitrite oxidation by free ammonia might be two phenomena playing a role in the biofilm function of this system. The microbial community was characterized by a high diversity of nitrifiers. The heterogeneous spatial distribution of the microbial populations below (aggregates of *N. europaea/eutropha* and *Nitrosococcus mobilis*) or above (*Nitrospira* spp. and *Nitrobacter* spp.) a scale relevant for diffusion limitations, however, limited the insights gained by the microsensor-FISH approach. To reveal mechanisms of coexistence, future studies on complex biofilm communities should include methods suitable to access as well

the local function on the population and single cell level. Combinations of FISH and microautoradiography (MAR) have already been used successfully to access single cell activity (21). Thus, MAR could be used to link analysis with FISH and microsensors for a more detailed picture of structure and function in complex biofilm communities.

## ACKNOWLEDGEMENTS

This work was supported by the German Research Foundation (SFB 411, Project A1-Research Center for Fundamental Studies of Aerobic Wastewater Treatment, Munich, Germany). L. B. was supported by a grant within the framework of the SFB 411 from the DFG to M.W. Holger Daims is acknowledged for help with the confocal laser scanning microscopy and for valuable discussions, and Anja Eggers, Gaby Eickert, and Ines Schröder for providing oxygen microelectrodes.

## REFERENCES

1. **Amann, R. I., B. J. Binder, R. J. Olson, S. W. Chisholm, R. Devereux, and D. A. Stahl.** 1990. Combination of 16S rRNA-targeted oligonucleotide probes with flow cytometry for analyzing mixed microbial populations. *Appl. Environ. Microbiol.* **56**:1919-1925.
2. **Anthonisen, A. C., R. C. Loehr, T. B. S. Prakasam, and E. G. Srinath.** 1976. Inhibition of nitrification by ammonia and nitrous acid. *J. Water Pollut. Cont. Fed.* **48**:835-852.
3. **Arnold, E., B. Böhm, and P. A. Wilderer.** 2000. Application of activated sludge and biofilm sequencing batch reactor technology to treat reject water from sludge dewatering systems: a comparison. *Water Sci. Technol.* **41**:115-122.
4. **Bock, E., I. Schmidt, R. Stüven, and D. Zart.** 1995. Nitrogen loss caused by denitrifying *Nitrosomonas* cells using ammonium or hydrogen as electron donors and nitrite as electron acceptor. *Arch. Microbiol.* **163**:16-20.
5. **Boetius, A., K. Ravensschlag, C. J. Schubert, D. Rickert, F. Widdel, A. Gieseke, R. Amann, B. B. Jørgensen, U. Witte, and O. Pfannkuche.** 2000. A marine microbial consortium apparently mediating anaerobic oxidation of methane. *Nature.* **407**:623-626.
6. **Broecker, W. S., and T.-H. Peng.** 1974. Gas exchange rates between air and sea. *Tellus.* **26**:21-35.
7. **Burrell, P., J. Keller, and L. Blackall.** 1998. Microbiology of a nitrite-oxidizing bioreactor. *Appl. Environ. Microbiol.* **64**:1878-1883.
8. **Christensen, B. E., and W. G. Characklis.** 1990. Physical and chemical properties of biofilms, p. 93-130. *In* W. G. Characklis and K. C. Marshall (eds.), *Biofilms*. John Wiley & Sons, Inc., New York.

9. **Daims, H., A. Brühl, R. Amann, K.-H. Schleifer, and M. Wagner.** 1999. The domain-specific probe EUB338 is insufficient for the detection of all *Bacteria*: Development and evaluation of a more comprehensive probe set. *Syst. Appl. Microbiol.* **22**:434-444.
10. **Daims, H., P. Nielsen, J. L. Nielsen, S. Juretschko, and M. Wagner.** 2000. Novel *Nitrospira*-like bacteria as dominant nitrite-oxidizers in biofilms from wastewater treatment plants: diversity and *in situ* physiology. *Water Sci. Technol.* **41**:85-90.
11. **Daims, H., U. Purkhold, L. Bjerrum, E. Arnold, P. A. Wilderer, and M. Wagner.** 2001. Nitrification in sequencing batch reactors: lessons from molecular approaches. *Water Sci. Technol.* **43**:9-18.
12. **de Beer, D., A. Schramm, C. M. Santegoeds, and M. Kühl.** 1997. A nitrite microsensor for profiling environmental biofilms. *Appl. Environ. Microbiol.* **63**:973-977.
13. **de Beer, D., and P. Stoodley.** 1999. Microbial biofilms. In M. Dworkin (ed.), *The Prokaryotes: An Evolving Electronic Resource for the Microbiological Community*, 3rd ed. Springer, New York.
14. **Fagerbakke, K. M., M. Heldal, and S. Norland.** 1996. Content of carbon, nitrogen, oxygen, sulfur and phosphorus in native aquatic and cultured bacteria. *Aquat. Microb. Ecol.* **10**:15-27.
15. **Gieseke, A., U. Purkhold, M. Wagner, R. Amann, and A. Schramm.** 2001. Community structure and activity dynamics of nitrifying bacteria in a phosphate-removing biofilm. *Appl. Environ. Microbiol.* **67**:1351-1362.
16. **Hwang, B.-H., K.-Y. Hwang, E.-S. Choi, D.-K. Choi, and J.-Y. Jung.** 2000. Enhanced nitrite build-up in proportion to increasing alkalinity/NH<sub>4</sub><sup>+</sup> ratio of influent in biofilm reactor. *Biotechnol. Lett.* **22**:1287-1290.
17. **Jetten, M. S. M., S. Logemann, G. Muyzer, L. A. Robertson, S. de Vries, M. C. M. van Loosdrecht, and J. G. Kuenen.** 1997. Novel principles in the microbial conversion of nitrogen compounds. *Ant. Leeuw.* **71**:75-93.
18. **Jetten, M. S. M., M. Strous, K. T. van de Pas-Schoonen, J. Schalk, U. G. J. M. van Dongen, A. A. van de Graaf, S. Logemann, G. Muyzer, M. C. M. van Loosdrecht, and J. G. Kuenen.** 1999. The anaerobic oxidation of ammonium. *FEMS Microbiol. Rev.* **22**:421-437.
19. **Juretschko, S., G. Timmermann, M. Schmid, K.-H. Schleifer, A. Pommerening-Röser, H. P. Koops, and M. Wagner.** 1998. Combined molecular and conventional analysis of nitrifying bacterium diversity in activated sludge: *Nitrosococcus mobilis* and *Nitrospira*-like bacteria as dominant populations. *Appl. Environ. Microbiol.* **64**:3042-3051.
20. **Koops, H.-P., H. Harms, and H. Wehrmann.** 1976. Isolation of a moderate halophilic ammonia-oxidizing bacterium, *Nitrosococcus mobilis* nov. sp. *Arch. Microbiol.* **107**:277-282.
21. **Lee, N., P. H. Nielsen, K. H. Andreasen, S. Juretschko, J. L. Nielsen, K.-H. Schleifer, and M. Wagner.** 1999. Combination of fluorescent *in situ* hybridization and microautoradiography - a new tool for structure-function analyses in microbial ecology. *Appl. Environ. Microbiol.* **65**:1289-1297.
22. **Li, Y.-H., and S. Gregory.** 1974. Diffusion of ions in sea water and in deep-sea sediments. *Geochim. Cosmochim. Acta.* **38**:703-714.
23. **Manz, W., R. Amann, W. Ludwig, M. Wagner, and K.-H. Schleifer.** 1992. Phylogenetic oligodeoxynucleotide probes for the major subclasses of proteobacteria: problems and solutions. *Syst. Appl. Microbiol.* **15**:593-600.

24. **Mobarry, B. K., M. Wagner, V. Urbain, B. E. Rittmann, and D. A. Stahl.** 1996. Phylogenetic probes for analyzing abundance and spatial organization of nitrifying bacteria. *Appl. Environ. Microbiol.* **62**:2156-2162.
25. **Morgenroth, E., A. Obermayer, E. Arnold, A. Brühl, M. Wagner, and P. A. Wilderer.** 2000. Effect of long-term idle periods on the performance of sequencing batch reactors. *Water Sci. Technol.* **41**:105-113.
26. **Morgenroth, E., P. A. Wilderer, J. Banard, A. Boon, S. Williams, F. Xiong, A. Ware, T. Pitman, and E. de Jong.** 1998. Sequencing batch reactor technology: concepts, design and experiences. *J. CIWEM.* **12**:314-321.
27. **Muller, E. B., A. H. Stouthamer, and H. W. van Verseveld.** 1995. Simultaneous  $\text{NH}_3$  oxidaton and  $\text{N}_2$  production at reduced  $\text{O}_2$  tensions by sewage sludge subcultured with chemolithotrophic medium. *Biodegradation.* **6**:339-349.
28. **Okabe, S., H. Satoh, and Y. Watanabe.** 1999. In situ analysis of nitrifying biofilms as determined by in situ hybridization and the use of microelectrodes. *Appl. Environ. Microbiol.* **65**:3182-3191.
29. **Pommerening-Röser, A., G. Rath, and H.-P. Koops.** 1996. Phylogenetic diversity within the genus *Nitrosomonas*. *Syst. Appl. Microbiol.* **19**:344-351.
30. **Prosser, J. I.** 1989. Autotrophic nitrification in bacteria. *Adv. Microb. Physiol.* **30**:125-181.
31. **Purkhold, U., A. Pommerening-Röser, S. Juretschko, M. C. Schmid, H.-P. Koops, and M. Wagner.** 2000. Phylogeny of all recognized species of ammonia-oxidizers based on comparative 16S rRNA and *amoA* sequence analysis: Implications for molecular diversity surveys. *Appl. Environ. Microbiol.* **66**:5368-5382.
32. **Rath, G.** 1996. Entwicklung eines Nachweissystems zur *in situ*-Analyse nitrifizierender Bakterienpopulationen auf der Basis spezifischer 16S rRNA-Gensequenzen. PhD thesis. University of Hamburg, Hamburg, Germany.
33. **Revsbech, N. P.** 1989. An oxygen microelectrode with a guard cathode. *Limnol. Oceanogr.* **34**:474-478.
34. **Revsbech, N. P., and B. B. Jørgensen.** 1986. Microelectrodes: their use in microbial ecology. *Adv. Microb. Ecol.* **9**:293-352.
35. **Schmid, M., U. Twachtmann, M. Klein, M. Strous, S. Juretschko, M. S. M. Jetten, J. W. Metzger, K.-H. Schleifer, and M. Wagner.** 2000. Molecular evidence for genus level diversity of bacteria capable of catalyzing anaerobic ammonium oxidation. *Syst. Appl. Microbiol.* **23**:93-106.
36. **Schramm, A., D. de Beer, A. Gieseke, and R. Amann.** 2000. Microenvironments and distribution of nitrifying bacteria in a membrane-bound biofilm. *Environ. Microbiol.* **2**:680-686.
37. **Schramm, A., D. de Beer, J. C. van den Heuvel, S. Ottengraf, and R. Amann.** 1999. Microscale distribution of populations and activities of *Nitrosospira* and *Nitrospira* spp. along a macroscale gradient in a nitrifying bioreactor: Quantification by in situ hybridization and the use of microsensors. *Appl. Environ. Microbiol.* **65**:3690-3696.
38. **Schramm, A., D. de Beer, M. Wagner, and R. Amann.** 1998. Identification and activities in situ of *Nitrosospira* and *Nitrospira* spp. as dominant populations in a nitrifying fluidized bed reactor. *Appl. Environ. Microbiol.* **64**:3480-3485.

39. Schramm, A., L. H. Larsen, N. P. Revsbech, N. B. Ramsing, R. Amann, and K.-H. Schleifer. 1996. Structure and function of a nitrifying biofilm as determined by *in situ* hybridization and the use of microelectrodes. *Appl. Environ. Microbiol.* **62**:4641-4647.
40. Strous, M., J. A. Fuerst, E. H. M. Kramer, S. Logemann, G. Muyzer, K. T. van de Pas-Schoonen, R. Webb, J. G. Kuenen, and M. S. M. Jetten. 1999. Missing lithotroph identified as new planctomy-cete. *Nature.* **400**:446-449.
41. Wagner, M. pers. comm. .
42. Wagner, M., R. Amann, P. Kämpfer, B. Assmus, A. Hartmann, P. Hutzler, N. Springer, and K.-H. Schleifer. 1994. Identification and *in situ* detection of gram-negative filamentous bacteria in activated sludge. *Syst. Appl. Microbiol.* **17**:405-417.
43. Wagner, M., G. Rath, R. Amann, H. P. Koops, and K.-H. Schleifer. 1995. *In situ* identification of ammonia-oxidizing bacteria. *Syst. Appl. Microbiol.* **18**:251-264.
44. Wagner, M., G. Rath, H. P. Koops, J. Flood, and R. Amann. 1996. *In situ* analysis of nitrifying bacteria in sewage treatment plants. *Water Sci. Technol.* **34**:237-244.



## **Chapter 6**

### ***In situ* Substrate Conversion and Assimilation in a Nitrifying Model Biofilm as Studied with a Combination of Methods**

A. Gieseke, J. L. Nielsen, H. Jonkers, R. Amann, P. H. Nielsen, and D. de Beer

Manuscript in preparation



## ***In situ* Substrate Conversion and Assimilation in a Nitrifying Model Biofilm as Studied with a Combination of Methods**

Armin Gieseke<sup>1\*</sup>, Jeppe Lund Nielsen<sup>2</sup>, Henk Jonkers<sup>1</sup>, Rudolf Amann<sup>1</sup>, Per Halkjær  
Nielsen<sup>2</sup>, and Dirk de Beer<sup>1</sup>

<sup>1</sup>*Molecular Ecology Group, Max Planck Institute for Marine Microbiology, D-28359 Bremen, Germany*

<sup>2</sup>*Department of Environmental Engineering, Aalborg University, DK-9000 Aalborg, Denmark*

A combination of microsensor measurements, fluorescence *in situ* hybridization (FISH), microautoradiography (MAR), and a new quantitative beta microimaging technique was used to study nitrification in a model biofilm. An agarose suspension of two ammonia-oxidizing populations (related to *Nitrosomonas europaea/eutropha* and to *N. oligotropha*) and one nitrite-oxidizing population (*Nitrospira* spp.) was incubated with [<sup>14</sup>C]-bicarbonate under different conditions (oxygen, ammonium, nitrite). Simultaneously, microprofiles of oxygen, ammonium, nitrite, and nitrate were measured. Thin sections of fixed biofilm were subsequently subjected to FISH and MAR. In a subset local [<sup>14</sup>C]-bicarbonate uptake was quantified with a high resolution beta microimaging device. Results of the four methods were generally in good agreement. Microprofiles reflected limitation of either oxygen or substrate. Active oxygen consumption and substrate conversion, as well as assimilation of bicarbonate, were restricted to a surface layer of different thickness in the various experiments. Depending on incubation conditions, cells of either a single or several populations were mostly MAR-positive within this active zone. Uptake profiles of [<sup>14</sup>C] were in agreement in shape and intensity with activity as measured with microsensors. *In situ* cell yields determined from the data were in the lower range of those reported for pure cultures of nitrifying bacteria.

## **INTRODUCTION**

Intensive recent application of *in situ* techniques like microsensor measurements or fluorescence *in situ* hybridization (FISH) has strongly increased our understanding of the structure and function of microbial communities. These techniques are of particular use when applied to complex environments, or on organisms that are difficult to cultivate, like nitrifying bacteria. This latter group of bacteria is of considerable economical importance as nitrifiers

can cause extensive loss of fertilizer ammonium from soils and subsequent eutrophication of natural waters (30), but are also responsible for first steps in nitrogen removal from sewage (28).

FISH with oligonucleotide probes specific for various groups of nitrifying bacteria has been successfully used for identification (13, 16, 22, 26, 31, 34-37, 39, 40), quantification (13, 34, 39), and localization of ammonia-oxidizing bacteria (AOB) and nitrite-oxidizing bacteria (NOB) in activated sludge flocs (16, 22, 35) and biofilms (13, 26, 34, 37). A 16S rRNA-based detection, however, provides only indirect evidence for the physiological potentials and recent activity of the respective population. Therefore, these methods have been combined with techniques for *in situ* analysis of function. Several recent studies combined FISH with micro-sensor measurements to characterize the microenvironment and activity of nitrifying populations in biofilms (13, 26, 34-37). The correlation of both the measured activity and the spatial distribution allows direct conclusions towards the ecology and *in situ* physiology of a defined population. In this way, the calculation of cell-specific conversion rates (13, 35) and *in situ* substrate affinities (35) have been achieved.

On the applied technical scale or in multifunctional systems, however, microbial communities in flocs or biofilms are often complex. The coexistence of several populations of AOB and NOB has been shown in biofilms from a membrane reactor (34), from a trickling filter (37), and from sequencing batch systems (13, 22; this thesis, chapter 5). These communities often lack a clear-cut layered organization along substrate gradients (13; this thesis, chapter 5). Close spatial co-occurrence of microcolonies (13, 22, 37) and significant diversity of AOB and NOB (this thesis, chapter 5) have been reported. The application of FISH and micro-sensor measurements in such systems is not sufficient to resolve the specific contribution of different populations or individual cells to the overall or local activity in different micro-environments.

A combination of FISH with microautoradiography (MAR) has been proposed and successfully applied to investigate whether a population actively metabolizes a substrate under certain environmental conditions (18, 24, 27). The method allowed studies down to the single cell level. This approach, however, is difficult to apply for quantitative analysis of cellular activities.

Beta microimaging has been recently suggested as a sensitive technique to measure the two-dimensional distribution of a radiotracer in a sample with high spatial resolution (10  $\mu\text{m}$ ) (17). While not accessing the single cell level, the uptake can be quantified from monitored signals.

In this study we describe an experimental approach in which FISH, microsensor measurements, MAR and quantitative beta microimaging techniques are combined in order to get deeper insights into the function and its correlation to structure in a model biofilm. The aim of this study was to quantify local bicarbonate assimilation under different conditions in a model biofilm and to relate this information (i) to the distribution of active populations revealed by MAR/FISH and (ii) to their local activity as measured with microsensors. The combination of methods permitted us to study activity on different scales, i.e., the whole biofilm community, the individual populations, and the single cell.

## **MATERIALS AND METHODS**

**Nitrifying fluidized bed reactor.** A fluidized bed reactor operated as described previously (11) served as a source for nitrifying aggregates. The conical shaped reactor was fed with a medium composed of  $\text{NH}_4\text{Cl}$  (5.7 mM),  $\text{Na}_2\text{SO}_4$  (0.5 mM),  $\text{K}_2\text{HPO}_4$  (0.25 mM), and trace elements ( $\text{MgCl}_2$ ,  $2.9 \times 10^{-2}$  mM;  $\text{FeCl}_3$ ,  $1.8 \times 10^{-2}$  mM;  $\text{MnCl}_2$ ,  $3.5 \times 10^{-3}$  mM;  $\text{MoO}_4^{2-}$ ,  $1.4 \times 10^{-3}$  mM; in 0.2 M HCl).  $\text{Na}_2\text{CO}_3$  (0.6 M) was used to keep the pH at 8.0, leading to a total carbonate concentration of 2 mM. The system had been operated under stable conditions for more than 16 months before the time of sampling.

**Preparation of model biofilm.** For every experiment, a fresh sample was taken from the reactor by aid of a long tube introduced from above. This ensured a mixed vertical sample from the whole reactor column. After the flocs in this sample were broken down into smaller aggregates by vortexing, 750  $\mu\text{l}$  of the suspension was mixed with an equal amount of low melting agarose (melting temp. 26°C to 30°C) kept at 30°C. The mixture was then portioned in sterile cut-off 8 x 4 mm lids (d x h) from 2 ml Eppendorf tubes using a syringe with an injection needle, and the suspension was immediately solidified on ice. The model biofilm was kept covered with liquid medium until experimental incubation.

**Experimental setup.** Model biofilm were glued by their support to the bottom of a 100 ml wide-neck glass bottle by use of small amounts of silicone grease. A volume of 12 ml of the respective medium was added to cover the sample. This incubation chamber was closed by a lid with two holes. A small curved glass capillary for aeration and convection of the medium was inserted through the peripheral hole. The opening of the capillary was placed directly above the medium surface to avoid aerosol formation. A second central opening in the lid was used to access the sample with microsensors during incubation. The liquid medium was com-

parable to that fed to the reactor, except that  $K_2HPO_4$  was replaced by  $Na_2HPO_4$ , and fixed amounts of  $NH_4Cl$ ,  $NaNO_2$  (Table 1) and  $Na_2CO_3$  were added. The pH was adjusted to 7.8 by addition of either acid or base. The exact total carbonate concentration in the medium was determined with a total organic carbon analyzer (TOC 5050A, Shimadzu Europe, Duisburg, Germany), and in all incubations was  $1.49 \pm 0.08$  mM (mean  $\pm$  SD). Several experiments with different conditions were performed as shown in Table 1. In case of the experiments with a decreased oxygen concentration (C and E), aeration was done with Argon.

TABLE 1. Experimental conditions.

Designation	Experimental conditions	Ammonium added [mM]	Nitrite added [ $\mu$ M]	Oxygen conc. [% air sat.]
A	Standard	0.7	-	100
B	Ammonium limitation	0.03	-	100
C	Oxygen limitation	0.3	-	15
D	Nitrite oxidation	-	0.6	100
E	Nitrifier denitrification	0.3	0.3	20
N	Negative control	-	-	100

**Radiotracer incubation and microsensor measurements.** Each experiment was started by adding 5.9 MBq of [ $^{14}C$ ]-bicarbonate per 12 ml medium. Incubation was performed for a period of 8.8 h. Parallely, microprofiles were measured with an amperometric oxygen microsensor (32) and ion-selective microelectrodes for ammonium, and either nitrite or nitrate (10). Measurements were started after 1 h of incubation to allow for development of a steady state. Between 14 and 20 microprofiles were recorded in each individual experiment.

**FISH.** Samples from the source reactor were fixed directly with fresh paraformaldehyde (PFA) for 4 h as described earlier (1). After washing in PBS and transfer to PBS/EtOH, the samples were ultrasonicated with an amplitude of 126  $\mu$ m for 3 x 20s to suspend the bacterial aggregates. Aliquots of 6  $\mu$ l per well were spread on gelatin-coated microscopic slides with wells, dried at room temperature, and subjected to FISH according to earlier descriptions (21). Probes and hybridization conditions are listed in Table 2. The AOB populations were quantified by microscopic counting on an epifluorescence microscope (Zeiss Axiophot II, Carl Zeiss, Jena, Germany).

Incubated model biofilm samples were carefully removed from their support to ensure homogeneous fixation, and then fixed with PFA accordingly directly after incubation. Thereafter, the samples were transferred to cryoembedding medium (Jung tissue embedding medium, Leica GmbH, Nussloch, Germany), incubated for 24h, frozen on dry ice, and then

sliced vertically on a cryomicrotome (HM505E, Microm, Walldorf, Germany). The sections of 20 µm thickness were immobilized on gelatin-coated cover glasses (18). After drying, the embedding compound and non-incorporated bicarbonate were removed by careful washing with distilled water, and samples were stored at 4°C until further processing.

TABLE 2. Probes and hybridization conditions applied in this study.

Probe	Probe Sequence (5' to 3')	Target site <sup>a</sup>	Target organism(s)	FA [%] <sup>b</sup>	NaCl [mM] <sup>c</sup>	Ref.
EUB338	GCTGCCTCCCCTAGGAGT	16S (338-355)	Domain <i>Bacteria</i>	20	225	(1)
Nso1225	CGCCATTGTATTACGTGTGA	16S (1225-1244)	Ammonia-oxidizing β-proteobacteria	35	80	(22)
NEU <sup>d</sup>	CCCCTCTGCTGCACTCTA	16S (653-670)	Halophilic / halotolerant <i>Nitrosomonas</i> spp.	40	56	(39)
Nse1472 <sup>e</sup>	ACCCCAGTCATGACCCCC	16S (1472-1489)	<i>N. europaea</i>	50	28	(16)
Nmo218	CGGCCGCTCCAAAGCAT	16S (218-235)	<i>N. oligotropha</i> -lineage	35	80	(13)
NOLI191 <sup>d</sup>	CGATCCCCCACTTTCCTC	16S (191-208)	various members of the <i>N. oligotropha</i> -lineage	30	112	(13)
Ntspa712 <sup>d,f</sup>	CGCCTTCGCCACCGGCTTCC	16S (712-732)	Phylum <i>Nitrospira</i>	35	80	(8)
Ntspa662 <sup>d,f</sup>	GGAATTCCGCGCTCTCT	16S (662-679)	Genus <i>Nitrospira</i>	35	80	(8)

<sup>a</sup> rRNA position according to *E. coli* numbering (7).

<sup>b</sup> Percentage of formamide in the hybridization buffer.

<sup>c</sup> Concentration of sodium chloride in the washing buffer.

<sup>d</sup> Applied together with equimolar amount of unlabeled competitor oligonucleotide as indicated in the reference.

<sup>e</sup> Referred to as S\*-Nse-1472-a-A-18.

<sup>f</sup> Referred to as S\*-Ntspa-0712-a-A-21 and S-G-Ntspa-0662-a-A-18, respectively, in the reference.

**Microautoradiography and FISH.** The vertical cryosections of the biofilm from each experiment were immobilized on gelatin-coated cover glasses and allowed to dry at room temperature (18). To remove any traces of precipitated [<sup>14</sup>C]-bicarbonate within the biofilm an additional gentle washing step with a 0.1 M glycine buffer solution, pH 3, followed by rinsing in distilled water, was applied after drying. Hybridization with the different probes (Table 2) was performed directly on the coverglass using common hybridization procedures (21). The sections were subsequently covered with a photographic emulsion for microautoradiography and allowed to expose for approximately 7 days before development as described earlier (2). The developed slides were dried and immediately inspected under the microscope.

**Beta microimaging.** Uptake of bicarbonate was quantified by use of a beta emission microimager (Micro Imager, Biospace Mesures, Paris, France). For that purpose, washed and dried cryosections were covered with a scintillation foil and mounted in the device. The working principle of the beta microimager is described elsewhere (17). Shortly, scintillation signals were enhanced in an array of microphotomultipliers with an individual diameter of 10 µm. Each signal event was then retranslated into an optical signal, detected via a CCD chip and recorded on a PC. For each experimental condition, 6 thin sections were scanned. The

scan time was 45 min. Within the counting period, between 7500 and 17500 counts were obtained for each individual thin section, with the exception of the negative control, where a maximum of 2200 counts was obtained in 45 min. For determination of counting efficiency, a set of thin sections was first scanned on the beta microimager. Then, the samples were washed off by incubation in trichloroacetic acid at 95°C for 30 min. Radioactivity in the liquid phase was subsequently quantified by scintillation counting and compared to the results from beta microimaging.

**Nitrification and bicarbonate uptake rates.** The microprofiles were used to calculate total areal uptake or release rates of  $O_2$ ,  $NH_4^+$ ,  $NO_2^-$ , and  $NO_3^-$  for the whole biofilm, and local volumetric consumption rates of oxygen in different layers. For the areal uptake/release rates, fluxes through the diffusive boundary layer (DBL) were calculated according to earlier descriptions (37). The molecular diffusion coefficients in water of  $2.12 \times 10^{-5} \text{ cm s}^{-1}$ ,  $1.76 \times 10^{-5} \text{ cm s}^{-1}$ ,  $1.65 \times 10^{-5} \text{ cm s}^{-1}$ , and  $1.71 \times 10^{-5} \text{ cm s}^{-1}$  for oxygen, ammonium, nitrite, and nitrate, respectively, were taken from literature data (6, 19) and adjusted to experimental temperature of 20°C accordingly. Local conversion rates were obtained by a step-size calculation procedure for each profile as previously described (9). In case of local volumetric rate calculation within the biofilm, the effective diffusion coefficient in the matrix, i.e., 0.75% agarose, was assumed to be  $0.96 \times D_0$  (4). The resulting mean rates were smoothed by adjacent averaging to reduce noise effects.

Images of the bicarbonate uptake were analyzed with the Betavision software package provided by the manufacturer (Micro Imager, Biospace Mesures, Paris, France). After visual determination of the surface, counts were horizontally averaged for each depth interval (i.e., 10  $\mu\text{m}$ ) over a width of 1.5 to 2.5 mm and down to a depth of 4 mm. The resulting profiles were used to quantify the vertical distribution of bicarbonate uptake according to:

$$C = z \cdot (\delta \cdot v \cdot A \cdot t)^{-1}$$

with  $C$ : bicarbonate uptake rate [ $\text{nmol cm}^{-3} \text{ h}^{-1}$ ];  $z$ : measured radioactivity [Bq];  $\delta$ : counting efficiency [-];  $v$ : voxel size [ $\text{cm}^3$ ], given by imaging resolution ( $1 \times 10^{-3} \text{ cm}$ ), vertical averaging ( $5 \times 10^{-3} \text{ cm}$ ), and section thickness ( $2 \times 10^{-3} \text{ cm}$ );  $A$ : molar radioactivity [ $\text{Bq nmol}^{-1}$ ];  $t$ : incubation time in the experiment [h]. Rates were corrected for unspecific uptake and bicarbonate precipitates by subtracting results of the negative control from each profile.

## RESULTS

**Nitrifying activity under different conditions.** Under standard conditions (experiment A) profiles of oxygen, ammonium and nitrate reflected nitrifying activity. Oxygen penetration depth was about 2 mm. Ammonium consumption and nitrate production took place exclusively within this horizon (Fig. 1A, top panel), as visible from the curvature of the profiles. Local oxygen consumption rates were more or less homogeneously distributed over the oxic horizon (Fig. 1A, bottom). Activity of the whole biofilm in terms of oxygen uptake, as quantified by the areal uptake rates (Fig. 2), was highest in experiment A compared to all other experiments. For full nitrification, 2 mols oxygen and 1 mol ammonium are consumed for 1 mol nitrate produced (20). With respect to this stoichiometry, observed areal uptake rates of oxygen and ammonium matched the release rate of nitrate within the range of error (Fig. 2).

Decreased concentrations of ammonium or oxygen (experiments B and C) had a significant effect on the nitrifying activity. In experiment B (ammonium limitation), oxygen fully penetrated the biofilm. Within the active surface layer of 1.4 mm thickness, the oxygen concentration was decreased to 70% air saturation according to 200  $\mu\text{M}$  (Fig. 1B). Consumption was highest at the surface (Fig. 1B, bottom). Ammonium was depleted within the oxygen-consuming layer (Fig. 1B, top). Both the total (areal) uptake rate of oxygen and even more of ammonium were clearly reduced (Fig. 2). Whereas nitrite was not measured in this experiment, nitrate release corresponded to the uptake of ammonium (1:1 ratio), indicating full nitrification to prevail (Fig. 2). However, oxygen uptake rates were stoichiometrically too high for the observed nitrification (Fig. 2). A certain minor uptake of oxygen in the order of  $11\% \pm 3\%$  of that under standard conditions, however, was also observed, when neither ammonium nor nitrite were present (negative control, N; Fig. 2).

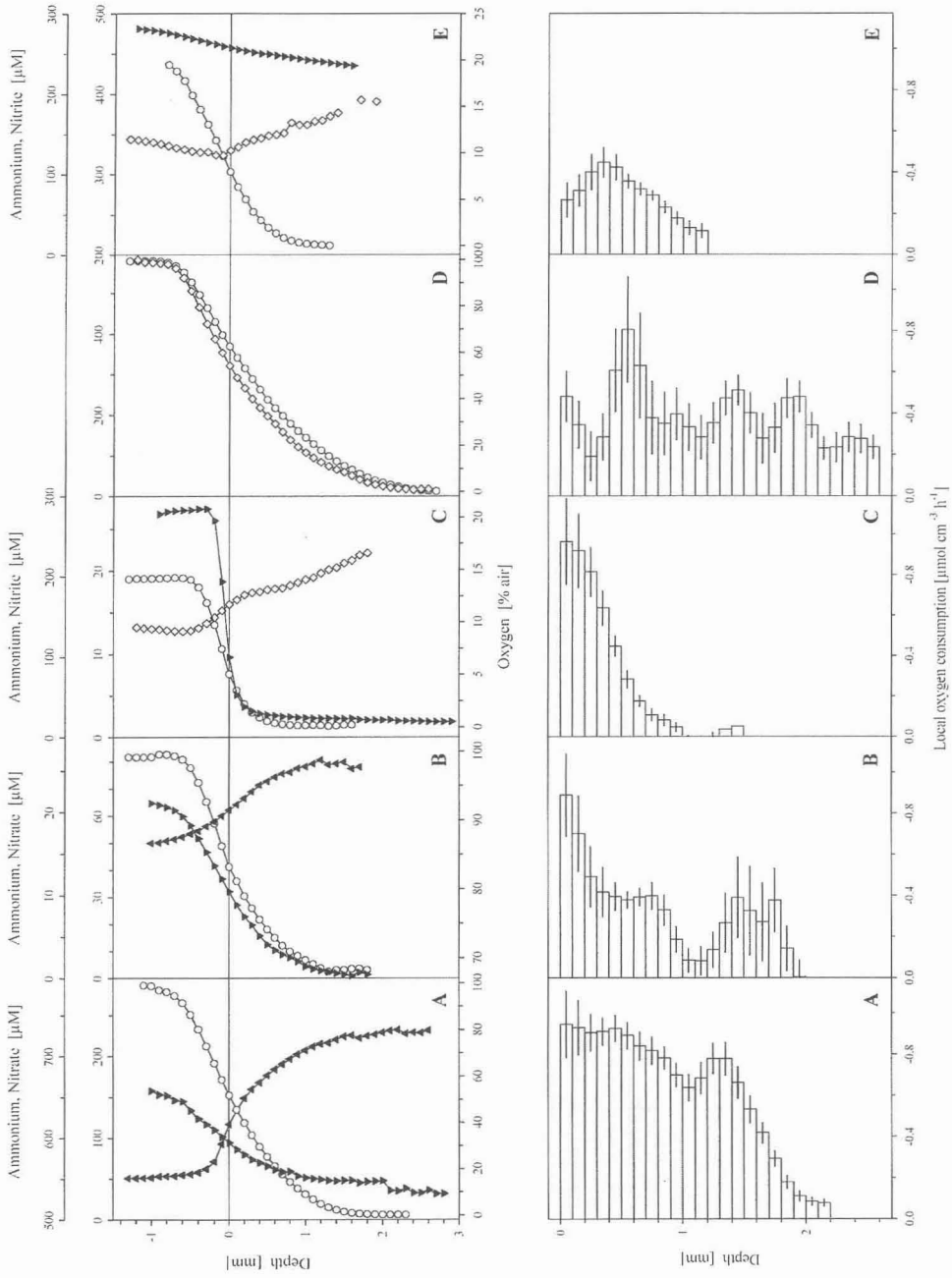
Compared to experiment B, the effect of oxygen limitation (experiment C) was much more profound: In contrast to A and B, oxygen was completely consumed within the upper 0.7 mm. Both the areal uptake rate (Fig. 2) and maximum local oxygen uptake, i.e.,  $1 \mu\text{mol cm}^{-3} \text{ h}^{-1}$ , were on the same magnitude as those found in experiment B. However, consumption quickly decreased with depth (Fig. 1C, bottom). Areal uptake of ammonium by the biofilm was found to be extremely high compared to all other experimental conditions: The very steep gradient through the DBL indicated a 10-fold increase in the areal uptake compared to standard conditions (Fig. 2). Whereas no microprofile data is available for nitrate, the nitrite production did not account for the uptake of ammonium and oxygen (Fig. 1C, top).

When only nitrite was present as an electron donor (experiment D), profiles of oxygen and nitrite were very similar in shape (Fig. 1D, top). The areal oxygen uptake rate was slightly lower than under standard conditions (Fig. 2). We also found the oxygen to be homogeneously consumed over the whole aerated zone, i.e., down to a depth of 2.4 mm (Fig. 1D, bottom). Nitrite was visibly consumed within the oxic horizon, as indicated by the profile shape similar to that of oxygen (Fig. 1D, top). Stoichiometry of nitrite oxidation is 0.5 mol of oxygen consumed per mol of nitrite consumed. Areal uptake rates determined for both solutes are in agreement with this stoichiometry (Fig. 2). In this experiment, traces of ammonium were present, which might have originated from accidental transfer from the source reactor through the unwashed sample. Profiles of ammonium, however, only indicated a very minor uptake at the surface (not shown).

Under conditions, where the oxygen concentration was reduced to 20 % and both ammonium and nitrite were present in high concentrations (experiment E), only a weak uptake of ammonium could be observed. Oxygen penetrated deeper, i.e., down to 1 mm. The oxygen uptake was only slightly lower than in experiments B and C (Fig. 2). Highest local oxygen consumption within the biofilm, however, took place about 0.5 mm below the surface (Fig. 1E, bottom), and was clearly decreased compared to experiment C, where no nitrite was added. The consumption of oxygen in the surface was clearly decreased compared to the other experiments (except D). The data does not allow to state whether nitrite oxidation took place as well. In any case the activity of the biofilm was as low as, or even lower than, in experiment B (ammonium limitation).

---

FIG. 1. Concentration profiles of oxygen ( $\circ$ ), ammonium ( $\blacktriangledown$ ), nitrite ( $\odot$ ), and nitrate ( $\blacktriangle$ ) (top), and distribution of local oxygen uptake rates with depth (bottom) in the model biofilm. The designations A to E, and N refer to the different incubation conditions as listed in Table 1. Note the different scales. The top offset axis refers to the concentration of ammonium, the one below to either nitrate (A and B) or nitrite (C to E), respectively.



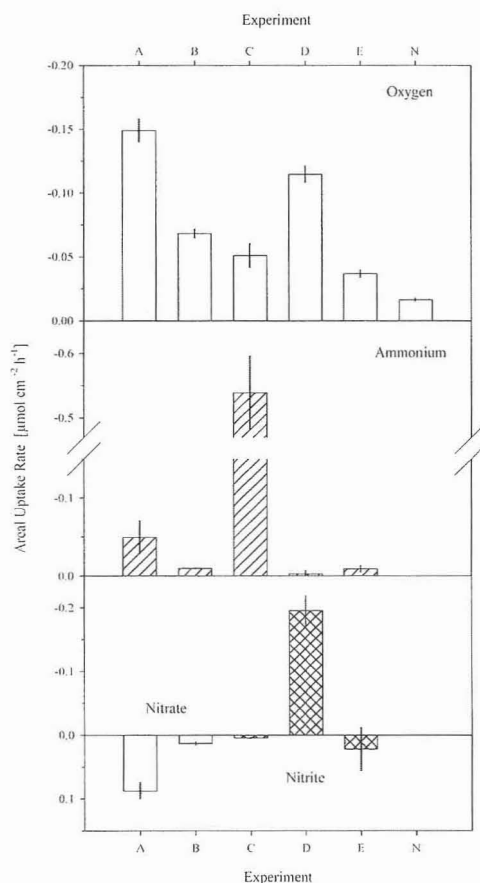


FIG. 2. Areal uptake rates of oxygen (grey) and ammonium (hatched), and areal conversion rates of nitrite (white) and nitrate (cross-hatched) under different experimental conditions. Values were calculated based on the concentration gradients through the diffusive boundary layer. Positive data correspond to a release, negative data to an uptake of the respective solute.

**Microbial populations.** Hybridization of the suspension from the reactor with various probes revealed the presence of three main populations in the system. One population hybridized with probes Nso1225, NEU, and with probe Nse1472, indicating its affiliation to the *Nitrosomonas europaea*-lineage. A second population of AOB gave signals after hybridization with probes Nso1225, NOLI, and Nmo218, indicative for strains belonging to the *N. oligotropha*-lineage. Both AOB populations were equally abundant in the suspension from the source reactor: Their numbers were  $6.9$  and  $5.5 \times 10^7 \text{ cm}^{-3}$ , respectively. One population of NOB occurred in dense clusters of small cells affiliated to the genus *Nitrospira*, as evident by hybridization with probes Ntspa712 and Ntspa662 (Table 2). Due to their dense clustering and irregular occurrence a reliable quantification was not possible. Their abundance, however,

was estimated to be at least one order of magnitude higher than that of the AOB. These populations accounted for the majority of signals resulting from hybridization of EUB338.

Hybridization of the thin sections revealed that the aggregates were not totally disrupted by vortexing, but some aggregations persisted. These consisted not only of the typical mono-species microcolonies, but were also composed of the different populations. Aggregates were heterogeneously dispersed throughout the sections without any accumulation in the bottom part.

**Microautoradiography and FISH (MAR-FISH).** The combination of microautoradiography and fluorescence *in situ* hybridization was used to study details of the uptake of [ $^{14}\text{C}$ ]-bicarbonate in the biofilm. A dark layer of silver grains covered cells with an active uptake of [ $^{14}\text{C}$ ]-bicarbonate (Fig. 3). The thin cryosections usually resulted in widely distributed aggregates that were easily distinguishable from other cells. It was thus possible to relate the MAR signal to specific cells identified by *in situ* hybridization. The agarose was partly dissolved by the FISH procedure leaving the cells intact on the cover glass. However, it was possible to determine the surface of the biofilm from the density of the MAR signal and by the fluorescence signal deriving from FISH. Unspecific background signal originating from precipitated bicarbonate was low in all slides.

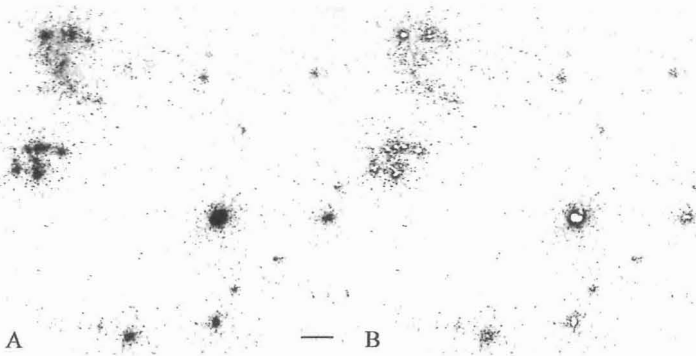


FIG. 3. Example of MAR-FISH micrographs from experiment E. Microautoradiographic image (A) and overlay of MAR image with fluorescence micrograph (B) after hybridization with probes Ntspa712 (red) and EUB338 (green). Cells appearing yellow hybridized to both probes. Scale bar is 20  $\mu\text{m}$ .

Results of MAR are summarized in Table 3. In the aerated biofilm with the presence of 0.7 mM ammonium (experiment A), cells hybridizing with the probes Ntspa712 and Nmo218 were MAR-positive throughout the biofilm, with only a slightly higher silver grain density in the top of the biofilm compared to the middle and bottom of the biofilm. Under decreased ammonium concentration of 0.03 mM (experiment B) the MAR pattern of cells hybridizing

both probe Nmo218 and Ntspa712 was changed. Only a few of the Nmo218 and half of the Ntspa712 positive cell clusters were MAR-positive in the top of the biofilm. In the middle and bottom of the biofilm all Nmo218- and Ntspa712-positive cells were MAR-negative. When only nitrite was added to the incubation (experiment D), no Nmo218-hybridized cells were covered with silver grains in any layer, except that colonies near to the surface were weakly MAR-positive. Cells hybridizing with Ntspa712 were found to be strongly MAR-positive throughout the biofilm. However, a few colonies near to the surface were negative. Some algal contaminants present in the biofilm were MAR-positive throughout the biofilm.

In the presence of ammonium and nitrite, and limited amounts of oxygen (experiment E) a few Nmo218-positive cells were MAR-positive at the surface. However most cells were MAR-negative throughout the biofilm. Cells hybridizing with the Ntspa712 probe were MAR-positive in the top and in the middle of the biofilm but MAR-negative near the bottom. Preparations of experiment C caused problems with detachment of sample material. Thus, no MAR results could be determined for this experiment.

TABLE 3. MAR-FISH results for the different experiments.

Probe	Experiment				
	A	B	C	D	E
Nmo218					
Top <sup>a</sup>	+++ <sup>b</sup>	(++) <sup>c</sup>	nd <sup>f</sup>	+	(++) <sup>c</sup>
Middle	++	-	nd	-	-
Bottom	++	-	nd	-	-
Ntspa712					
Top	+++	++ <sup>d</sup>	nd	+++ <sup>e</sup>	+++ <sup>e</sup>
Middle	++	-	nd	+++	++
Bottom	++	-	nd	+++	-

<sup>a</sup> Refer to depth of the investigated layer as follows: top 0-0.2 mm, middle 0.2-1.5 mm, bottom >1.5 mm.

<sup>b</sup> Signs refer to estimated silver grain density around probe positive cells as follows: +++ very high density, ++ high density, + low density, - no silver grains.

<sup>c</sup> MAR signal associated only with a few probe-positive cells.

<sup>d</sup> MAR signal associated with about half of all probe-positive colonies.

<sup>e</sup> MAR signal associated with the majority of all probe-positive colonies.

<sup>f</sup> nd: not determined.

**Quantitative beta microimaging.** Beta microimaging was used to detect the distribution and quantity assimilated bicarbonate in the biofilm. The distribution of [<sup>14</sup>C] in the biofilm (Fig. 4) showed the same heterogeneity of signals as found by hybridization of the thin sections (data not shown). Although the images were not correlated directly with micrographs of hybridized sections, it was obvious that the [<sup>14</sup>C] specifically occurred in aggregates of nitrifying bacteria. Fig. 4 visualizes that uptake of bicarbonate in experiment A was high. In

contrast, the negative control (N) showed some minor amount of tracer incorporation homogeneously distributed throughout the biofilm. In experiment D, bicarbonate assimilation also occurred deeper in the biofilm. In contrast, this took place mostly at the surface in experiments B, C and E, with the exception of a few isolated local spots with tracer situated deeper in the biofilm. It can be seen from the examples, that the signal intensity in general is slightly higher in experiment D compared to B, and clearly higher in experiment C compared to E. Quantification of the [ $^{14}\text{C}$ ]-bicarbonate uptake along vertical profiles is shown in Fig. 5.

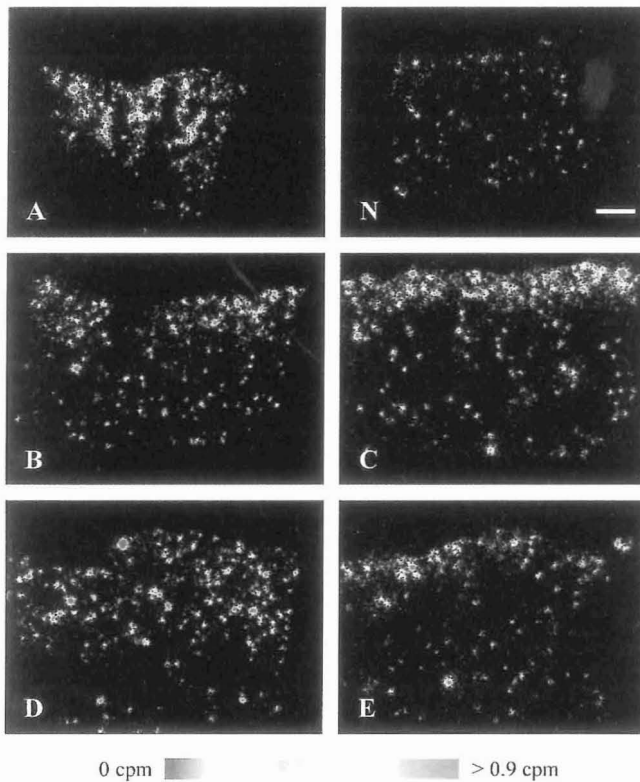


FIG. 4. Distribution of incorporation of [ $^{14}\text{C}$ ]-bicarbonate in the model biofilm as visualized in high resolution by beta microimaging. Signal intensity is shown by color coding with an identical scale applied for all images. Designations A to E, and N refer to the experimental conditions as described in Table 1. Scale bar is 1 mm. cpm: counts per minute.

Quantitative profiling of [ $^{14}\text{C}$ ] distribution in the sections by beta microimaging revealed that the uptake of bicarbonate correlated in general with the distribution of the limiting compound, i.e., oxygen (experiments A, and C to E) or ammonium (experiment B; Fig. 5). Uptake rates for bicarbonate in all experiments except D were highest at the surface, i.e., in the upper 400  $\mu\text{m}$ , and decreased with depth. No bicarbonate uptake occurred below the oxic-anoxic

boundary in experiments D and E, or below the penetration limit of ammonium in experiment B, respectively. In these experiments, the distribution of the local volumetric oxygen uptake (Fig. 1, bottom) correlated to that of the bicarbonate uptake rates: In experiments B and E, carbon uptake rates were highest at the surface and decreased with depth, whereas they were more or less homogeneously in the upper 2.5 mm in experiment D. In all three experiments, the same effect was observed for the oxygen uptake rates (Fig. 1B, D, E, bottom). Differences between the experiments B, D, and E become evident, when considering the total uptake rate of carbon. This can be calculated by integration of local uptake rates over the whole depth of activity. For the reason of comparability between the experiments, we integrated the rates of the upper 2.5 mm in each experiment. In experiment B, a total carbon uptake of  $0.30 \mu\text{mol cm}^{-2} \text{h}^{-1}$  was calculated, whereas the biofilm consumed  $0.44 \mu\text{mol cm}^{-2} \text{h}^{-1}$  in experiment D. This effect was mostly due to the contribution of deeper layers below 1 mm in experiment D. In contrast, total carbon uptake was  $0.20 \mu\text{mol cm}^{-2} \text{h}^{-1}$  in experiment E.

With respect to the correlation between carbon and oxygen uptake, experiment C was markedly different. Carbon uptake rates in the aerated surface layer were very high and even higher than under standard conditions (experiment A) where much more oxygen was available. The total (areal) uptake of bicarbonate in experiment C was  $1.04 \mu\text{mol cm}^{-2} \text{h}^{-1}$ , and, thus, in sharp contrast to experiment A, where the biofilm assimilated  $0.76 \mu\text{mol cm}^{-2} \text{h}^{-1}$ . Furthermore, assimilation of carbon occurred in deeper parts of the model biofilm below 1 mm in C. Assimilation in this layer was also observed in experiment A. However, these layers were clearly oxic in experiment A. In experiment C, the distribution of  $[^{14}\text{C}]$  in these layers appeared in isolated patches causing the larger standard errors observed in the peak regions of the profile.

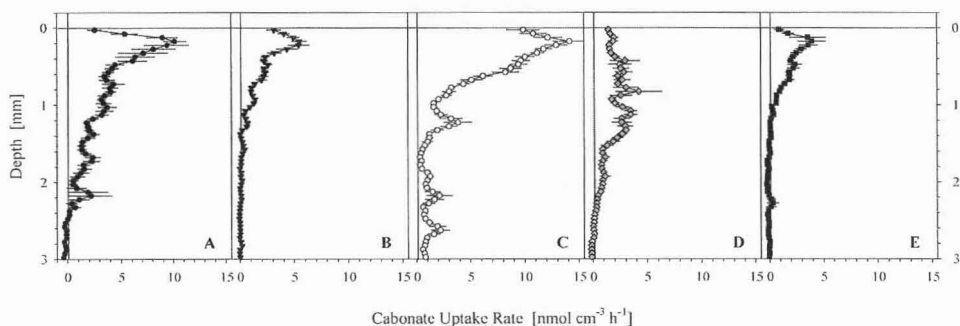


FIG. 5. Local bicarbonate uptake rates under different experimental conditions. The shaded areas show the penetration depth of the limiting solute, i.e., either oxygen (A, and C to E) or ammonium (B) in the respective experiment (see also Fig. 1).

Table 3 summarizes the uptake of carbon, nitrogen, and oxygen for all experimental conditions. The data were calculated from depth-integrated volumetric rates. Nearly equal ratios were obtained when calculated by the fluxes of ammonium and nitrite across the DBL (data not shown). The carbon-to-oxygen ratio was quite stable: Carbon uptake was corresponded to about 0.5% of the oxygen uptake rates in all experiments, except for experiment C. The nitrogen-to-oxygen ratios of uptake rates were much more variable, and highest in experiments C and D. In both experiments, the uptake of the nitrogen compound was too high as compared to the oxygen consumption.

TABLE 3. Molar ratios of carbon, nitrogen, and oxygen uptake under different conditions.

Name	Experiment	Carbon [ $\times 10^{-3}$ ]	Nitrogen [ $\times 10^{-1}$ ]	Oxygen
A	Standard	5.7	3.2	1
B	Ammonium limitation	4.9	1.5	1
C	Oxygen limitation	25.6	96.2	1
D	Nitrite oxidation	4.5	16.9 <sup>a</sup>	1
E	Nitrifier denitrification	5.9	4.1 <sup>b</sup>	1

<sup>a</sup> Data based on uptake of nitrite.

<sup>b</sup> Data based on uptake of ammonium (54%) and nitrite (46%).

## DISCUSSION

**Evaluation of the integrated approach.** In general, the different methods gave consistent results. Nitrification as followed by the formation of nitrite and nitrate, and the consumption of oxygen with microsensors was mostly limited to a certain depth in the model biofilm. Correspondingly, this depth limit of activity was reflected by the distribution of MAR-positive cells, and by the depth distribution of uptake rates of [ $^{14}\text{C}$ ]-bicarbonate. The approach indeed demonstrated the feasibility to measure activity on the community, population and single cell level.

**Activity on the community level.** Our experiments addressed the question of the nitrifying activity of the biofilm and individual contribution of AOB and NOB populations to it under various conditions. Both microsensor data and bicarbonate assimilation as quantified by beta microimaging demonstrate that the community is typically limited by oxygen. If the substrate, ammonium or nitrite, is added in saturating concentration, i.e., it is not depleted within the biofilm, its uptake is directly related to the amount of available oxygen. Vertical distributions of the activity as followed with microsensors was well correlated with assimi-

lation activity as detected by beta microimaging. This is furthermore supported by the overall results of the microautoradiography, which are consistent with both findings. However, results of experiment C (ammonium addition, oxygen limitation) are an exception to this result. The high total uptake of ammonium and bicarbonate cannot be explained by the activity in the aerobic zone alone. Furthermore, ammonium was completely taken up in the aerated layer. However, we detected some assimilation in the anoxic part of the biofilm in experiment C, that might explain the high total activity. It was reported before, that *N. europaea* and *N. eutropha* under microaerobic or anoxic conditions are capable to perform a denitrifying metabolism, using nitrite as electron acceptor and hydrogen or ammonium as electron donors, causing a net nitrogen loss by gaseous products (5). The relevance of this process has been suggested for activated sludge (23) and biofilms (14, 33, 38). While the appropriate population was present in our system, no evidence is obtained from microprofiles, that this type of metabolism occurred in our experiment: Ammonia was virtually not present in the deeper layers, and microprofiles did not suggest any nitrite consumption in these horizons. In experiment E we applied as well oxygen-limiting conditions, but added ammonium and nitrite to promote the potential activity of this "nitrifier denitrification" (15). However, the activity here was restricted to the aerobic layer, and neither distinct consumption of ammonium and/or nitrite, nor assimilation of bicarbonate has been observed in the anaerobic layer. It could be argued that the high concentrations of nitrite in experiment E might have inhibited *N. europaea/eutropha*. Inhibition was described to be caused by free nitrous acid at concentrations higher than 0.22 to 2.8 mg  $\text{HNO}_2 \text{ l}^{-1}$  (3). Under the conditions of experiment E, however, free nitrous acid is several orders of magnitude below these values. Therefore, nitrifier denitrification under anoxic conditions is ruled out as an explanation here. Thus, it is most likely that some artefacts occurred during the incubation in experiment C.

***In situ* assimilation.** In most of the experiments the carbon assimilation was quite constant at a molar ratio of 0.005 of the oxygen uptake (except C). This stable carbon yield as calculated with respect to oxygen for most of the experiments supports the role of the oxygen concentration as the controlling parameter in our experiments. Typical carbon yields reported in the literature refer to ammonia, and are in a range of 0.014 and 0.096 for various pure cultures of AOB (29). Carbon yield on nitrite, as determined with *Nitrobacter* sp. and *Nitrosococcus mobilis*, is typically between 0.0125 and 0.03 (29). Referenced to ammonium and/or nitrite uptake, the carbon yield in our experiments varied depending on the incubation conditions. From Table 3, an *in situ* carbon yield of 0.003 (experiments C and D) to 0.032 (B) can be calculated. Thus, the yield determined here is in the lower range of literature data reported for

pure cultures. However, it has to be noted that the yield determined here is measured *in situ*, which, to our knowledge, has not yet been done. Effects like competition for oxygen between the populations are suggested to lower the carbon yield *in situ* compared that obtained from pure cultures.

**Contribution of the individual populations.** Microautoradiography revealed how much the individual populations detected by FISH were involved in the observed nitrification. The three populations, affiliated to the ammonia-oxidizing *N. europaea/eutropha*, *N. oligotropha*, and to the nitrite-oxidizing *Nitrospira* sp., were found to be all active under standard conditions. Obviously, none of the populations were forced to inactivity by competition with another in any horizon, suggesting no cut-off limitation in either oxygen or substrate. MAR results also supported the finding of beta microimaging: Below the oxic-anoxic transition zone in experiment E, or the layer of ammonium depletion in experiment B, no bicarbonate assimilation occurred in any of the populations (Table 2) including the *N. europaea/eutropha*-like cells (data not shown). Thus, MAR independently confirms the absence of an anaerobic bicarbonate fixing metabolism.

Some of the Nmo218-positive cells were able to assimilate carbon under nitrite-oxidizing conditions in B. Traces of ammonium present obviously were sufficient and oxygen uptake by the nitrite-oxidizing population, *Nitrospira* sp., is not as high as to cause severe competition with the active *N. oligotropha*-related cells as this population was not completely inactive. The adaptation to low substrate concentrations of the latter population is also supported by results of experiment B (ammonium limitation), where MAR showed a small part of this population to be active in the top 0.2 mm layer.

We could not find indications for any denitrifying activity of *N. europaea/eutropha* despite the presence of suitable conditions (experiment E). In contrast, the dominating activity in experiment E is nitrite oxidation. Microsensor data did not show uptake of nitrite, which, however, could be partly due to overlapping activity of ammonia and nitrite oxidation. At least a minor ammonia-oxidizing activity at the surface is supported by MAR. Strongly MAR-positive *Nitrospira* sp., however, were found in the biofilm down to the penetration limit of oxygen. This supports the hypothesis of adaptation of *Nitrospira* sp. to very low oxygen levels through high affinity as suggested earlier (13, 34, 35; this thesis, chapter 5). The low total bicarbonate uptake, mainly associated to the activity of *Nitrospira* sp. in experiment D also confirms earlier findings of a low growth rate in pure cultures (12, 41) and *in situ* evidence (26, 35). As shown above, the carbon yield with respect to nitrite uptake was only 0.003. In contrast, inhibition of the activity of *Nitrospira* sp. under high oxygen concentration as alter-

natively suggested to explain its predominant occurrence in deeper biofilm layers (25) are not confirmed by our MAR results from experiment A, B and D. In all three experiments, oxygen concentration was high at the surface, and *Nitrospira* cells were clearly MAR positive under these conditions. Concerning these results, earlier speculations are confirmed, suggesting members of the genus *Nitrospira* sp. to be typical K strategists with a high affinity for oxygen, a low maximum substrate conversion rate, and a low growth rate and growth yield (35).

## CONCLUSIONS

The single methods produced consistent results. Distribution of MAR-positive cells correlated with the assimilation profiles as measured with the beta microimager. The combined approach facilitated the investigation of activity on the community, population, and single cell level. Together with FISH its application to an environmental biofilm opens new possibilities in studying the role of single populations in complex environments.

## ACKNOWLEDGEMENTS

Anja Eggers Gaby Eickert and Ines Schröder are acknowledged for the preparation of oxygen microelectrodes. Tim Ferdelman is acknowledged for his help with the isotopic work.

## REFERENCES

1. **Amann, R. I., B. J. Binder, R. J. Olson, S. W. Chisholm, R. Devereux, and D. A. Stahl.** 1990. Combination of 16S rRNA-targeted oligonucleotide probes with flow cytometry for analyzing mixed microbial populations. *Appl. Environ. Microbiol.* **56**:1919-1925.
2. **Andreasen, K., and P. H. Nielsen.** 1997. Application of microautoradiography to the study of substrate uptake by filamentous microorganisms in activated sludge. *Appl. Environ. Microbiol.* **63**:3662-3668.
3. **Anthonisen, A. C., R. C. Loehr, T. B. S. Prakasam, and E. G. Srinath.** 1976. Inhibition of nitrification by ammonia and nitrous acid. *J. Wat. Pollut. Cont. Fed.* **48**:835-852.
4. **Beuling, E.** Mass Transfer Properties of Biofilms. 1998. PhD thesis. University of Amsterdam, Amsterdam (NL).

5. **Bock, E., I. Schmidt, R. Stüven, and D. Zart.** 1995. Nitrogen loss caused by denitrifying *Nitrosomonas* cells using ammonium or hydrogen as electron donors and nitrite as electron acceptor. *Arch. Microbiol.* **163**:16-20.
6. **Broecker, W. S., and T.-H. Peng.** 1974. Gas exchange rates between air and sea. *Tellus.* **26**:21-35.
7. **Brosius, J., T. J. Dull, D. D. Sleeter, and H. F. Noller.** 1981. Gene organization and primary structure of a ribosomal RNA operon from *Escherichia coli*. *J. Mol. Biol.* **148**:107-127.
8. **Daims, H., P. Nielsen, J. L. Nielsen, S. Juretschko, and M. Wagner.** 2000. Novel *Nitrospira*-like bacteria as dominant nitrite-oxidizers in biofilms from wastewater treatment plants: diversity and *in situ* physiology. *Water Sci. Technol.* **41**:85-90.
9. **de Beer, D.** 2000. Micro-electrodes. In R. H. Wijffels (ed.), *Immobilized Cells*. Springer, Heidelberg.
10. **de Beer, D., A. Schramm, C. M. Santegoeds, and M. Kühl.** 1997. A nitrite microsensor for profiling environmental biofilms. *Appl. Environ. Microbiol.* **63**:973-977.
11. **de Beer, D., J. C. van den Heuvel, and S. P. P. Ottengraf.** 1993. Microelectrode measurements of the activity distribution in nitrifying bacterial aggregates. *Appl. Environ. Microbiol.* **59**:573-579.
12. **Ehrich, S., D. Behrens, E. Lebedeva, W. Ludwig, and E. Bock.** 1995. A new obligately chemolithoautotrophic, nitrite-oxidizing bacterium, *Nitrospira moscoviensis* sp. nov. and its phylogenetic relationship. *Arch. Microbiol.* **164**:16-23.
13. **Gieseke, A., U. Purkhold, M. Wagner, R. Amann, and A. Schramm.** 2001. Community structure and activity dynamics of nitrifying bacteria in a phosphate-removing biofilm. *Appl. Environ. Microbiol.* **67**:1351-1362.
14. **Helmer, C., S. Kunst, S. Juretschko, M. C. Schmid, K.-H. Schleifer, and M. Wagner.** 1999. Nitrogen loss in a nitrifying biofilm system. *Water Sci. Technol.* **39**:13-21.
15. **Jetten, M. S. M., S. Logemann, G. Muyzer, L. A. Robertson, S. de Vries, M. C. M. van Loosdrecht, and J. G. Kuenen.** 1997. Novel principles in the microbial conversion of nitrogen compounds. *Ant. Leeuw.* **71**:75-93.
16. **Juretschko, S., G. Timmermann, M. Schmid, K.-H. Schleifer, A. Pommerening-Röser, H. P. Koops, and M. Wagner.** 1998. Combined molecular and conventional analysis of nitrifying bacterium diversity in activated sludge: *Nitrosococcus mobilis* and *Nitrospira*-like bacteria as dominant populations. *Appl. Environ. Microbiol.* **64**:3042-3051.
17. **Laniece, P., Y. Charon, A. Cardona, L. Pinot, S. Maitrejean, R. Matrippolito, B. Sandkamp, and L. Valentin.** 1998. A new high resolution radioimager for the quantitative analysis of radiolabelled molecules in tissue section. *J. Neurosci. Meth.* **86**:1-5.
18. **Lee, N., P. H. Nielsen, K. H. Andreasen, S. Juretschko, J. L. Nielsen, K.-H. Schleifer, and M. Wagner.** 1999. Combination of fluorescent *in situ* hybridization and microautoradiography - a new tool for structure-function analyses in microbial ecology. *Appl. Environ. Microbiol.* **65**:1289-1297.
19. **Li, Y.-H., and S. Gregory.** 1974. Diffusion of ions in sea water and in deep-sea sediments. *Geochim. Cosmochim. Acta.* **38**:703-714.
20. **Madigan, M. T., J. M. Martinko, and J. Parker.** 2000. *Brock Biology of Microorganisms*, 9th ed. Prentice-Hall, Upper Saddle River (NJ, USA).

21. **Manz, W., R. Amann, W. Ludwig, M. Wagner, and K.-H. Schleifer.** 1992. Phylogenetic oligodeoxynucleotide probes for the major subclasses of proteobacteria: problems and solutions. *Syst. Appl. Microbiol.* **15**:593-600.
22. **Mobarry, B. K., M. Wagner, V. Urbain, B. E. Rittmann, and D. A. Stahl.** 1996. Phylogenetic probes for analyzing abundance and spatial organization of nitrifying bacteria. *Appl. Environ. Microbiol.* **62**:2156-2162.
23. **Muller, E. B., A. H. Stouthamer, and H. W. van Verseveld.** 1995. Simultaneous NH<sub>3</sub> oxidaton and N<sub>2</sub> production at reduced O<sub>2</sub> tensions by sewage sludge subcultured with chemolithotrophic medium. *Biodegradation.* **6**:339-349.
24. **Nielsen, P. H., K. Andreasen, M. Wagner, L. L. Blackall, H. Lemmer, and R. J. Seviour.** 1998. Variability of type 021N in activated sludge as determined by *in situ* substrate uptake pattern and *in situ* hybridization with fluorescent rRNA targeted probes. *Water Sci. Technol.* **37**:423-430.
25. **Okabe, S., K. Hirata, Y. Ozawa, and Y. Watanabe.** 1996. Spatial microbial distributions of nitrifiers and heterotrophs in mixed population biofilms. *Biotechnol. Bioeng.* **50**:24-35.
26. **Okabe, S., H. Satoh, and Y. Watanabe.** 1999. In situ analysis of nitrifying biofilms as determined by in situ hybridization and the use of microelectrodes. *Appl. Environ. Microbiol.* **65**:3182-3191.
27. **Ouverney, C. C., and J. A. Fuhrman.** 1999. Combined microautoradiography-16S rRNA probe technique for determination of radioisotope uptake by specific microbial cell types in situ. *Appl. Environ. Microbiol.* **65**:1746-1752.
28. **Painter, H. A.** 1986. Nitrification in the treatment of sewage and wastewaters. *Spec. Publ. Soc. Gen. Microbiol.* **20**:185-213.
29. **Prosser, J. I.** 1989. Autotrophic nitrification in bacteria. *Adv. Microb. Physiol.* **30**:125-181.
30. **Prosser, J. I.** 1986. Nitrification, vol. 20. Society for General Microbiology, Oxford (UK).
31. **Purkhold, U., A. Pommerening-Röser, S. Juretschko, M. C. Schmid, H.-P. Koops, and M. Wagner.** 2000. Phylogeny of all recognized species of ammonia-oxidizers based on comparative 16S rRNA and *amoA* sequence analysis: Implications for molecular diversity surveys. *Appl. Environ. Microbiol.* **66**:5368-5382.
32. **Revsbech, N. P.** 1989. An oxygen microelectrode with a guard cathode. *Limnol. Oceanogr.* **34**:474-478.
33. **Schmid, M., U. Twachtmann, M. Klein, M. Strous, S. Juretschko, M. S. M. Jetten, J. W. Metzger, K.-H. Schleifer, and M. Wagner.** 2000. Molecular evidence for genus level diversity of bacteria capable of catalyzing anaerobic ammonium oxidation. *Syst. Appl. Microbiol.* **23**:93-106.
34. **Schramm, A., D. de Beer, A. Gieseke, and R. Amann.** 2000. Microenvironments and distribution of nitrifying bacteria in a membrane-bound biofilm. *Environ. Microbiol.* **2**:680-686.
35. **Schramm, A., D. de Beer, J. C. van den Heuvel, S. Ottengraf, and R. Amann.** 1999. Microscale distribution of populations and activities of *Nitrosospira* and *Nitrospira* spp. along a macroscale gradient in a nitrifying bioreactor: Quantification by in situ hybridization and the use of microsensors. *Appl. Environ. Microbiol.* **65**:3690-3696.
36. **Schramm, A., D. de Beer, M. Wagner, and R. Amann.** 1998. Identification and activities in situ of *Nitrosospira* and *Nitrospira* spp. as dominant populations in a nitrifying fluidized bed reactor. *Appl. Environ. Microbiol.* **64**:3480-3485.

37. **Schramm, A., L. H. Larsen, N. P. Revsbech, N. B. Ramsing, R. Amann, and K.-H. Schleifer.** 1996. Structure and function of a nitrifying biofilm as determined by in situ hybridization and the use of microelectrodes. *Appl. Environ. Microbiol.* **62**:4641-4647.
38. **Siegrist, H., S. Reithaar, G. Koch, and P. Lais.** 1998. Nitrogen loss in a nitrifying rotating contactor treating ammonium-rich wastewater without organic carbon. *Water Sci. Technol.* **38**:241-248.
39. **Wagner, M., G. Rath, R. Amann, H. P. Koops, and K.-H. Schleifer.** 1995. *In situ* identification of ammonia-oxidizing bacteria. *Syst. Appl. Microbiol.* **18**:251-264.
40. **Wagner, M., G. Rath, H. P. Koops, J. Flood, and R. Amann.** 1996. *In situ* analysis of nitrifying bacteria in sewage treatment plants. *Water Sci. Technol.* **34**:237-244.
41. **Watson, S. W., E. Bock, F. W. Valois, J. B. Waterbury, and U. Schlosser.** 1986. *Nitrospira marina* gen. nov. sp. nov.: a chemolithotrophic nitrite-oxidizing bacterium. *Arch. Microbiol.* **144**:1-7.



## **Chapter 7**

### **Discussion and Summary**



## Discussion

The aim of this thesis was the investigation of nitrifying populations in complex biofilms. Complexity occurred in function and structure. The reactor systems studied mostly incorporated either several functions (Chapters 2 to 4) or simply were not as controlled as lab-scale experiments (Chapter 5). In terms of the microbial community structure, all systems harbored several coexisting populations of AOB and NOB: Populations related to *N. europaea*/*N. eutropha* and to *Nitrosospira* sp., and *Nitrobacter* sp. as well as *Nitrosospira* sp. were found in a membrane-bound biofilm under opposed gradients of oxygen and substrate; members of the *N. europaea*/*N. eutropha*-, *N. oligotropha*-, and *N. communis*-lineages were the components of the ammonia-oxidizing community in a nitrifying phosphate-removing sequencing batch system; populations affiliated to *N. europaea*/*N. eutropha*, *Nitrosococcus mobilis*, and *N. oligotropha*, and to *Nitrobacter* sp. and *Nitrosospira* sp. occurred in a pilot-scale sequencing batch system designed for nitrification of highly ammonium-loaded wastewaters; even the controlled lab-scale fluidized bed reactor providing nitrifying bacteria for the final integrated study harbored two AOB populations, related to *N. europaea*/*N. eutropha* and to *N. oligotropha*.

How can the coexistence of several populations with identical function be explained? In most of the studies presented here distinct microniches were assumed, and partly could be shown to explain this apparent redundancy.

Most of the systems provide enough niches to allow this coexistence. The data on the membrane-bound biofilm supported the hypothesis of adaptation of *Nitrosospira* sp. and *Nitrosospira* sp. to low, and of *N. europaea*/*N. eutropha* and *Nitrobacter* sp. to high substrate concentrations. The populations were found spatially separated, according to their substrate affinities. In two studies on a phosphate-removing nitrifying SBBR (Chapter 3 and 4), it has been shown that time might play a similar role in sequencing batch systems. The coexistence of nitrifiers with heterotrophic phosphate-removing and glycogen-accumulating bacteria was suggested to be based on activity at different times during the reactor cycle, and this might have been also true for the coexistence of surface populations of *N. europaea*/*N. eutropha*- and *N. oligotropha*-like AOB in this biofilm. It can be argued here that this could have been concluded as well from macroscopic bulk measurement data. However, based on such indirect evidence, opposing hypotheses of a spatial coexistence have been risen suggesting, e.g., internal coupling of nitrification and denitrifying phosphate uptake in a biofilm (6). No such coupling could be revealed in the studies presented in Chapter 2 and 3. This clearly

demonstrates the relevance of addressing the microscale in order to find direct evidence of how processes occur in time and specific microenvironments.

However, the niche concept is probably not sufficient to explain the coexistence of several AOB in a nitrifying biofilm. Adaptation to different substrate concentrations does not explain spatial patterns in case of the three coexisting AOB populations in a nitrifying SBBR on the pilot scale (Chapter 5). No layered organization was found in this biofilm. In contrast, *Nitrosococcus mobilis*- and *N. europaea*/*N. eutropha*-related populations appeared in dense microcolonies in which *N. europaea*/*N. eutropha*-like cells surrounded spherical *Nitrosococcus mobilis*-affiliated microcolonies. The size of these objects, which was typically between 10 and 20  $\mu\text{m}$ , is definitely beyond a scale for the formation of relevant concentration gradients. The time for diffusion to have an effect over such distances is in the range of seconds [e.g., (4)], and any local uptake inside such an aggregate will be counterbalanced by rapid diffusional transport. As a consequence adaptation to different substrate concentrations cannot explain a separation on this scale (i.e., a few  $\mu\text{m}$ ). Due to the physical nature of diffusion, the microsensor approach is not suitable to study the coexistence on this spatial scale. The data, however, might demonstrate activity in a distinct layer that causes a concentration gradient. This activity can be indirectly related to an abundant population detected in this layer. If multiple populations are present within chemically homogeneous microenvironments, their individual activity cannot be inferred from microsensor data.

The detectability of several populations does not necessarily reflect their activity. Nitrifiers can withstand long periods of inactivity without substantial decrease of ribosomes compared to heterotrophs (5). This enables them to rapidly regain their activity when suitable conditions recur, especially when present in high numbers as found in biofilms (2). In conjunction with the huge abundance of *Nitrospira* sp in rather inactive deeper horizons, a seedling hypothesis has been suggested in Chapter 5. A backwashing event in the reactor every few days regularly removed substantial parts of biomass (1). On a microscale, this could allow detached microcolonies to get access to oxygen, spread to different zones in the reactor, and thrive temporarily (i.e., during and immediately after the backwashing event), before they are overgrown again by fast-growing populations.

This hypothesis goes beyond the frame of the niche concept, which is based on the assumption of an equilibrium in the community composition. In contrast, it implies a non-equilibrium situation. This appears to be plausible for a batch system with recurrent changes (cycle) and frequent impacts (backwashing). Macroecology offers alternative non-equilibrium

hypotheses to explain diversity, i.e., assuming the community composition not to reflect a steady state. One such hypothesis is based on intermediate disturbance (3, 7). Shortly, this hypothesis suggests highest diversity at an intermediate rate and intensity of disturbance events. Rare and/or mild disturbance would lead to a few dominating, very well adapted and competitive populations. In contrast, frequent and/or strong disturbance events will cause a community to be dominated by populations, that either resist the disturbance or are able to quickly recolonize a free niche. The intermediate case will lead to the presence of both and, hence, to a community with highest diversity.

Could this hypothesis be of use to explain the phenomena of diversity of nitrifiers in the studied biofilms? The phenotypical plasticity of prokaryotes in contrast to eukaryotic organisms makes it difficult to speculate on that. However, a non-equilibrium situation should be kept in mind especially when interpreting the structure of the biofilm communities in SBBR systems.

As long as the contribution of single populations in such multispecies communities is not revealed, any explanation is speculative. In Chapter 6, an integrated approach was used, which combined microsensor measurements and FISH with microautoradiography (MAR) and quantitative beta microimaging. MAR can be used to show activity of single cells and populations qualitatively, and the uptake of radioactively labeled compounds can be quantified on the microscale with new techniques. The integrated approach proved to be suitable to reveal the qualitative and quantitative activity on both, the community as well as the single population level in a nitrifying community of a model biofilm. While appearing complex and sophisticated, the approach was shown to be feasible and led to consistent data. It allowed to overcome the limitations shown above. The combination of various *in situ* methods is necessary to study in depth the structure and function of complex microbial communities in applied systems in the future. As stated earlier "...complexity remains an inherent quality of these systems..." (8). Nevertheless, the new methods allow for new insights into many aspects of this complexity.

1. **Arnold, E., B. Böhm, and P. A. Wilderer.** 2000. Application of activated sludge and biofilm sequencing batch reactor technology to treat reject water from sludge dewatering systems: a comparison. *Water Sci. Technol.* **41**:115-122.
2. **Batchelor, S. E., M. Cooper, S. R. Chhabra, L. A. Glover, G. S. A. B. Stewart, P. Williams, and J. I. Prosser.** 1997. Cell density-regulated recovery of starved biofilm populations of ammonia-oxidizing bacteria. *Appl. Environ. Microbiol.* **63**:2281-2286.
3. **Connell, J. H.** 1978. Diversity in tropical rainforests and coral reefs. *Science.* **199**:1302-1310.
4. **Jørgensen, B. B.** 2000. Life in the diffusive boundary layer, p. 348-373. *In* B. P. Boudreau (ed.), *The Benthic Boundary Layer: Transport Processes and Biogeochemistry*. Oxford University Press, Oxford, UK.
5. **Morgenroth, E., A. Obermayer, E. Arnold, A. Brühl, M. Wagner, and W. P. A.** 2000. Effect of long-term idle periods on the performance of sequencing batch reactors. *Water Sci. Technol.* **41**:105-113.
6. **Pastorelli, G., R. Canziani, L. Pedrazzi, and A. Rozzi.** 1999. Phosphorus and nitrogen removal in moving-bed sequencing batch biofilm reactors. *Water Sci. Technol.* **40**:169-176.
7. **Petraitis, P. S., R. E. Latham, and R. A. Niesenbaum.** 1989. The maintenance of species diversity by disturbance. *Quart. Rev. Biol.* **64**:393-418.
8. **Tolker-Nielsen, T., and S. Molin.** 2000. Spatial organization of microbial biofilm communities. *Microb. Ecol.* **40**:75-84.

## Summary

The chemolithoautotrophic nitrifying bacteria gain their energy from aerobic oxidation of  $\text{NH}_4^+$  to  $\text{NO}_2^-$  (ammonia-oxidizing bacteria, AOB) and from  $\text{NO}_2^-$  to  $\text{NO}_3^-$  (nitrite-oxidizing bacteria, NOB). This process is the precondition for the removal of bound reduced nitrogen to atmospheric  $\text{N}_2$  via denitrification. Handling and control of nitrification is of major importance in modern sewage treatment. Advanced wastewater systems with complex functionality require detailed knowledge on the nitrifying populations and their activities. Microsensors and fluorescence *in situ* hybridization (FISH) are ideal tools to address structure and function *in situ*.

An initial study on an experimental multispecies nitrifying biofilm grown along opposed supply of  $\text{O}_2$  and substrate supported the hypothesis of high substrate affinity of *Nitrosomonas*- and *Nitrobacter*-related populations, which were outcompeted in microenvironments with low concentrations of  $\text{O}_2$  and  $\text{NO}_2^-$  by *Nitrospira* sp. and *Nitrospira* sp., resulting in a layered organization of the community.

The second study demonstrated that heterotrophic biological phosphate removal can be combined with substantial nitrification in a sequencing batch biofilm reactor (SBBR). An increase in  $\text{NH}_4^+$ -concentration led to intensified nitrification, as demonstrated by bulk measurements, and increased presence of nitrifiers. Nitrification contributed significantly to the budget of  $\text{O}_2$  uptake in the end of each cycle. In-depth investigation of nitrification and the composition and spatial organization of the nitrifying community revealed three populations of AOB related to *N. europaea*/*N. eutropha*, *N. communis*, and *N. oligotropha*, and the NOB *Nitrospira* sp. A partly distinct spatial distribution, the sequential activity of P removal and nitrification, and the transiency of the process could explain the coexistence on a microscale. The effects of the transient conditions on nitrifying activity, and the community structure of nitrifiers in SBBR systems was studied on a pilot-scale. This study revealed a pronounced diversity of AOB and NOB populations. Microsensor measurements showed a N loss and inefficiency of nitrification during most of the process. However, spatial heterogeneity of the individual populations was high, and did not allow an assignment of individual contributions.

This problem was addressed by an integrated approach combining microautoradiography and quantitative beta microimaging with the aforementioned techniques. A study was performed on a model biofilm. This approach might be suitable to access both, the community and the single population level quantitatively in complex biofilms.

## Zusammenfassung

Die chemolithoautotrophen Nitrifikanten gewinnen Energie aus der Oxidation von  $\text{NH}_4^+$  zu  $\text{NO}_2^-$  (ammoniakoxidierende Bakterien, AOB) und von  $\text{NO}_2^-$  zu  $\text{NO}_3^-$  (nitritoxidierende Bakterien, NOB). Dieser Prozeß ist Voraussetzung für die Überführung des gebundenen zu atmosphärischem Stickstoff durch eine anschließende Denitrifikation. In der modernen Abwasser-aufbereitung spielt die Kontrolle und Integration dieses Prozesses eine wichtige Rolle. Neue Aufbereitungssysteme mit komplexen Funktionen, und ihre Anpassung an den angewandten Maßstab benötigen detaillierte Kenntnisse über die nitrifizierenden Populationen und die Bedingungen für deren Aktivität. Mikrosensormessungen und die Fluoreszenz-*in situ*-Hybridisierung (FISH) sind geeignete Methoden um die Funktion und Struktur solcher Gemeinschaften *in situ* zu untersuchen.

In einer ersten Studie wurde ein Biofilm mit mehreren Nitrifikantenpopulationen untersucht, der unter entgegengesetzten Gradienten von  $\text{O}_2$  und Substrat gewachsen war. Die Hypothese einer Anpassung von *Nitrosomonas*- und *Nitrobacter*-verwandten Populationen an hohe und von *Nitrospira* sp. und *Nitrospira* sp. an niedrige Substratkonzentrationen fand Unterstützung in dem gefundenen stratifizierten Vorkommen der Populationen.

Ein Sequencing-Batch-Biofilm-Reaktor wurde in einer weiteren Studie daraufhin untersucht, inwieweit Nitrifikation mit dem heterotrophen Prozess der biologischen Phosphat-entfernung kombiniert werden kann. Erhöhte  $\text{NH}_4^+$ -Konzentrationen führten zu einer stärkeren Nitrifikation. Dies konnte sowohl anhand der Analyse des Mediums, als auch der mikrobiellen Struktur und auch der Bilanz der  $\text{O}_2$ -Aufnahme gezeigt werden. Eine detaillierte Analyse zeigte, daß drei Populationen von AOB vorhanden waren, die Verwandtschaft mit *N. europaea*/*N. eutropha*, *N. communis*, bzw. *N. oligotropha* aufwiesen. Die NOB gehörten zur Gattung *Nitrospira* sp. Die Koexistenz verschiedener AOB könnte durch räumliche und sequenzielle Aktivität von P-Entfernung und Nitrifikation erklärt werden. Der Einfluß sich ändernder Bedingungen auf die Struktur und Funktion eines Biofilms wurde an einem nitrifizierenden Pilot-SBBR-System untersucht. Mikrosensormessungen zeigten einen deutlichen N-Verlust und eine Ineffizienz der Nitrifikation während längerer Prozeßphasen. Die Diversität und räumliche Heterogenität der AOB und NOB erlaubte jedoch keine räumlich-zeitliche Auflösung der Aktivität der einzelnen Populationen.

Durch einen integrierten Ansatz in einer abschließenden Studie wurde dieses Problem angegangen. Der Ansatz kombinierte FISH und Mikrosensormessungen mit der Mikroautoradiographie und einer quantitativen hochauflösenden Aufzeichnung der [ $^{14}\text{C}$ ]-Verteilung an

einem Modellbiofilm. Dadurch konnte die Nitrifikation zusätzlich auf der Populationsebene detaillierter untersucht werden. Im Rahmen der Studie konnten *in situ*-Assimilationsraten und -Zellerträge der autotrophen Nitrifizierer ermittelt werden. Dieser Ansatz kann in zukünftigen Studien zur Aufklärung der Struktur und Funktion einzelner mikrobieller Populationen in komplexen technischen Biofilmen von Nutzen sein.



## List of Publications

### *Contributions to the manuscripts presented in this thesis*

- Schramm, A., D. de Beer, A. Gieseke, and R. Amann. 2000. Microenvironments and distribution of nitrifying bacteria in a membrane-bound biofilm. *Environ. Microbiol.* **2**(6):680-686.
- Gieseke, A., P. Arnz, R. Amann, P. Wilderer, and A. Schramm. 2002. Simultaneous P and N removal in a sequencing batch biofilm reactor: insights from reactor- and microscale investigations. *Water Res.* **36**(2):501-509.
- Gieseke, A., U. Purkhold, M. Wagner, R. Amann, and A. Schramm. 2001. Community structure and activity dynamics of nitrifying bacteria in a phosphate-removing biofilm. *Appl. Environ. Microbiol.* **67**(3):1351-1362.
- Gieseke, A., L. Bjerrum, M. Wagner, and R. Amann. Structure and activity of multiple nitrifying bacterial populations coexisting in a biofilm. In prep. for *Environ. Microbiol.*
- Gieseke, A., J. L. Nielsen, H. Jonkers, R. Amann, P. H. Nielsen, and D. de Beer. A polyphasic approach to study in situ substrate conversion in a nitrifying community. In prep.

### *Further publications*

- Boetius, A., K. Ravensschlag, C.J. Schubert, D. Rickert, F. Widdel, A. Gieseke, R. Amann, B.B. Jørgensen, U. Witte, and O. Pfannkuche. 2000. A marine microbial consortium apparently mediating anaerobic oxidation of methane. *Nature* **407**:623-626.
- Wickham, S., A. Gieseke, and U.-G. Berninger. 2000. Benthic ciliate identification and enumeration: an improved methodology and its application. *Aquat. Microb. Ecol.* **22**:79-91.

